Peer Review File

Manuscript Title: Autonomous Self-burying Seed Carriers for Aerial Seeding

Reviewer Comments & Author Rebuttals

Reviewer Reports on the Initial Version:

Referees' comments:

Referee #1 (Remarks to the Author):

The manuscript reports on artificial seeds, inspired by natural (i.e., Erodium) seeds, which are able to penetrate soil, thanks to hygromorphic actuation, and to release functional payload, including symbiotic species (such as cherry belle radish seeds and mycorrhizal fungi), as remarkably demonstrated in the supporting videos.

The paper demonstrates a truly bioinspired approach, starting from material choice. Indeed, natural wood was used to fabricate the artifical seed, with remarkable gains in hygroscopic passive actuation, robustness (as also demonstrated by releasing the seeds from drones) and biodegradability, namely key assets for the envisioned real-world applications of reforestation. Even the reliance of seed cyclic coiling/uncoiling on large humidity variations, as occurring when passing from dry to rainy days, is totally consistent with the pursued approach, since, e.g., even germination relies on the same wet conditions.

More in detail, a clever delignification process was preliminarily performed, which permits to code the coiled seed shape with tight curvature, as functional to subsequent elongation/drilling. It is worth remarking that such an enabling manufacturing step was previously reported in ref[23] (which is correctly acknowledged in the ms), where, however, a basic seed design was adopted compared to the one introduced in the ms. Indeed, the ms report a clever three tail design for the artificial seed, which enables a more favourable initial penetration angle compared to the natural model that only features a single tail (and the reported enhanced successful penetration rate of the artificial seeds corroborate the proposed design).

Hygromorphic behavior was characterized by considering a simplified bending segment, by also introducing some complementary analytical models, wherease the coupled torsion was discussed based on through-thickness variation of the hygroscopic fibers naturally present in the considered material samples. Moreover, soil penetration was experimentally characterized, by also measuring the axial force produced by uncoiling and by introducing some numerical models. Overall, the ms reports a convincing amount of work, yet the following comments should be considered to improve the paper.

- The quantitative analysis that is detailed through supporting note 1, aimed at complementing figures (2g,h), should be improved by considering the following points.
> The densification process is not suitably described: the note should better detail its physical mechanisms and how they are reflected in the model (in particular concerning the stiffening deformation region, as currently appears). Even the curve in fig.2g deserves some additional explanation
> Both fig(2g,h) may share the same x-range
> The factor \beta is an empirical ex-post correction. This should be clearly written. Indeed, physically speaking, it is expected to depend on the specific microstuctural properties of the sample (including fiber angle variation and dispersion), yet a single value is reported in the ms, and this seems to be just a single fit to the data in fig.2h
> Eq.(9) in section B of the curvature analysis methods reports a simple scaling between k_w and k_d, based on the corresponsing sample thickness. This seems to be plausible for the purely

plastic case, as detailed in supporting note1. The ms claims that is holds even for the stiffening case, yet this seems not to be immediate, since in supporting note 1 and specifically in Eq.(16), h appears even alon (i.f., not as k*h). In other words, the scaling with thikness (from h to h') seems to be more complex than what is stated in the ms
> Eq.(9) in section B of the curvature analysis methods lacks E in the rightmost term
> In supporting note 1, and specifically concerning Eq.(3), why torque equilibrium is not invoked? It clearly adds a constraint: does it affect the resulting curvature k in Eq.(5)? The question stems from the fact that, for many of the introduced expressions, a clear description of which are the independent variables, the dependent variables, and the additional parameters seems to be missing. The presentation should be improved by reflecting them
- In supporting note 1, many expressions are defined by cases (on the y range). The current in-line writing stykle make them hard to be read. Conventional vertical stacking (with left brace) might improve readabilty
- In supporting note1 and specifically in figS1, the y_k should not be indicated as distances, since they are signed quantities in the reported expressions

- The quantitative analysis that is detailed through supporting notes 2, 3 and 4, aimed at complementing figures (3b,c,d,e), should be improved by considering the following points.
> The methods used to generate fig.(3b,c) which shows simulated data coming from a comparison between single tail and three tail configurations, should be reported with some more details. Which were the considered configurations? Likely, they correspond to those depicted in fig.3(d,e), yet their choise deserves some more explanation. Indeed, the anchoring points/conditions are expected to strongly affect the results, in particular for the single tail seed.
> The results in fig.(3b,c) seem not to be significanly different from one another: which is the lesson that simulation offers? Moreover, time was not explicitly accounted for in simulation (rather, hygroscopic strain was incrementally enforced) so, no truly dynamical simulations can be claimed, and seed elongation (instead of time) should be used to parameterize force
> The simulated results in fig.3d should be commented in more detail. Which are their scalebar units and significance? Indeed, they seem to be relatively qualitative at the present stage, also because the assumed frictional contact cannot accurately describe drilling engagement. This aspect should be clearly discussed, and some sensitivity to the boundary conditions should be considered to make stronger claims. Finally, the black inner region featuring in the rightmost figure in fig.3d (and in particular for the left contact) should be checked/discussed, since it seems hard to decipher from a physical viewpoint.
> A technical point should be clarified. As far as I understand, the hygroscopic strain is applied in the Lagrangian coordinates, and the seed changes its configuration as a consequence of the imposed strain and the external contact boundary conditions. Is it correct? Are the aforementioned conditions compatible with each other (in particular in Abaqus)? These details should appear in the supporting notes.
> The parameters involved in the numerical model were calibrated to match experimental results, yet this calibration seems to be poorly reported. Which are the experimental results considered for calibration? A clear report of what has been done seems to be needed, also because parameter fitting was not leading to a unique set of parameters, as reported in the current supporting note 3.
> As regards frictional contact introduced to mimick anchoring: was it imposed on a couple of surfaces?

- The considered hygroscopic actuation leverages humidity transport to synergistically modulate strain and stiffness in plant tissue. Although a complete modeling treatment is still very challenging (both for stable implementation in numerical solvers and model calibration), some works dealing with hygroscopically actuated bilayers appear in literature, which include modeling contributions bridging humidity transport and derived strain. See, e.g., (Krüger et al., Biomimetics, 6(4), 58, 2021, [doi.org/10.3390/biomimetics6040058]; Lunni et al., Advanced Materials Interfaces, 7(4), 1901310, 2020, [DOI: 10.1002/admi.201901310]). In light of previously published contributions, the ms should also discuss the importance to further enrich the proposed modeling approach by also embarking the real actuation driver, i.e., water transport, to further advance the design of the devised aerial seeds

- Experimental data seems to miss relevant details on repetitions and statistical variations (e.g., though std and error bars). At least 3 repetitions should be reported for each experimental data (better 6). All data should be reported as mean value ± standard deviation.

- Nematodes release is of interest, yet poorly discussed. Additional details, including.e.g, some figures (over time) or supplementary movie should be added.

- Double layer seeds are reported, besides single layer ones (and no surprise that the former are stronger than the latter). Fabrication variability should be nonetheless discussed

- Fiber angle variation thorugh thickness was presented a the key physical element to couple bending and coiling. How was it possible to succesfully obtain coiling in the prototyped artificial seeds without checking/imposing the correct direction of fiber angle gradient before coiling the initial wood strip in the mechanical molding fabrication step? This should be definitely clarified.

- Title could be improved so as to better reflect the proposed material. “Self-drilling” seems to be lisleading, since the seed is not drilling itself. “Superior” is not very clear. Maybe, a more descriptive title could be “Autonomous Self-burying Seed Carriers for Aerial Seeding”.

- The SEM measurements of the fibrillar angles are quite at poor magnification, from the images it is not clear the arrangement of the fibrils. A SEM imaging at higher resolution could help. Furthermore, authors should perform measurements on several samples and report the results with the error bars.

- In the manufacturing process it is clear that the wet molding procedure relies on the operator skills (made by hand). It is quite evident that the radius can be fabricated with high reproducibility, given a fixed cylindrical mold diameter, instead the pitch could change during the wet molding. Authors could provide a comment and an evaluation on the variability of the pitch.

- A few typos are around (including the whole sentence in supporting note 1, which appears between Eq.(9a) and Eq.(9b)). Further proofreading is recommended.

- Extended Data Figure 7: some pictures have very low quality. Please, replace them with better quality pictures.

Referee #2 (Remarks to the Author):

The authors report the design and fabrication of seed carriers made of wood veneer, which can self-drill into the soil, inspired by Erodium seeds. The key advantages of their seed carriers are argued to be a higher drilling success rate than Erodium seeds thanks to three-tailed structure, and a wider range of payloads. The authors also provide some theoretical accounts on curvature change and actuation of their actuators. Although the veneer-based self-drilling actuators look intriguing, this work does not appear to present significant scientific/technological advances for the following reasons.

(1) The most serious question raised after reading this manuscript is the value (necessity, meaning or advantage) of making self-drilling actuators inspired by Erodium or other similar kinds of plant species using plant-based materials (veneer in this case). It is well known that plant-based materials are hygroscopic, and their applications for soft actuation have been reported. Artificial materials, including hygroscopic polymers, have also been explored for hygroscopic actuation. Fascinated by the amazing motility of some seeds capable of self-burial, many previous works have analyzed the mechanics behind the shape-morphing and actuation of both the natural

and artificial coiling actuators. Many of those previous works have been cited by the authors, although there have been few attempts to replicate the self-drilling ability of Erodium and other plant species.

The actuators made by the authors indeed seem capable of self-drilling with a very high success rate. However, if we ever want to attach self-propelling tails to seeds we want to disperse over land, why do we not just use seed awns of Erodium or other similar kinds of plant species?
- There are many seeds with motile awns (providing the ability of self-dispersal and self-burial), e.g. black oat grass (Stipa avenacea), wiregrass (Aristida tuberculosa), wheat (Triticum sp.), mouse barley (Hordeum murinum), Erodium and Pelargonium species. Many of them can be easily purchased over the internet.
- The size range is very wide - let alone small seeds of Erodium and Pelargonium species (a few mm long), large awns of Stipa species seeds are as long as 25 cm - so that a wide range of payloads can be covered.
- The authors attribute the high success rate of anchoring or establishing to the three-tailed structure of their actuators. Aristida has three awns (please see figure 1 of Cerros-Tlatilpa et al. Am. J. Botany 98, 1868-1886, 2011), so it is doubtful whether the authors' design is creative.
- As seen in Fig. 1f of the manuscript, the elastic modulus of existing seed awns is not inferior to that of the veneer used in this work.
- To fabricate self-drilling actuators with veneer, the authors used multi-step processes including sawing, cutting, chemical washing, rinsing, drying and moulding. Considering the cost, time, energy and amount of carbon produced to make each actuator, it is questionable whether this kind of work is environmentally friendly and economically viable.

(2) A significant portion of the main text describes and explains the curvature change of a bent piece of treated veneer. Although this is an important starting point to understand the shape-morphing of coiled actuators, the actual deformation of the actuator involves the change of pitch as well as curvature of the helix, which leads to coiling and uncoiling. Although numerical simulations with many simplified assumptions and fitting parameters for coiled actuation are presented in Supplementary Note, focusing on the mere curvature of the bent piece in the main text can mislead readers to think that this work has analyzed the shape-morphing with enough depth. The authors need to present theoretical analysis for the pitch and curvature of the helix with drying or to refine their numerical simulations to correlate the internal structure (including MFA) and mechanical properties with coiling deformations.

(3) Below equation (5) in Methods, they mentioned that they ignored the modulus reduction effect, which needs to be justified (for other mechanical models in this work, too).

Referee #3 (Remarks to the Author):

This manuscript reports development of seed vehicles inspired by self-drilling plant seeds. They used wood – biodegradable and ecosystem-safe material – to create the hygromorphic machines, achieving 45 times more deformation capacity than previously reported. The new technology is employed to develop sustainable solutions for plant/fungus/nutrients dispersal in soil and vegetation restoration. The work is comprehensive, spanning from material processing to design exploration and functional tests in laboratory and field conditions. Generally, it is done with thoughtfulness and attention to detail and documented and explained clearly in this manuscript.

Major points:
1. The elephant in the room question I had while reading this manuscript is: “This is a very nice and interesting work, but does it have broad significance expected for publications in Nature?”. The wide-reaching significance of this work, I think, lies in being able to make a dynamic water-activated morphing with wood, which has diverse applications. The authors mention this but only

one sentence at the beginning and end of the report. Can you elaborate by expanding in the discussion?
Throughout the history of materials development, wood and new modifications to enhance its performance (e.g., bent wood, plywood) unlocked whole new ranges of innovations and manufacturing capability. Do you think this could do the same?
2. More starting materials? A specific starting material (white oak) was chosen for the best spec – but the observations made may only be relevant for the specific material. Have you tried other types of wood?
3. What was the key driver of your innovation? How could you achieve the 45 times better bending curvature? This is critical information and could be articulated with more highlighting. I read that it was because of the chemical treatment – is it the case? If so, please elaborate the development of the method further. Did you try different ways to make to complaisant while maintaining the strength? Why did you choose this method?
4. Making artificial replica is effective in gaining insights into the why behind biological design. (And such cross-disciplinary impacts could enhance the broader relevance of this work.) You have found the natural form turned out to not so functional (cannot drill as efficiently as three tailed engineered design). Can you discuss why the natural selection has settled on the not so effective form? Do you find double/triple tailed seeds in nature?

Minor points:
5. Why scalable? The molding procedure and assembly sound quite complex, and it does not sound so scalable.
6. I read that the samples they used did not pay attention to cellular size differences across the height of the wood piece used. The molding creates the gradient of sizes. It is worth emphasizing, especially because wood is quite heterogenous in cell size and they are arranged in layers across the radius of the trunk.
7. Quantification is needed in the soil drilling test. Figure 1-3 are done with nice quantitation, while Figure 4 and 5 could have much more.
8. Soil granularity and surface topology – can you specify this for all the conditions you used (in lab and field)?
9. More field work needed (currently only one field test, which had a surprise storm)
More details also needed; for example, what was the germination rate of unlodged and non-lodged seeds (never lodged)?
10. Do they tangle with each other upon storage and dispensing? That would be a drawback of the three tailed design.

Author Rebuttals to Initial Comments:

Response to Reviewers

Reviewer comments are set on grey background, the responses to the comments and newly added text in the revised manuscript and SI are shown in blue.

Referee #1 (Remarks to the Author):

Comment #1: The manuscript reports on artificial seeds, inspired by natural (i.e., Erodium) seeds, which are able to penetrate soil, thanks to hygromorphic actuation, and to release functional payload, including symbiotic species (such as cherry belle radish seeds and mycorrhizal fungi), as remarkably demonstrated in the supporting videos.

The paper demonstrates a truly bioinspired approach, starting from material choice. Indeed, natural wood was used to fabricate the artifical seed, with remarkable gains in hygroscopic passive actuation, robustness (as also demonstrated by releasing the seeds from drones) and biodegradability, namely key assets for the envisioned real-world applications of reforestation. Even the reliance of seed cyclic coiling/uncoiling on large humidity variations, as occurring when passing from dry to rainy days, is totally consistent with the pursued approach, since, e.g., even germination relies on the same wet conditions.

More in detail, a clever delignification process was preliminarily performed, which permits to code the coiled seed shape with tight curvature, as functional to subsequent elongation/drilling. It is worth remarking that such an enabling manufacturing step was previously reported in ref[23] (which is correctly acknowledged in the ms), where, however, a basic seed design was adopted compared to the one introduced in the ms. Indeed, the ms report a clever three tail design for the artificial seed, which enables a more favourable initial penetration angle compared to the natural model that only features a single tail (and the reported enhanced successful penetration rate of the artificial seeds corroborate the proposed design).

Hygromorphic behavior was characterized by considering a simplified bending segment, by also introducing some complementary analytical models, wherease the coupled torsion was discussed based on through-thickness variation of the hygroscopic fibers naturally present in the considered material samples. Moreover, soil penetration was experimentally characterized, by also measuring the axial force produced by uncoiling and by introducing some numerical models.

Our response: We thank the referee for the positive comments and suggestions for improvement.

Comment #2: Overall, the ms reports a convincing amount of work, yet the following comments should be considered to improve the paper.

- The quantitative analysis that is detailed through supporting note 1, aimed at complementing figures (2g,h), should be improved by considering the following points.

Our response: we thank the reviewer for the insightful comments to improve the quality of our manuscript. We have updated the manuscript and included a point-to-point response to each individual comment.

Comment #3: > The densification process is not suitably described: the note should better detail its physical mechanisms and how they are reflected in the model (in particular concerning the stiffening deformation region, as currently appears). Even the curve in fig.2g deserves some additional explanation

Our response: Here, the "densification process" refers to collapsing of the cellular network under compressive loading; as the cell walls contact each other, the elastic modulus increases after the plastic deformation region. In our theoretical analysis, the modulus increase is modeled as the stress-strain curve for compressive strain value larger than \epsslion_Y2 (the red line in Fig. 2f). Since "densification process" is also used in literature to describe the wood processing, to avoid confusion we will use the term, "stiffening region", in our manuscript. We agree with the reviewer that Fig. 2g needs more explanation.

Our modification to the manuscript: Under method, on page 23, lines 549-550, we explicitly described the physical picture of the stiffening region and added references:

"plastic model with an ideal plastic region followed by a stiffening region (Fig. 2f)[40,50]. The increase of modulus in the stiffening region is due to the contact of the collapsed cell walls[51]."

Ref. 51. Reiterer, Alexander, and Stefanie E. Stanzl-Tschegg. "Compressive behaviour of softwood under uniaxial loading at different orientations to the grain." *Mechanics of materials* 33, no. 12 (2001): 705-715.

In the main text, on page 8, lines 152-157, we added a discussion of Fig. 2g:

"All experimental data collapse onto two master curves (Fig. 2g), determined by a dimensionless variable, κh, where κ is the bending curvature with respect to the neutral axis of the wood sheet during molding. The gray master curve describes the increase dimensionless curvature, κ_w/κ, due to the accumulation of the plastic strain. The decrease of κ_w/κ in the black master curve can be attributed to the fact that the compression strain in the stiffening regime becomes reversible."

Comment #4: > Both fig(2g,h) may share the same x-range

Our response: We adjusted both x-ranges in Fig. 2g,h as [0 0.9]. Please see the updated figures in our responses to **Comment #19**.

Comment #5: > The factor \beta is an empirical ex-post correction. This should be clearly written. Indeed, physically speaking, it is expected to depend on the specific microstuctural properties of the sample (including fiber angle variation and dispersion), yet a single value is reported in the ms, and this seems to be just a single fit to the data in fig.2h

Our response: We agree with the reviewer that the real physical process is complicated. The current single value of \beta is an empirical ex-post correction. We made it more clear in the revised manuscript.

Our modification to the manuscript: In the main text, on page 9, lines 184-186, we changed the text to:

"where β is an empirical parameter that describes the coupling between the mechanical strain and shrinkage. Our experimental data can be reasonably well-captured in Fig. 2h with $\beta = 0.6$."

Under the Method, on page 26, line 610, we added the following statement:

" β is an empirical parameter"

On page 26, lines 612-616, we expanded the discussion of the parameter β:

"Note that we compared the curvatures at the two end states and neglected the kinetic effects. In principle, β will also depend on the strain values. Here, since our focus was to identify the key actuation mechanism, a constant value of β is preferred for deriving a closed form solution. A numerical solution to address the dynamic process will be investigated in the future[53]."

Ref. 53. Fortino, S., Mirianon, F. & Toratti, T. A 3D moisture-stress FEM analysis for time dependent problems in timber structures. *Mech. Time-Depend. Mater.* **13**, 333 (2009)."

Comment #6: > Eq.(9) in section B of the curvature analysis methods reports a simple scaling between k_w and k_d, based on the corresponsing sample thickness. This seems to be plausible for the purely plastic case, as detailed in supporting note1. The ms claims that is holds even for the stiffening case, yet this seems not to be immediate, since in supporting note 1 and specifically in Eq.(16), h appears even alon (i.f., not as k*h). In other words, the scaling with thikness (from h to h') seems to be more complex than what is stated in the ms

Our response: We thank the reviewer's insightful comments. Indeed, the bending curvature for the stiffening case is much more complicated than the ideal plastic case. As the reviewer pointed out, two more dimensionless variables appear in the equation. As y_2 and y_4 will change proportionally to the thickness, so does the change of the wet and dry curvatures due to the thickness change. The simple scaling is rooted in our assumption that the wet and dry states have the same plastic strain, which is supported by the nearly reversible actuation of our actuators. We believe the simple treatment reported here is sufficient to provide a good explanation of our experimental data. Nevertheless, the real deformation in the wood veneer could be much more complicated, which will need more careful modeling and analysis in future studies.

Our modification to the manuscript: Under Method, on page 26, lines 597-600, we added the following discussion:

"For the bending curvature of the case with stiffening defined in Equation (3), it contains not only κh but also two more dimensionless variables $\frac{y_4}{h}$ and $\frac{y_2}{h}$, making the analysis more complicated than the ideal plastic case in our simple model. As y'_2 and y'_4 will change proportionally to h, this leads to $\frac{y_4}{h} = \frac{y'_4}{h'}$ and $\frac{y_2}{h} = \frac{y'_2}{h'}$. Therefore, the same relationship in Equation (9) also holds for the cases with stiffening."

In the Supplementary Note 6, we also updated Figure S10 to include the stress distributions of wet and dry wood veneers in the plastic deformation regime with stiffening:

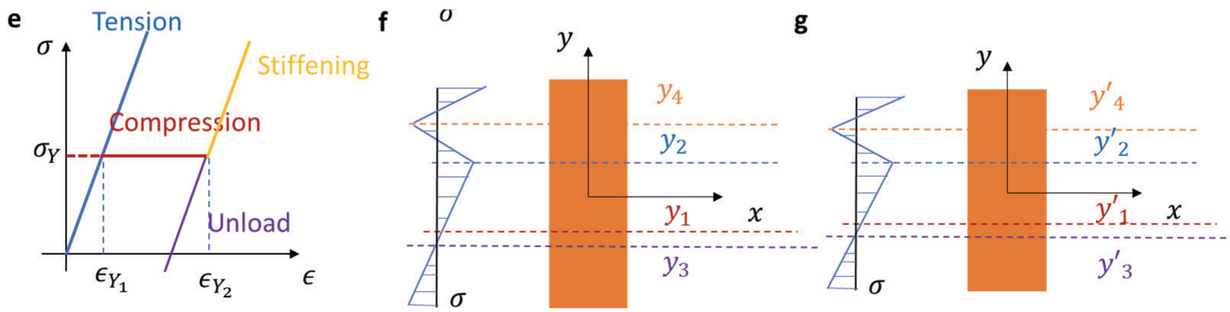

Newly added **Figure S10 e-g**. **The thickness shrinkage effect during drying on the curvature change**. **e**, Plastic deformation with stiffening. **f**, The stress distribution at the wet state for wood veneers in the plastic deformation regime with stiffening. **g**, The stress distribution at the dry state for wood veneers in the plastic deformation regime with stiffening. The wet and dry y-axis satisfy $\frac{y}{y'} = \frac{h}{h'}$.

Comment #7: > Eq.(9) in section B of the curvature analysis methods lacks E in the rightmost term

Our response: we thank the reviewer for the careful reading of our manuscript. Young's modulus E is now included in Eq. (13).

Our modification to the manuscript: Under Method, on page 27, line 623, we added "E" to the rightmost term.

Comment #8: > In supporting note 1, and specifically concerning Eq.(3), why torque equilibrium is not invoked? It clearly adds a constraint: does it affect the resulting curvature k in Eq.(5)? The question stems from the fact that, for many of the introduced expressions, a clear description of which are the independent variables, the dependent variables, and the additional parameters seems to be missing. The presentation should be improved by reflecting them

Our response: the analysis in the Supplementary Note 6 only focused on the curvature analysis of the bending wood strips. Therefore, there is no torque under this condition. We agree that "a clear description of which are the independent variables, the dependent variables, and the additional parameters" should be clearly laid out at the beginning of the analysis.

Our modification to the manuscript: We changed the title of Supplementary Note 6 on page 60, line 1059, to "**Supplementary Note 6: Curvature of Bending Actuators in the Wet State just After Release**" to clearly indicate the analysis on the bending deformation of the wood strips. On page 60, lines 1060-1067, we added the following definition and discussion:

"This note aims to establish a relationship between the bending curvature in the wet state just after release (κ_w) and the material (e.g., plastic deformation behaviors) and geometrical (e.g., thickness h) properties of the wood veneers and the radius of the mold (R). Since our focus is on bending actuators, the wood veneer can be modeled as a beam. In the analysis, the wood veneer thickness, h, and the mold radius, R, can be directly measured from experiments. The key material properties include two critical strains associated with plastic deformation, ϵ_{Y_1} and ϵ_{Y_2}, which are fitting parameters and will be extracted by comparing the theoretical predictions with experimental results."

Under the Method, on page 23, line 544, we modified the sentence as "**Curvature analysis of the bending actuators**" to make this clear in the manuscript as well.

In the main text, on page 8, lines 143-145, we added a sentence to explicitly indicate that our analysis of the curvature formation and actuation is based on bending actuators

"To reveal the underlining mechanism of curvature formation and actuation, we first analyze the deformation behaviors of the bending actuators, made from the three-step molding process (Fig. 2a-d)."

We also removed the comment on "leading to a tight coiling" in the original manuscript.

Comment #9: - In supporting note 1, many expressions are defined by cases (on the y range). The current in-line writing style make them hard to be read. Conventional vertical stacking (with left brace) might improve readabilty

Our response: We thank the reviewer's suggestion to improve the readability. We updated the equations in supporting note 1, which becomes "Supplementary Note 6" in the revised manuscript as we include more supplementary materials.

Our modification to the manuscript: In Supporting note 6, on page 61, line 1079, Eq. (2) was rearranged as

$$\sigma = \begin{cases} (y_1 - y)\kappa E, \; y < y_2, \\ -\sigma_Y, \; y > y_2, \end{cases}.$$

On page 62, line 1098, Eq. (8) was rearranged as

$$\sigma = \begin{cases} (y_3 - y)\kappa_w E, \; y < y_2, \\ \big((y_3 - y)\kappa_w - (y_2 - y)\kappa\big)E, y > y_2. \end{cases}$$

On page 62, line 1110, Eq. (11) was rearranged as

$$\sigma = \begin{cases} (y_1 - y)\kappa E,\ y < y_2 \\ -\sigma_Y,\ y_2 < y < y_4 \\ -\sigma_Y + \left((y_1 - y)\kappa + \epsilon_{Y_2}\right)E,\ y > y_4 \end{cases}$$

On page 63, line 1123, Eq. (14) was rearranged as

$$\epsilon_p = \begin{cases} 0,\ y < y_2 \\ (y_2 - y)\kappa,\ y_2 < y < y_4 \\ \epsilon_{Y_1} - \epsilon_{Y_2},\ y > y_4 \end{cases}$$

On page 64, line 1125, Eq. (15) was rearranged as

$$\sigma = \begin{cases} (y_3 - y)\kappa_w E,\ y < y_2 \\ \left((y_3 - y)\kappa_w - (y_2 - y)\kappa\right)E,\ y_2 < y < y_4 \\ \left((y_3 - y)\kappa_w + \epsilon_{Y_2} - \epsilon_{Y_1}\right)E,\ y > y_4 \end{cases}$$

Comment #10: - In supporting note1 and specifically in figS1, the y_k should not be indicated as distances, since they are signed quantities in the reported expressions

Our response: we agree with the reviewer and removed the arrows associated to y_k (k=1,2,3,4).

Our modification to the manuscript:

The original Figures S1-S3 become Figures S8-S10 in the revised manuscript because we included more supplementary figures.

The updated Figure S8c,f are

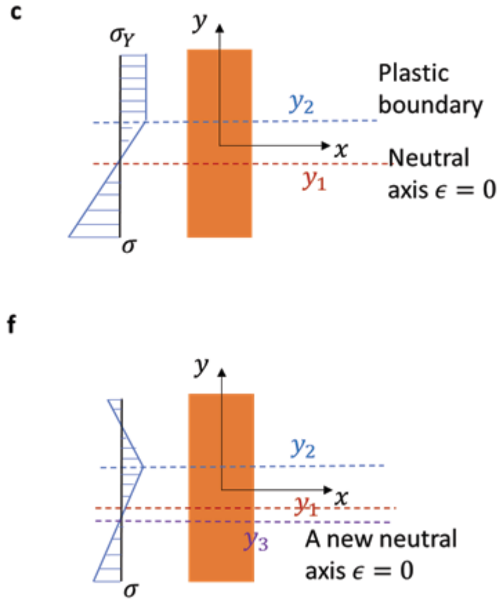

Updated **Figure S8 c,f. Bending curvatures after the release of the wood veneer from the mold within the ideal plastic region**. **c**, The stress distribution along the thickness direction. **f**, The stress distribution in the released sample.

The updated Figure S9c,f are:

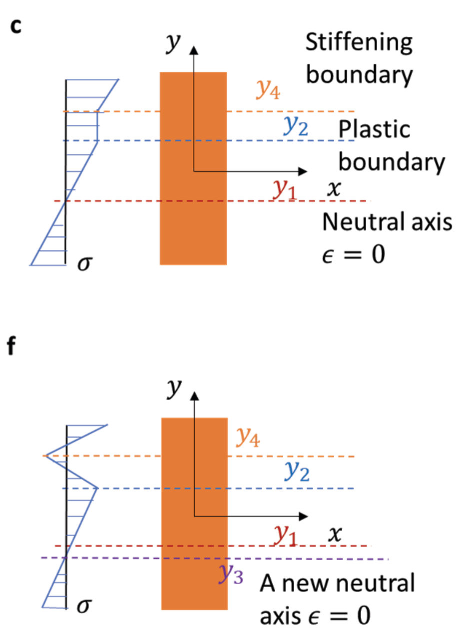

Updated **Figure S9. Bending curvatures after release of the wood veneer from the mold within the stiffening region c**, The stress distribution along the thickness direction. **f**, The stress distribution in the released sample.

The updated Figure S10 c,d are

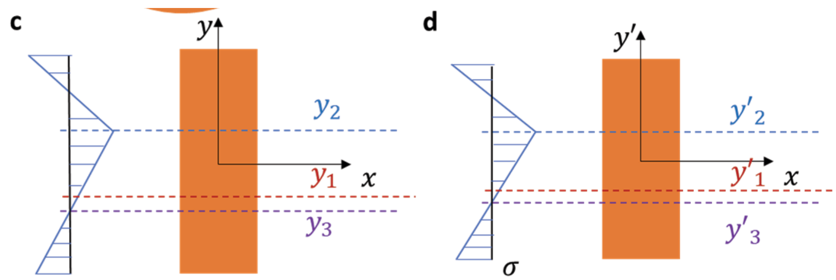

Updated **Figure S10. The thickness shrinkage effect during drying on the curvature change**. **c**, The stress distribution at the wet state for wood veneers in the ideal plastic deformation regime. **d**, The stress distribution at the dry state for wood veneers in the ideal plastic deformation regime.

Comment #11: - The quantitative analysis that is detailed through supporting notes 2, 3 and 4, aimed at complementing figures (3b,c,d,e), should be improved by considering the following points.

Our response: We thank the reviewer for the insightful comments to improve the quality of our manuscript.

Comment #12: > The methods used to generate fig.(3b,c) which shows simulated data coming from a comparison between single tail and three tail configurations, should be reported with some more details. Which were the considered configurations? Likely, they correspond to those depicted in fig.3(d,e), yet their choise deserves some more explanation. Indeed, the anchoring points/conditions are expected to strongly affect the results, in particular for the single tail seed.

Our response: we have added more descriptions of the methods used to generate Fig. 3b and Fig. 3c. Yes, the force for seed carriers with tip anchoring corresponds to simulation snapshots shown in Fig3. d-e. We added more discussion on the choice simulation parameters under the Methods section and supplementary note 4. We agree with the reviewer that the anchoring points/conditions are very important in the drilling. Therefore, we have conducted new simulations and experiments to better show their effects.

Our modification to the manuscript: In the main text, on page 11, lines 220-226, we added discussion of the Fig. 3b and Fig. 3c as

"As seen in Fig. 3b, the three-tailed design generates a much larger thrust force than the single-tailed design. Figure 3c shows that the body of tail 2 and the tip of tail 3 of the three-tailed design anchor initially (left image in Fig. 3d), then both tips of tail 1 and 2 start anchoring on the ground (right image in Fig. 3d) to generate larger forces as the tails become more hydrated. For both designs, an anchoring seed tip can significantly increase the thrust force; the representative dynamic hydration process both in experiments and simulations are shown in Fig. 3d-e and Supplementary Video 4."

Under Methods, on page 27, lines 671-677, we added discussion on the drilling process on hard and smooth surfaces:

"We conducted further experiments and simulations of seed carrier drilling on a surface that was hard and smooth (Supplementary Note 9) and found a substantial rotation of the seed carriers, due to the low frictional force and lack of anchoring points (Extended Data Fig. 9). The three-tailed design rotated less than the single-tailed design, as it can establish contact not only at two tails but also at the seed tip, due to the initially inclined angle on the surface. This further validates that our simulations can capture the interaction between engineered seed carriers and different ground types, despite the simplification of the model."

The Extended Data Figure 9 is given in response to **Comment #14**.

In supplementary note 9, on page 77, lines 1368-1372, we added a summary of the four simulations shown in Fig. 3b

"Seed carrier drilling was simulated from four possible scenarios, including single-tailed design without anchor, single-tailed design with anchor, three-tailed design without anchor and three-tailed design with an anchor. The simulated thrust force between the seed tip and the ground is shown in Fig. 3b, suggesting that the three-tailed design with an anchor can generate the largest thrust force."

Comment #13: > The results in fig.(3b,c) seem not to be significantly different from one another: which is the lesson that simulation offers? Moreover, time was not explicitly accounted for in simulation (rather, hygroscopic strain was incrementally enforced) so, no truly dynamical simulations can be claimed, and seed elongation (instead of time) should be used to parameterize force

Our response: Figure 3b compares the drilling forces for single-tailed and three-tailed designs under different anchoring conditions, providing direct support for our three-tailed design. Figure 3c presents the forces of different parts for the three-tailed design with an anchored seed tip. It offers more detailed information on the dynamical interactions between different parts of the seed carrier with the ground.

The time variation of the hygroscopic strain field is obtained by fitting the thrust force measurement. We agree that the time scale shown in the *x*-axis cannot be claimed as generic for different applications as it can change depending on the experimental setup. In addition, the real hygroscopic strain variations may not be a continuous function of time. Therefore, we changed the *x*-axis in Fig. 3b,c as a state variable that maps the transition from the dry state (0) to the wet (1) state.

Our modification to the manuscript: In the main text, we added a more detailed discussion about Fig. 3b and Fig. 3c (see the response to an earlier **Comment #12**). We update the figure caption of Fig. 3b to explain the hydration state, on page 10, lines 193-195:

"**b,** Comparison of simulated thrust force between the seed tip and the ground from the three-tailed and the single-tailed designs as a function of the normalized hydration state (Methods) that maps the transition from the dry state (0) to the wet state (1)."

In Supplementary Note 9, on page 77, lines 1372-1380, we added discussions about the motivation of plotting forces in terms of hydration state and how we defined the hydration state.

"In these drilling simulations, we adopted the same time-dependent state variable in Eq. (22) to describe the uncoiling process. The time scale was obtained from the thrust force measurements with controlled environmental moisture, which is likely to change, subject to the environmental conditions of the indoor and field tests. The time scale may not be very meaningful by comparing the simulation with experiments. Therefore, we presented the forces in terms of the hydration state, instead of time, as shown in Fig. 3b,c. The hydration state, denoted as η , was equal to 0 in the dry state and 1 in the wet state, respectively, which can be computed through a linear mapping of the state variable ξ as:

$$\eta = \frac{1-\xi}{1-\xi^{w}}. \tag{24}$$"

Comment #14: > The simulated results in fig.3d should be commented in more detail. Which are their scale bar units and significance? Indeed, they seem to be relatively qualitative at the present stage, also because the assumed frictional contact cannot accurately describe drilling engagement. This aspect should be clearly discussed, and some sensitivity to the boundary conditions should be considered to make stronger claims. Finally, the black inner region featuring in the rightmost figure in fig.3d (and in particular for the left contact) should be checked/discussed, since it seems hard to decipher from a physical viewpoint.

Our response: we added more discussions on Fig. 3d. The scale bar unit is kPa and presented in the figure caption. We intentionally chose a small upper limit of the contact pressure to make the contact region more visible. Therefore, the exact value (0.1 kPa) does not provide a physical meaning of the level of the pressure. We added the units to the figure and explained our choice more clearly.

We agree with the reviewer that our simulation can only provide a qualitative explanation of the experiments and we will clarify this in the manuscript. On the other hand, our simulation can capture the trend of the drilling process on different types of ground quite well. We add more discussion on the modeling and simulations of drilling and have conducted new experiments and simulations of drilling on both hard and smooth ground.

The left contact point in Fig. 3d is attributed to the establishment of the anchoring point of that tail. The tail anchoring effect is modeled as a larger coefficient of friction, which can capture the dynamics of the anchoring formation. We have added more discussion on this.

Our modification to the manuscript: In the main text, on page 11, lines 217-220, we highlighted that our simulations provide a qualitative explanation:

"We conduct further finite element (FE) simulations to quantitatively predict the coiling actuator performance taking into consideration of the frictional interaction between the seed carriers and soil, and the potential anchoring effect (Methods)."

We added the unit for the scale bar in Fig. 3d: 0 - 0.1 (kPa).

On page 10, lines 201-202, we added the discussion of the scale bar in the caption of Fig. 3d:

"The color bar represents the contact pressure, which is larger than 0.1 kPa. The small upper bound helps visualize the contact regions."

On page 11, lines 223-226, we added the discussion about the contacts in Fig. 3d:

"The body of tail 2 and the tip of tail 3 of the three-tailed design anchor initially (left image in Fig. 3d), then both tips of tail 1 and 2 start anchoring on the ground (right image in Fig. 3d) to generate larger forces as the tails become more hydrated (Fig. 3c)."

Under Methods, on pages 28-29, lines 665-677, we added discussions on the modeling of the anchoring effect and comparisons between simulations and experiments of drilling on different types of surfaces:

"Our experiments show that the tails and seed tip can penetrate the soil surfaces to form anchoring points. To mimic tail anchoring, we set a higher coefficient of friction at a small region near the tail tip. The seed tip is not included in the simulation model, as it is challenging to connect the tip with a non-stress-free coiled body. We show that the effects of the tip anchoring can be partially explained by fixing the in-plane motion of one point of the coiled body, which closely reproduces the corresponding drilling processes in experiments (Fig. 3d-e) on coconut coir with a LSMV of 1.62 mm^2. We conducted further experiments and simulations of seed carrier drilling on a surface that was hard and smooth (Supplementary Note 9) and found a substantial rotation of the seed carriers, due to the low frictional force and lack of anchoring points (Extended Data Fig. 9). The three-tailed design rotated less than the single-tailed design, as it can establish contact not only at two tails but also at the seed tip, due to the initially inclined angle on the surface. This further validates that our simulations can capture the interaction between engineered seed carriers and different ground types, despite the simplification of the model."

The newly added Extended Data Figure 9 is:

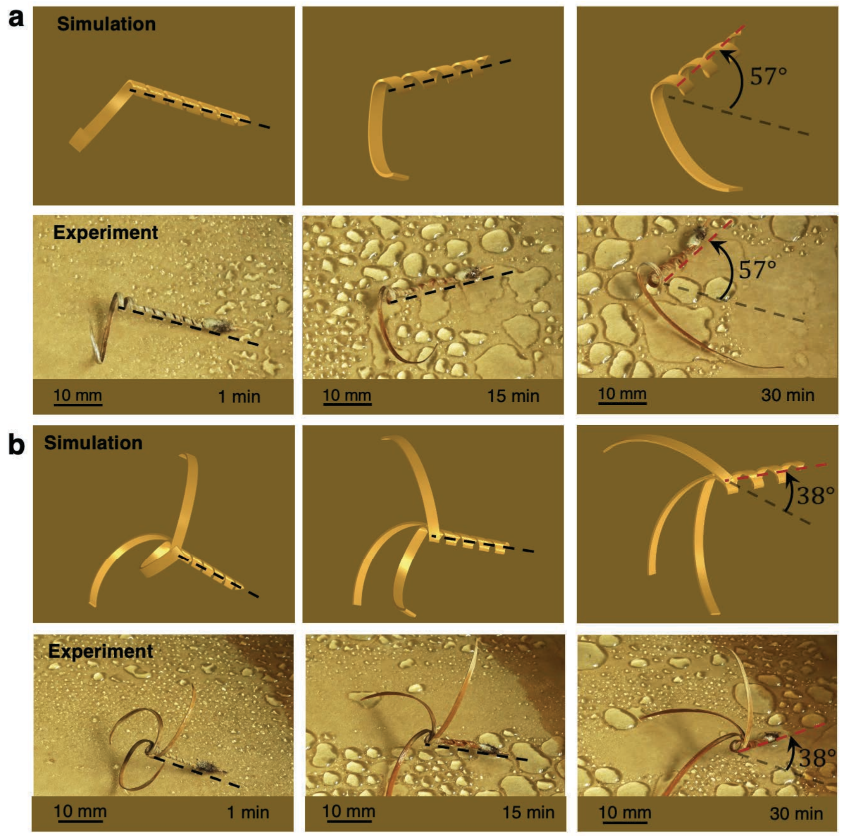

Added **Extended Data Figure 9. Experiments and simulations for seed carrier drilling on a surface that is hard and smooth. a**, Simulation (top) and experimental (bottom) snapshots of the drilling process of the single-tailed design seed carrier. **b**, Simulation (top) and experimental (bottom) snapshots of the drilling process of the three-tailed design seed carrier.

Comment #15: > A technical point should be clarified. As far as I understand, the hygroscopic strain is applied in the Lagrangian coordinates, and the seed changes its configuration as a consequence of the imposed strain and the external contact boundary conditions. Is it correct? Are the aforementioned conditions compatible with each other (in particular in Abaqus)? These details should appear in the supporting notes.

Our response: Yes, the reviewer correctly summarized our simulation process. One important point is that the configuration of the seed carriers is a direct geometrical mapping according to the imposed strain. The deformation simulated by ABAQUS contains two parts: one is associated with the imposed hygroscopic strain field and the other is associated with the degree of mechanical deformation. The imposed strain provides a driving force for the coiling. The non-uniform improved strain field further induces mechanical stress inside the wood strip at the coiling configuration and the deformation associated with the mechanical stress. These non-zero stresses indeed are determined by both the imposed strain and the contact boundary conditions.

Our modification to the manuscript: In Supplementary Note 7, on page 68, lines 1188-1193, we added discussions on the coil deformation under the prescribed hydration strain field.

"The non-uniform hydration strain field in Eq. (18) creates a driving force to deform the initially flat wood strip into helical configuration, to mimic the molding of the wood coils and the actuation of coils from the wet to the dry state. It is important to note that the helix configuration is not purely determined by the geometrical mapping from the hydration strain field. It is achieved through the balance between the stress associated with mechanical deformation and the hydration strain."

Comment #16: > The parameters involved in the numerical model were calibrated to match experimental results, yet this calibration seems to be poorly reported. Which are the experimental results considered for calibration? A clear report of what has been done seems to be needed, also because parameter fitting was not leading to a unique set of parameters, as reported in the current supporting note 3.

Our response: We thank the reviewer's suggestion that will enhance the quality of our manuscript. We now add more discussions on the calibration process in the Methods section and Supplementary Note. The original Supplementary Note 3 is Supplementary 8 in the revised manuscript as we include more supplementary materials.

Our modification to the manuscript: Under Method, On pages 27-28, lines 635-641, we added discussions about the model calibration:

"The wood strip starts from an initially flat state with its thickness, width and length matching the experimental sample. The hydration strain field is fitted with the coiling configuration (e.g., coil diameter and pitch) in the wet and dry states, respectively. The water transport is not directly modeled. Instead, we assigned an exponential time variation of the hydration strain with a characteristic time scale, fitted with the time variation of the measured forces in the experiments Fig. 3f. We further introduced a normalized hydration state to describe the transition of the coils from the dry to the wet state in Fig. 3b,c (Eq. 24 in Supplementary Note 9). The mechanical properties of the modeled material were obtained by fitting the thrust forces of the coils with different numbers, measured in the representative experiments (Supplementary Note 8). "

The detailed changes in the Supplementary notes 7 and 8 are listed as follows. On page 67, lines 1166-1173, we added descriptions of the simplification of the mechanical property calibration:

"As shown in Table S3, white oak has different anisotropic modulus ratios, along with the width and thickness directions, with an average value around 0.1. To simplify the material property calibration, we adopted this average value in our simulated model, such that $\frac{E_2}{E_1} = \frac{E_3}{E_1} = 0.1$. We further assumed that $\frac{G_{12}}{E_1} = \frac{G_{13}}{E_1} = \frac{G_{23}}{E_1} = 0.1$ and $v_{12} = v_{13} = v_{23} = 0.3$. After these simplifications, the only fitting material parameter is E_1, which will be extracted from the thrust force measurements of wood coils in Supplementary Note 8. Despite the limited parameter space of the material properties, our model can fit the experimentally measured thrust force by tunning Young's modulus, E_1."

On page 71, lines 1240-1256, we added a description of calibrating the effective hydration strain field parameters:

"We next outlined the calibration process of material properties. The flat wood sheet has a thickness (h) of 0.5 mm, and width (b) of 2.5 mm, according to our direct experimental measurement. The bending curvature in the dry state, κ_{coil}, was computed from Eq. (18) with $D^d_{\text{coil}} = 1.82\ mm$ and $P^d_{coil} = 2.00\ mm$ obtained from the experiments (Fig. S4a) and $\xi = 1$. By checking the thickness change of the wood strips from the wet to the dry state, we could obtain $\epsilon^0_{z'z'} = -0.20$. The density of the wood material was taken as $\rho = 1000\ \text{kg/m}^3$. Since the actuation is a slow process within the time scale of an hour, we do not expect that the kinetic energy, associated with density, will play a significant role in the coil deformation and force generation. We also included a small damping coefficient ($\alpha = 0.10$ for the mass proportional contribution to Rayleigh damping) to help the convergence of simulations. Following these analyses, we still needed to calibrate the following parameters, θ_l, Ψ_0, Ψ_1, $\epsilon^0_{x'x'}$, $\epsilon^0_{y'y'}$, E_1 and expected that the modulus, E_1 and the parameters associated with the hydration strain were only determined by the coil shape. Therefore, we first set a constant value of E_1 and conducted ABAQUS simulations to extract these parameters by comparing the simulations with experiments. During the simulation, we gradually increased the hydration state variable, ξ, from 0 to 1 to generate the dry coil. The coil in the wet state corresponded to the simulated coil at $\xi = \xi^w$. We found a set of parameters, namely, $\theta_l = 20°$, $\Psi_0 = 60°$, $\Psi_1 = 70°$, $\epsilon^0_{x'x'} = 0.10$, $\epsilon^0_{y'y'}$=-0.18, $\xi^w = 0.45$ from this calibration process."

On page 72, lines 1274-1281, we added a discussion about the calibration of the elastic modulus and the characteristic time scale associated with the water transport:

"The exponential decay was also observed in our experiments (Fig. 3f). Note that t_d depends on both the material properties and the environment conditions. We treated t_d as a fitting parameter to match the time variation of the measured forces in the experiments and found that $t_d = 1500\ s$ could result in a good agreement with the humidity chamber experiments. We tuned the modulus, E_1 , to match the force-time relationships of wood coils in our experiments and found $E_1 =$ 0.5 GPa provided a good prediction for all three coils of different lengths. Both simulations and experiments showed that the thrust forces decreased with coil length (Fig. 3f)."

In Supplementary note, we modified the caption of Table S6 (the original Table S3) to clearly state that the simulation parameters in the table are obtained from fitting a set of experiments, including the thrust force measurements and the seed carrier drilling. We also updated Table S6 to improve its readability. The new Table S6 is

Table S6. Mechanical properties and effective hydration parameters used in simulations of the coiled body thrust force calibration and the seed carrier drilling.

E_1(GPa)	E_2(GPa)	E_3(GPa)	v_{12}	v_{13}	v_{23}
0.5	0.05	0.05	0.3	0.3	0.3
G_{12} (GPa)	G_{13} (GPa)	G_{23} (GPa)	ρ (kg/m^3)	α	D^d_{coil} (mm)
0.05	0.05	0.05	10^3	0.1	1.82
P^d_{coil} (mm)	Ψ_0 (°)	Ψ_1 (°)	$\epsilon^0_{x'x'}$	$\epsilon^0_{y'y'}$	$\epsilon^0_{z'z'}$
2.0	60	70	0.1	-0.18	-0.2
ξ^w	θ_l (°)	$(\theta_l)_1$ (°)	$(\theta_l)_2$ (°)	$(\theta_l)_3$ (°)	t_d (s)
0.45	20	0	-5	-10	1500

Comment #17: > As regards frictional contact introduced to mimick anchoring: was it imposed on a couple of surfaces?

Our response: We considered two types of anchoring. One is the anchoring of the tail tips, and the other is the anchoring the seed tip. For the anchoring tail tip, yes, we assign a higher coefficient of friction of surfaces near the tail tip, highlighted in purple in Fig. S16. For anchoring of the seed tip, we adopted an indirect method to mimic it. This is because we do not explicitly include the seed tip in the modeling, which makes the simulation much more difficult. We constrain the in-plane motion of one point of the coil body to partially reproduce this anchoring effect.

Our modification to the manuscript:

We added more discussion on the modeling of the anchoring effect under method, on pages 28-29, lines 665-677. See response to **comment #14**.

We further expanded the caption of Fig. S16, on pages 76, lines 1350-1354 as:

"**Figure S16. Interaction between the coil system and ground.** The tail tip (purple) has a higher coefficient of friction than the body of tails (yellow) and the coil (yellow and greed) to mimic the anchoring of the tail tip. The coil end (green) is defined for computing the contact forces near the coil tip. The in-plane motion of point A (red) will be constrained for simulations with the anchoring seed tip. "

In Supplementary Note 9, on pages 77-78, lines 1384-1396, we added descriptions of the new experiments and simulations of the drilling on hard and smooth surfaces:

"To demonstrate the importance of the contact interaction between the seed carrier and the soil surface, we conducted experiments and simulations of drilling into a surface, which is hard and smooth. In the experiments, we placed both single-tailed and three-tailed carriers on top of an acrylic board and triggered the anchoring with one hydration circle for 30 min under the controlled drilling test condition described in Methods. The smooth surface and large Young's modulus led to a small coefficient of friction on the acrylic board. Furthermore, it was difficult for the tails and seed to penetrate the acrylic board to establish anchoring points. During the simulation, we found that a uniform friction coefficient of 0.4 for the interfaces between the seed carrier and ground can reproduce the seed carrier motion in experiments. Both experiments and simulations demonstrated a substantial rotation of the seed carriers, due to the low frictional force and lack of anchoring points (Extended Data Fig. 9). The three-tailed design rotated less than the single-tailed design, as it can establish contact not only at the two tails but also at the seed tip, thanks to the initially inclined angle on the surface."

The new Extended Data Figure 9 has been shown in response to an earlier **Comment #14**.

Comment #18: - The considered hygroscopic actuation leverages humidity transport to synergistically modulate strain and stiffness in plant tissue. Although a complete modeling treatment is still very challenging (both for stable implementation in numerical solvers and model calibration), some works dealing with hygroscopically actuated bilayers appear in literature, which include modeling contributions bridging humidity transport and derived strain. See, e.g., (Krüger et al., Biomimetics, 6(4), 58, 2021, [doi.org/10.3390/biomimetics6040058]; Lunni et al., Advanced Materials Interfaces, 7(4), 1901310, 2020, [DOI: 10.1002/admi.201901310]). In light of previously published contributions, the ms should also discuss the importance to further enrich the proposed modeling approach by also embarking the real actuation driver, i.e., water transport, to further advance the design of the devised aerial seeds

Our response: We agree with the reviewer's comments on the modeling of water transport and we thank the reviewer for sharing the important references. The reviewer offered a precise summary of the modeling challenges of this very complicated system. We have cited the literature [R1, R2], and highlighted the challenges we face for future studies. In addition, we would like to mention that the water transport process in field tests and applications is also highly sensitive to environmental conditions (e.g., moisture, temperature, rain), leading to non-linear relationships with time, in contrast to the well-controlled conditions in the lab. This also motivates us to avoid the direct modeling of water transport in our current work.

Our modification to the manuscript: Under Methods, page 29, lines 685-689, we added discussions about the future improvement of the model by including water transport:

"Furthermore, water transport inside the wood strips has been shown to play a critical role in determining the dynamic morphing process of hygroscopically actuated structures[54,55]. This will require integration of the current pure mechanical model in a proper kinetic model for moisture permeation in the wood in the future, to better capture real seed carrier actuation driven by water transport."

Ref. 54. Krüger, Friederike, Rebecca Thierer, Yasaman Tahouni, Renate Sachse, Dylan Wood, Achim Menges, Manfred Bischoff, and Jürgen Rühe. "Development of a material design space for

4D-printed bio-inspired hygroscopically actuated bilayer structures with unequal effective layer widths." *Biomimetics* 6, no. 4 (2021): 58.

Ref. 55 Lunni, D., Cianchetti, M., Filippeschi, C., Sinibaldi, E. & Mazzolai, B. Plant-inspired soft bistable structures based on hygroscopic electrospun nanofibers. Adv. Mater. Interfaces 7, 1901310 (2020).

Comment #19: - Experimental data seems to miss relevant details on repetitions and statistical variations (e.g., though std and error bars). At least 3 repetitions should be reported for each experimental data (better 6). All data should be reported as mean value ± standard deviation.

Our response: we have gone through all the experimental data presented in both the main and extended data figures, either adding information regarding statistical variations (mean value ± standard deviation), or clarifying why the data was plotted in a certain way. We have made our data available at https://doi.org/10.5281/zenodo.6555503.

Our modification to the manuscript:

For Fig 2e, g, and h: Due to the inherent heterogeneity of wood and unavoidable inconsistencies due to the manual laser cutting selection and molding process, the maximum bending curvature and actuation range vary across samples. As shown in Fig. 2e, even though the samples were prepared initially with relatively consistent thicknesses of 0.4 ± 0.0 mm, 0.5 ± 0.0 mm, and 0.7 ± 0.0 mm (N = 3), they show variations in both the thickness and wet-released curvature after chemical washing and molding. In addition, the thickness appears in the normalized x-axis for master curves in Fig. 2g and h, which makes the data analysis sensitive to the real sample thickness. As a result, instead of averaging samples of the same initial thickness, we chose to plot individual samples separately.

In the revised figures, we conducted a few more experiments to make sure that each set of experiments (e.g., fixed mold diameter and targeted wood strip thickness) has 3 different samples. All the experimental data collapse onto the two master curves shown in the updated Fig. 3g and h, providing a direct comparison between the experiments and theoretical prediction:

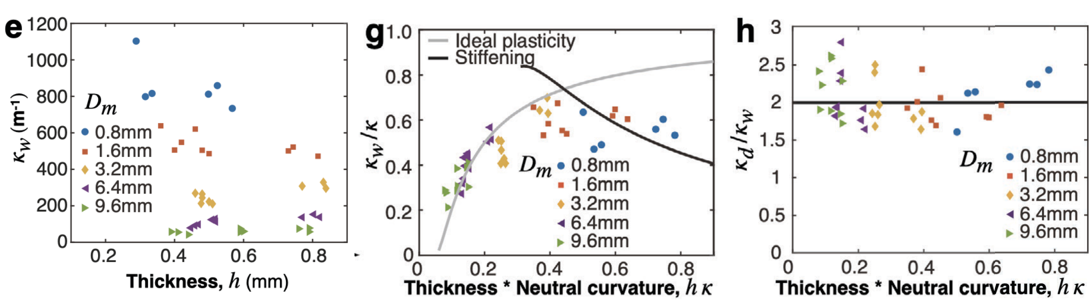

In the caption of Fig. 2, we added: "For (**e-h**), each test group contains three samples with an initial thickness of 0.4 ± 0.0 mm, 0.5 ± 0.0 mm and 0.7 ± 0.0 mm, respectively."

In Fig. 2i, we re-plotted a single triggering cycle with 3 repetitions with SD:

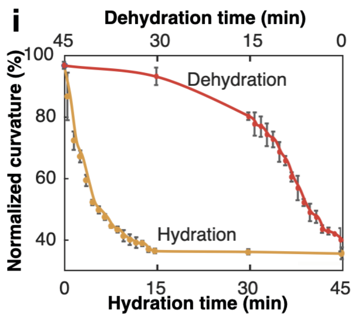

Updated **Figure 2. i**, Curvature changes of bending samples. Data are means $\pm$ SD. $N = 3$ triggering cycles.

In Fig. 2j, three repetitions of each data point with SD were plotted:

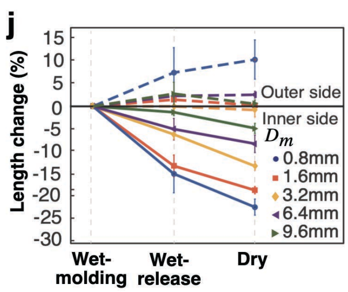

Updated **Figure 2. j,** Comparison of length changes of the inner and outer side of the wood strips, molded with mandrels of varying diameters. Data are means $\pm$ SD. $N = 3$ samples.

In Fig. 3a, to decrease the statistical variations, we tripled the number of samples for the controlled drilling tests, including 15 three-tailed seeds and 15 natural Erodium seeds in 5 continuous hydration and dehydration cycles. The conclusion remains the same: for relatively flat soil surface, the drilling success of the engineered three-tailed seeds is higher than the natural *Erodium* seed:

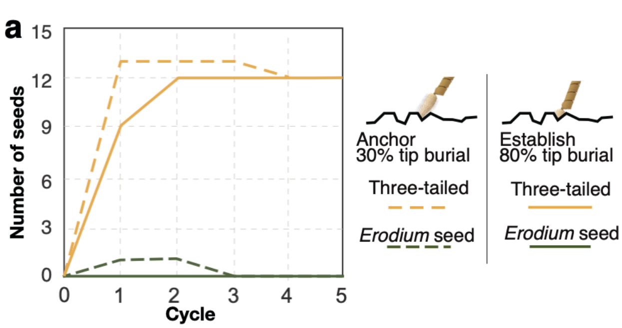

Updated **Figure 3. a,** Comparison of drilling success between the three-tailed and *Erodium* seeds on flat soil in five cycles (Methods). N =15 of each type.

In Fig. 3f, in the figure caption, on pages 10-11, lines 202-206, we added: "Comparison of peak extension force of coiling actuators with different coiling numbers. The solid lines are representative curves from the experimental results of three repetitions of each coiling number".

Since wood materials exhibit strong structural heterogeneities, averaging multiple samples of the same coiling number does not give us much insight. Instead, we added a new plot in Extended Data Figure 4 to show that even though the force-time relation is different among three 7-coiled samples, the amplitude of the thrust force is relatively constant across samples:

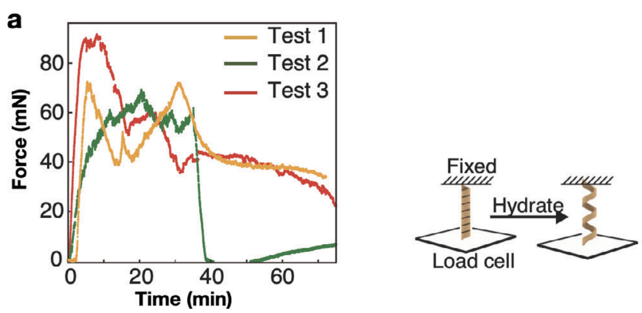

Updated **Extended Data Fig. 4. a**, Thrust force variations shown in three samples consisting of seven coils during one hydration-dehydration cycle. The detailed time variation of the forces is different; the amplitude of the thrust force is relatively constant across three samples.

For Fig. 3g, we replotted the rotational speed per coil and angle change per coil versus time, with SD:

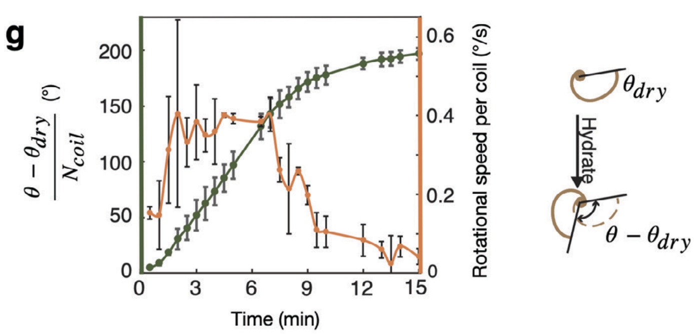

Updated **Figure 3. g,** Rotational range and speed of coiling actuators. Data are means $\pm$ SD. $N = 2$ samples consisting of 3.5 coils, 7 coils and 10.5 coils, respectively.

For the Extended Data Fig. 8b: we replotted three samples of each chemical washing duration (5 min, 10 min, 20 min respectively) to compare their curvature recovery:

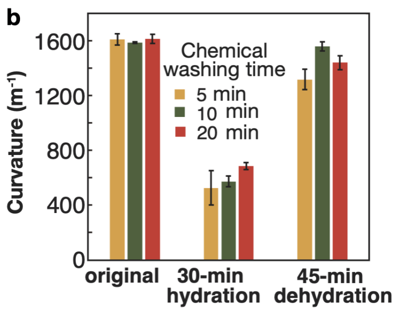

Updated **Extended Data Figure 8**. **d**, Effect of the chemical washing durations on the curvature changes. For both (**a**) and (**b**), data are means ± SD. $N = 3$ with a thickness of ~0.5 mm, length of ~3 mm and width of ~3 mm, molded with a mandrel, with a 0.8 mm diameter.

Comment #20: Nematodes release is of interest, yet poorly discussed. Additional details, including.e.g, some figures (over time) or supplementary movie should be added.

Our response: we have captured videos of living nematodes and added a supplementary video of them. In Methods, we explained our examination of nematode growth in more detail.

Our modification to the manuscript:

We added Supplementary Video S8. Living nematodes captured in the soil after nine days of seed burial. On page 13, line 265, we cited the Supplementary Video 8.

In Methods "Indoor germination and incubation", on page 22, line 524, we added: "We sampled soil 5 cm away from the seed every day with a light microscope, until we observed the nematode on the ninth day, as shown in Fig. 4d."

Comment #21: Double layer seeds are reported, besides single layer ones (and no surprise that the former are stronger than the latter). Fabrication variability should be nonetheless discussed

Our response: The double layer is molded by wrapping the second layer on top of the dried first layer. More details were added as Extended Data Figure 5 which describes the manufacturing process. In addition, we extended our Method to integrate this detail as well.

Our modification to the manuscript: In the newly added Supplementary Note 2: Fabrication Details, on page 51, line 937, we added "Once the first layer was molded, the coil was clamped and dried at room temperature for 12 hours. The second layer was then wrapped around the first layer and clamped to dry below room temperature for another 12 hours (Extended Data Fig. 5x)."

We also modified Extended Data Figure 5, to add additional steps needed when the double-coiled seed carrier is fabricated.

x

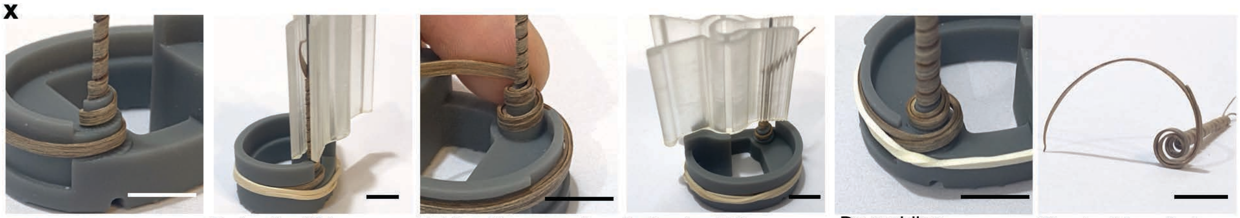

Added **Extended Data Figure 5. x**, The process of molding a double-coiled body. Scale bar is 10 mm unless otherwise specified.

Comment #22: Fiber angle variation through thickness was presented as the key physical element to couple bending and coiling. How was it possible to successfully obtain coiling in the prototyped artificial seeds without checking/imposing the correct direction of fiber angle gradient before coiling the initial wood strip in the mechanical molding fabrication step? This should be definitely clarified.

Our response: To clarify, the 'fiber angle variation through thickness' was induced by our molding process. Before molding, although the microfibril angle (MFA) can vary within trees and cells [R1], the average MFA of white oak is relatively uniform, ~ 10° across the thickness (as seen in Extended Data Fig.1b), which is consistent with the literature [R2]. The large difference in MFA was induced by molding. A more detailed discussion can be found in our responses to **Comment #24**.

To obtain a relatively consistent MFA gradient during the manual molding process, we optimized our processing pipeline in two ways. First, to ensure a relatively uniform fiber direction before coiling, we manually inspected the flat-sawn wood panels and selectively laser-cut strips along with the fiber in the longitudinal direction (see updated Extended Data Fig. 5a, g). Second, during the molding process, we use a customized mold to guide the helical steps with a pre-defined coiling angle to facilitate the starting point of the manual coiling process, which is further elaborated in **#Comment 25**. However, due to the inherent heterogeneity of wood in its MFAs, cellular sizes, and fiber orientations, and the unavoidable inconsistencies from the manual laser cutting selection and molding process, the maximum bending curvature and actuation range vary among samples. We have quantified the curvature variations in Fig. 2e (for the bending actuators) and Fig. 3g (for the coiling actuators). We discussed this point further in Methods.

[R1] Barnett, J. R. & Bonham, V. A. Cellulose microfibril angle in the cell wall of wood fibres. Biological Reviews 79, 461–472 (2004).

[R2] Jäger, A., Bader, Th., Hofstetter, K. & Eberhardsteiner, J. The relation between indentation modulus, microfibril angle, and elastic properties of wood cell walls. Composites Part A: Applied Science and Manufacturing 42, 677–685 (2011).

Our modification to the manuscript:

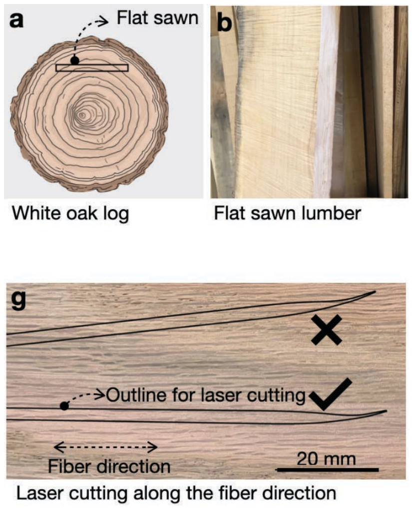

Updated **Extended Data Figure 5. a**, The process of turning a white oak log into a wood veneer with a specified thickness and fiber orientation. **g**, The process of laser cutting, chemical washing and manual molding of the wood strips.

On page 9, line 172, we added "By contrast, in the case of chemically washed yet unmolded wood veneers, the MFA is relatively uniform and small ($9 \pm 2°$, Extended Data Fig. 1b) across the thickness, indicating that the increased μ_{inner} can be attributed to the stress induced microfibril disorientation[41] during the molding and drying process."

We also shared more information in the newly added Supplementary Note 2: Fabrication Details

- On page 49, line 894, we added: "To ensure a relatively uniform fiber direction, we laser cut the strip along the wood fiber direction (see Extended Data Fig. 5g)."
- On 50, line 908-919, we added: "To achieve a fixed initial coiling angle, we customized a mold integrating guiding helical steps, with a pre-determined coiling angle, to facilitate the starting point of the manual coiling process (Fig. S1a)."(Newly added Supplementary Fig. 1 is discussed in **Comment #25**.)

In Methods "Bending curvature measurement" on page 21, line 480, we added: "Due to the inherent heterogeneity of wood and the unavoidable inconsistencies induced by the manual laser cutting selection and molding process, the curvature varied. In the case of samples that were prepared from the wood veneers with relatively consistent thicknesses of 0.5 ± 0.0 mm (N =3), we measured the maximum bending curvature as 1854.5 ± 96.9 m^{-1} and the actuation range as 1533.4 ± 56.1 m^{-1} to 596.8 ± 14.2 m^{-1}."

Comment #23: Title could be improved so as to better reflect the proposed material. "Self-drilling" seems to be misleading, since the seed is not drilling itself. "Superior" is not very clear. Maybe, a more descriptive title could be "Autonomous Self-burying Seed Carriers for Aerial Seeding".

Our modification to the manuscript: We thank the reviewer for the nice suggestion! We have changed the title to "Autonomous Self-burying Seed Carriers for Aerial Seeding".

Comment #24: The SEM measurements of the fibrillar angles are quite at poor magnification, from the images it is not clear the arrangement of the fibrils. A SEM imaging at higher resolution could help. Furthermore, authors should perform measurements on several samples and report the results with the error bars.

Our response: Following the referee's suggestion, we conducted new SEM imaging with a higher resolution to better show the fibrillar angles. In total, we imaged three bending samples and three straight samples. For each bending sample, we selected six cells to image, and for each straight sample, we imaged three cells. We added a Supplementary Note 3 to describe the SEM sample preparations and cell selections for imaging, as well as reported the changes in MFA and cellular morphology.

Our modification to the manuscript:

We have updated a set of SEM images for **Fig. 2**: k-l:

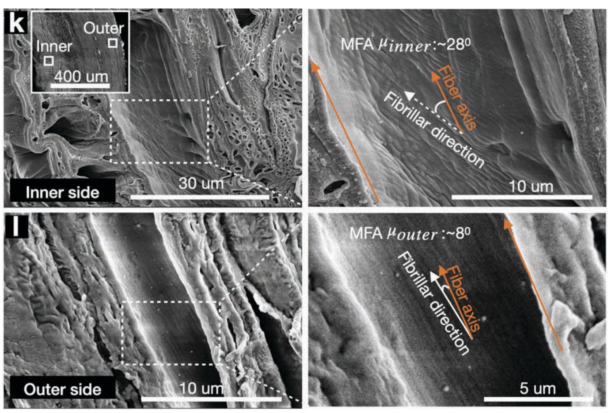

Fig. 2: **k-l**, A set of representative SEM images of the wood strip after molding and drying: the deformed cells towards the inner side tend to have larger microfibril angles (MFAs) than the cells towards the outer side with relatively smooth cell walls.

We have updated Extended Data Figure 1:

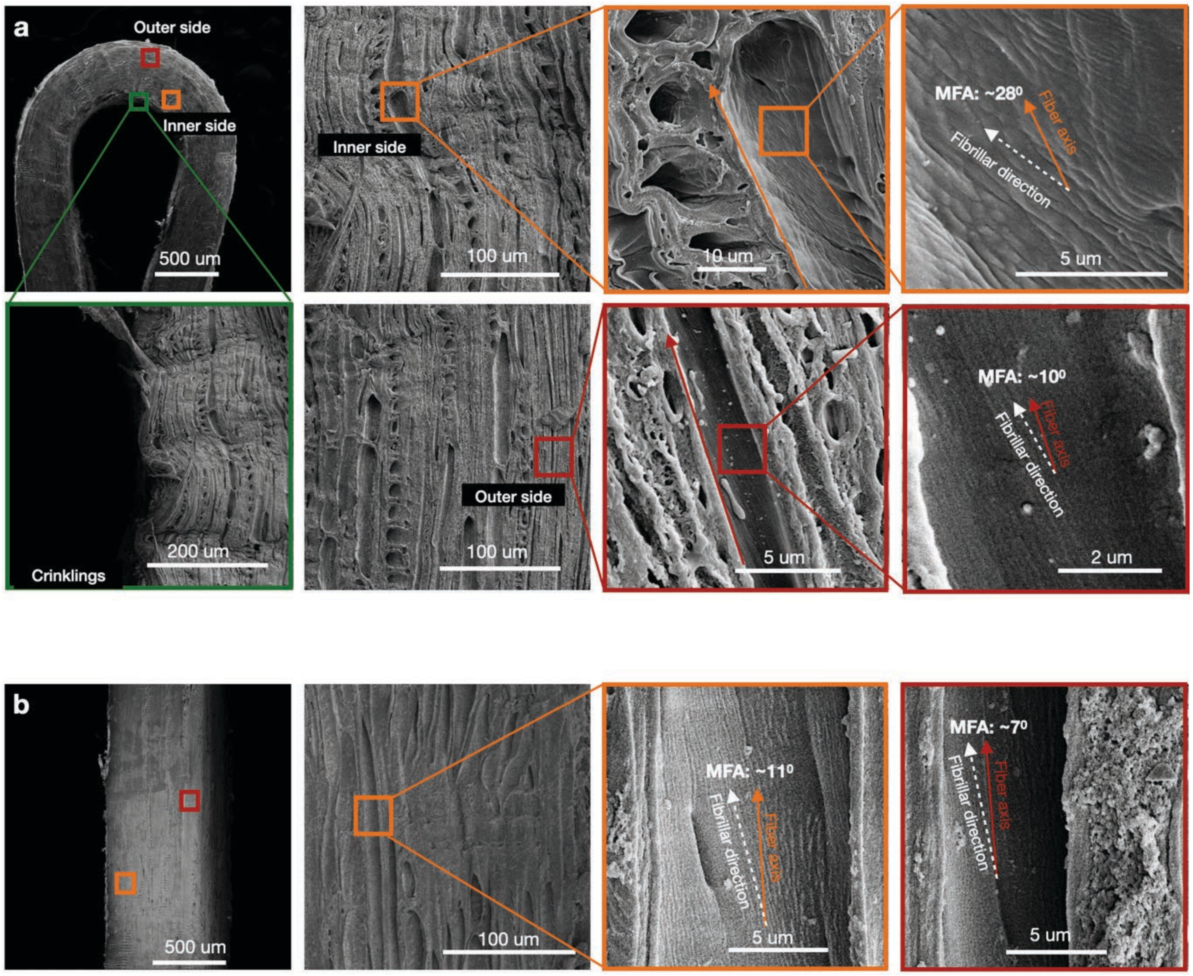

Extended Data Figure 1: SEM images of partially delignified wood veneer. a, Chemically washed and molded wood veneer (0.5 mm thick, 0.8 mm mandrel diameter). Wrinkled cell walls are caused by mechanical molding on the longitudinal cells on the inner side. The outer side cells show no obvious signs of deformation. **b**, The chemically washed but not molded wood veneer, showing uniform cell structure throughout the sample.

We also added **Supplementary Note 3: SEM Measurements of Cellular Structures in the Bending Samples**

"We carried out SEM to image the cellular structures in bending samples, which are ~0.8 mm thick and have a 1.6 mm molding diameter. We first imaged the sample at a relatively low magnification (500 x) to identify the target cells for imaging their fibrils. We looked for cells at the relative middle section of the arc (- 60°- 60° range as shown in Fig. S2a) with open cell walls and exposed S2 layers. We needed to identify three target cells on both the inner and the outer sides (see Fig. S2b). Ideally, the target cells should have equal distance to the neutral axis since the distance may contribute to different levels of compression or tension thus affecting the MFAs. However, in practice, it was almost impossible to find such target cells. Due to our laser-cutting approach for sample preparation, only a portion of cells could be cut in halves to expose the inner walls. Therefore, we looked for target cells that fell within the highlighted regions (h/4 - h/2 away from the neutral axis on both sides, as shown in Fig. S2a).

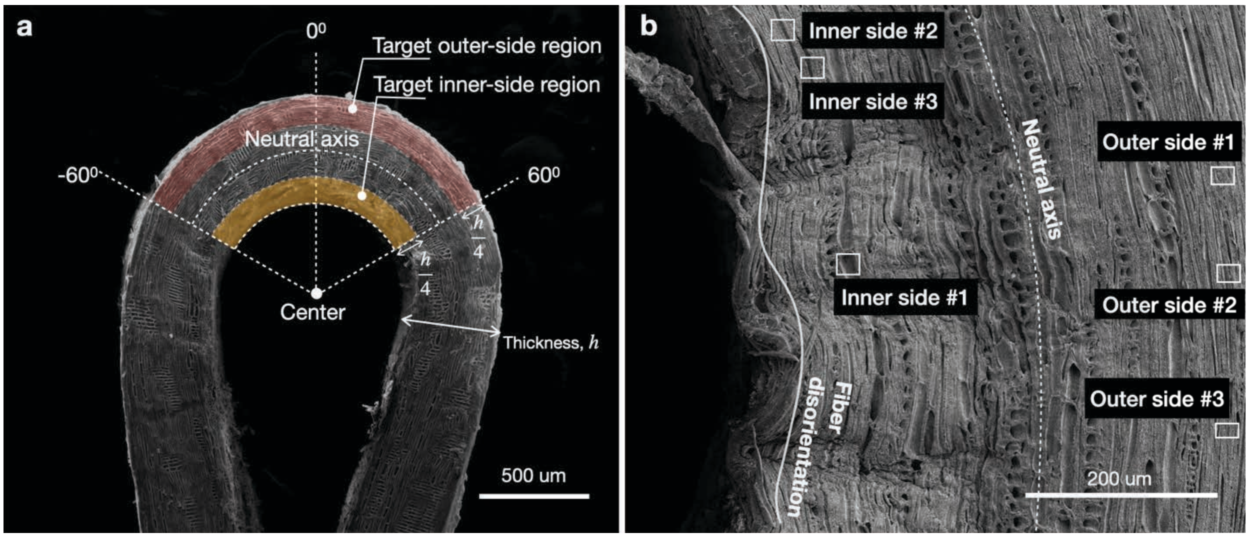

Figure S2. a, Methods to identify the target outer and inner sides of a bending actuator, annotated on top of the scanning electron microscopy (SEM) image of a bending actuator sample in a relatively low magnification (500 x). **b,** Sampling three cells from the target inner-side region and three from the target outer-side region.

We then imaged the MFA of the target cells. In total, we imaged three bending samples, and a set of images from a single sample is shown in Figures S3 and S4. SEM images show that the cells on the outer side (Fig. S3) have relatively straight microfibrils, with relatively consistent and small MFAs ($9 \pm 2°$, $N = 3\, cells \times 3\, samples$), which are similar to the MFAs ($9 \pm 2°$, $N = 3\, cells \times 3\, samples$) in the flat samples before molding.

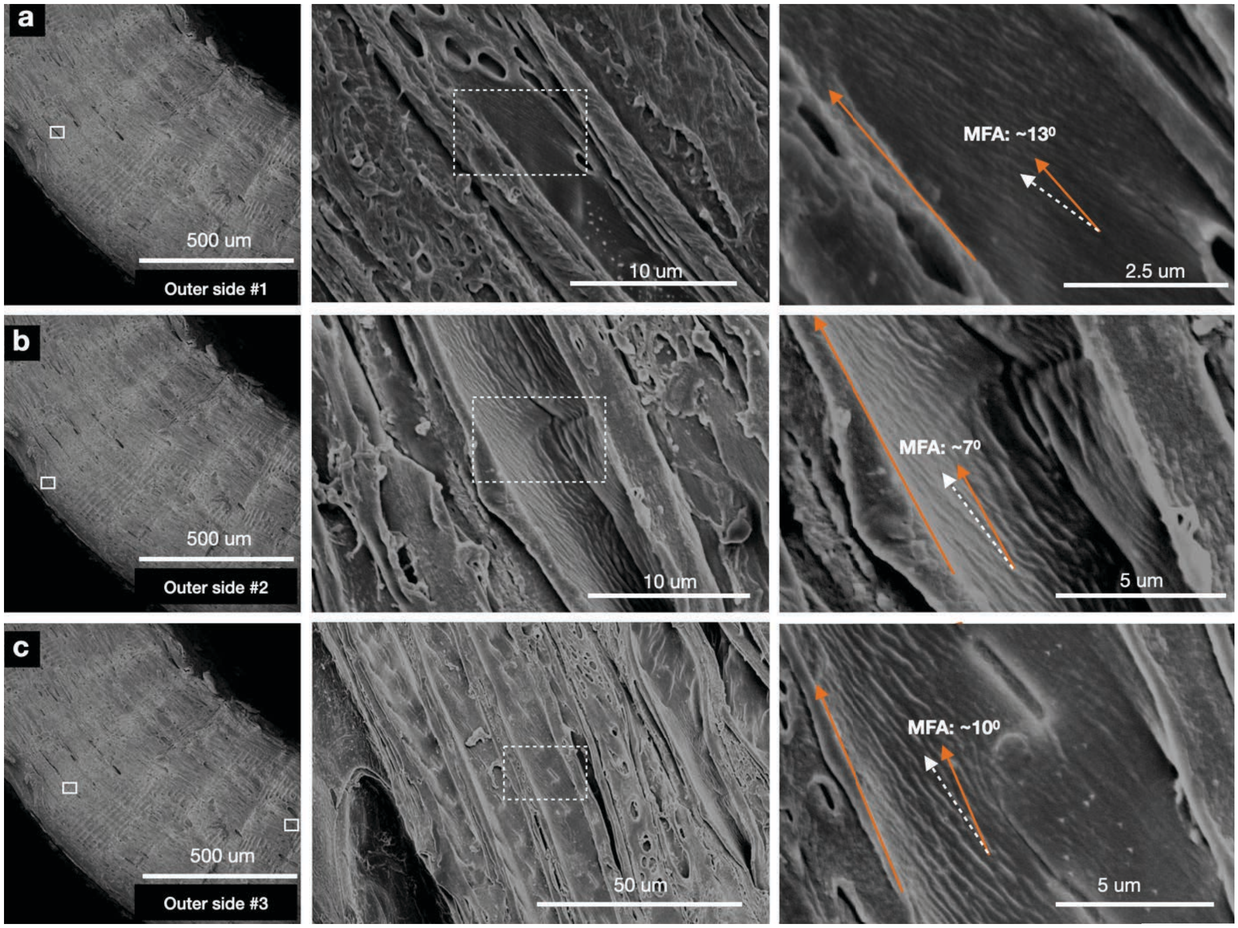

Figure S3. SEM images of cells from the outer side. The microfibrils are relatively straight, and the microfibril angles (MFAs) are relatively small ($9 \pm 2°$, $N = 3\, cells \times 3\, samples$) and consistent.

In contrast, the deformed cells towards the inner side under compression (Fig. S4) have disoriented microfibrils. In the case of the disoriented microfibrils identified in our SEM images, we observed a general increase in MFA ($23 \pm 7°$, $N = 3\, cells \times 3\, samples$). Previously, a distinct disorientation of the usually relatively straight microfibrils as a result of longitudinal compression was reported[41], and our observation of the deformed cells from the inner side was consistent with the literature.

Note that while certain cells show obvious microfibril disorientation and crinklings (Fig. S4a), cells that are relatively straight and non-deformed (with an MFA of ~11° that is comparable to the outer side) also exist on the inner side (Fig. S4b). In the case of some cells, crinklings and fibril disorientation only appear to exist within local regions (Fig. S4c). The non-uniform deformation of the cellular structures is likely to be due to the structural heterogeneities of the wood.

Our hypothesis is that the MFA change exhibits a gradient across the thickness, which is induced by the strain gradient. Although we were able to identify obvious increases in MFAs in a portion of cells towards the inner side but not the outer side, compared to the unmolded samples, it was challenging to quantify the gradient of MFA changes across the thickness. This is due to the cell wall collapsing towards the compression side and the laser cutting approach, therefore, we did not have a large number of cells with exposed S2 layers at different distances away from the neutral axis to quantify the error bars. A systematic study of the cellular network change under mechanical loading and moisture environment changes is needed to more accurately predict the curvature formation and the actuation of the molded wood in future studies.

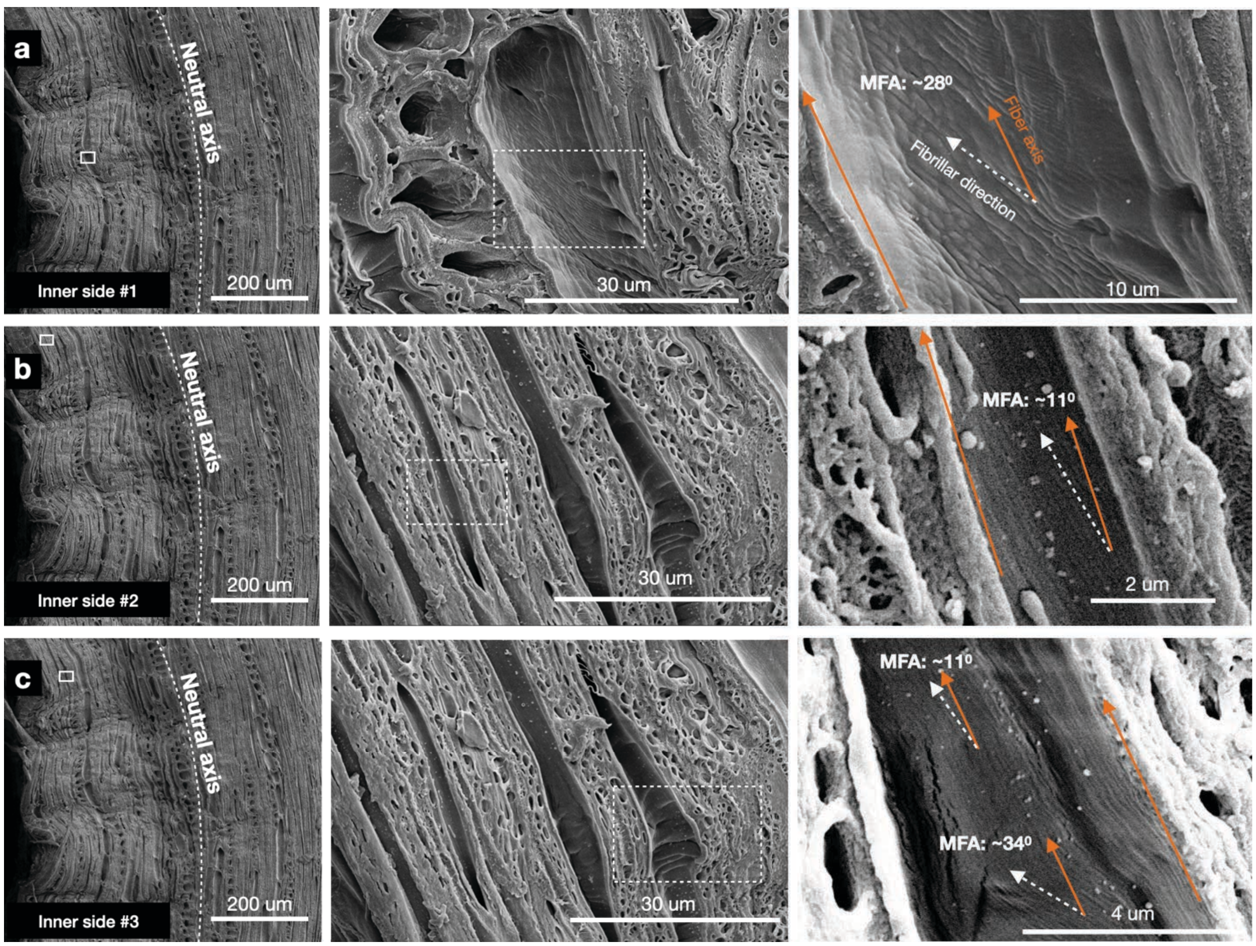

Figure S4. SEM images of cells from the inner side. Certain microfibrils are disoriented with an increased MFA (~28° - ~34°).

Ref. 41. Báder, M., Németh, R. & Konnerth, J. Micromechanical properties of longitudinally compressed wood. Eur. J. Wood Prod. 77, 341–351 (2019).

Comment #25: In the manufacturing process it is clear that the wet molding procedure relies on the operator skills (made by hand). It is quite evident that the radius can be fabricated with high reproducibility, given a fixed cylindrical mold diameter, instead the pitch could change during the wet molding. Authors could provide a comment and an evaluation on the variability of the pitch.

Our response: we added an additional figure and expanded the Methods to explain our design and processing strategy to minimize the pitch variation.

Our modification to the manuscript:

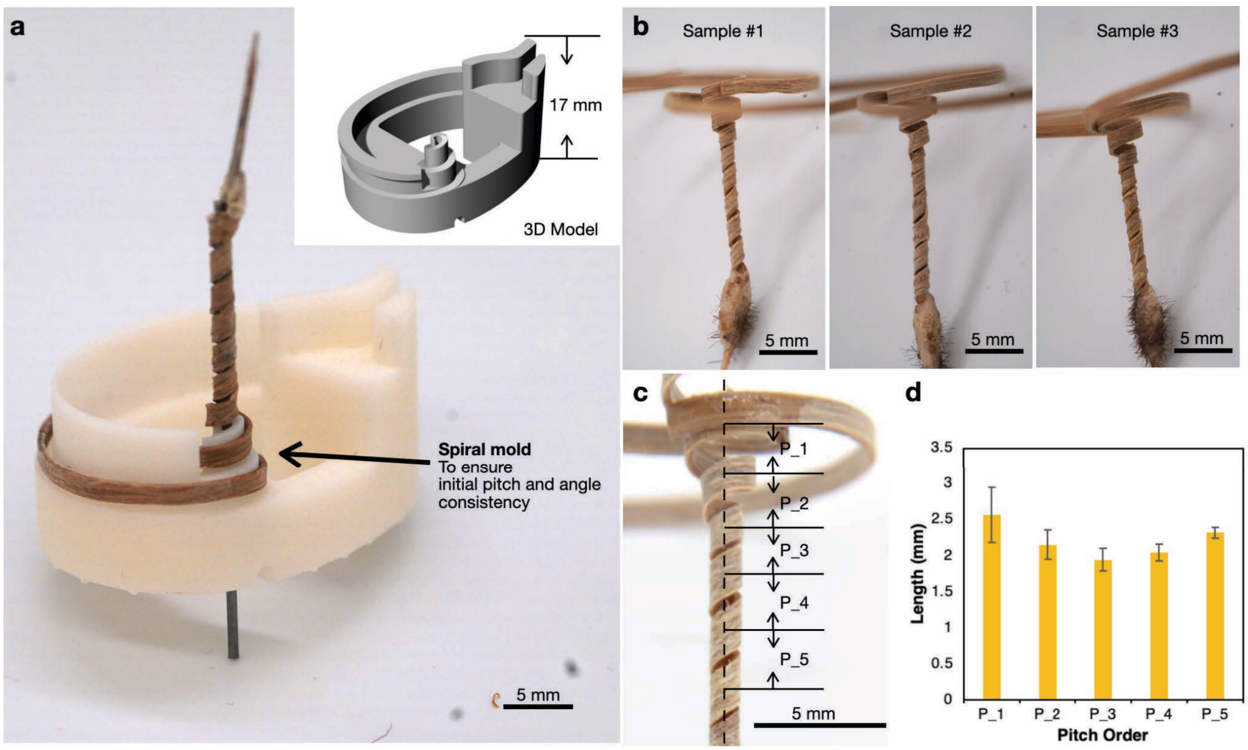

Added **Figure S1. Spiral mold design and measurements of pitch variations in coiled bodies. a**, The customized spiral mold to control the initial pitch angle consistency. **b,** Three samples show variations in pitch. **c-d**, Comparison of five pitches across the three samples shown in (**b**). Data are means ± SD.

On page 49, line 906, we added:

"The coil pitch is predominantly determined by three factors: the initial coiling angle, the variability caused by the manual coiling process, and the varied tightening performance during the released and drying step. To achieve a fixed initial coiling angle, we customized a mold integrating guiding helical steps, with a pre-determined coiling angle, to facilitate the starting point of the manual coiling process (Fig. S1a). During the coiling process, we ensured that the edge of the strip was always tightly connected without gaps or overlaps in between. In addition, due to the differences in cellular structures from different wood strips, the total shrinkage ratio between the released (Extended Data Fig. 5m) and drying (Extended Data Fig. 5n) stages may vary, which could also result in variability in the pitch. We measured the first five pitches of the coiled body

(N = 3) and observed that while the first two pitches had relatively large standard deviations, which was likely to be due to boundary effects; the third to the fifth pitches were reasonably consistent (Fig. S1b-d). ”

Comment #26: A few typos are around (including the whole sentence in supporting note 1, which appears between Eq.(9a) and Eq.(9b)). Further proofreading is recommended.

Our modification to the manuscript: On page 62, line 1097, between Eq.(9a) and Eq.(9b), we deleted the sentence as it is duplicated with the sentence in line 1099. We have done another round of thorough proofreading.

Comment #27: Extended Data Figure 7: some pictures have very low quality. Please, replace them with better quality pictures.

Our modification to the manuscript: we have replaced the low-resolution pictures with higher resolution ones in Extended Data Figure 7.

Referee #2 (Remarks to the Author):

Comment #28: The authors report the design and fabrication of seed carriers made of wood veneer, which can self-drill into the soil, inspired by Erodium seeds. The key advantages of their seed carriers are argued to be a higher drilling success rate than Erodium seeds thanks to three-tailed structure, and a wider range of payloads. The authors also provide some theoretical accounts on curvature change and actuation of their actuators. Although the veneer-based self-drilling actuators look intriguing, this work does not appear to present significant scientific/technological advances for the following reasons.

(1) The most serious question raised after reading this manuscript is the value (necessity, meaning or advantage) of making self-drilling actuators inspired by Erodium or other similar kinds of plant species using plant-based materials (veneer in this case). It is well known that plant-based materials are hygroscopic, and their applications for soft actuation have been reported. Artificial materials, including hygroscopic polymers, have also been explored for hygroscopic actuation. Fascinated by the amazing motility of some seeds capable of self-burial, many previous works have analyzed the mechanics behind the shape-morphing and actuation of both the natural and artificial coiling actuators. Many of those previous works have been cited by the authors, although there have been few attempts to replicate the self-drilling ability of Erodium and other plant species.

Our response: We agree that there is literature reporting the hygromorphic behaviors of both natural and engineered systems, which inspired the studies here. We compared several major hygromorphic materials (Fig. 1f and Supplementary Table 2), and chose wood over other engineered materials because it is one of the most abundant and environmentally friendly structural materials (suitable for the aerial seeding contexts). Importantly, wood offers superior mechanical strength (E ~10 GPa), and processibility at large scales (from centimeter to meter)[15,16] in comparison with other biodegradable water-responsive materials such as spider silk[28], bacterial spores[29], engineered silk film[30], pollen paper[31] and naturally derived hydrogels[32–35]. Coming with the high strength, however, is the small initial curvature (< 10 m^{-1}) and a limited range of curvature changes (< 30 m^{-1})[15–18]. Large initial curvature and curvature change upon exposure to water is critical to the performance of the hygroscopic actuators. Therefore, one of our major scientific contributions is to tackle this challenge:

- Through the combined processing optimization, geometrical factor, and material choice, we uncovered design principles that allow us to turn wood veneer into highly stiff (7.2 GPa when dry, and 1.2 GPa when wet) but hygromorphic bending or coiling actuators with an extremely large bending curvature (1854 m^{-1}), 45 times larger than that of reported wood-based bending actuators[15-18]. See more detailed elaboration in our response to **Comment #38**.
- Comparing the experiments with theoretical analysis and finite element simulations, we elucidate the curvature transformation and actuation mechanisms. The new insights to design and optimize the seed carriers as well as other moisture-sensitive actuators will offer broader societal benefits in the contexts of agriculture, environmental conservation, energy harvesting[46], biodegradable hygromorphic robotics[47] and sustainable responsive architecture[17].

As the referee pointed out, "there have been few attempts to replicate the self-drilling ability." The few attempts that do exist typically focus on creating a direct replica of the natural systems and do not show significant improvements in the drilling performance nor demonstrate the actuators are effective seed carriers. As we mentioned in the Introduction, page 4 and lines 63-66, the existing *Erodium* replica is limited in its drilling rate (0 - 20% establishment rate after the first cycle), limited to soil types with artificial crevices, and requires long chemical washing time (7 h). Therefore, there is a significant gap that could be filled by clever design and engineering for self-burying systems with superior drilling performance. To our knowledge, ours is the first design solution that is shown to outperform to the natural *Erodium* seed:

- We offer a bio-inspired design strategy for a self-burying seed carrier system enabled by wood based actuators with large curvatures. It can be geometrically configured for various target payloads, environmental and terrain conditions. The engineered system can take advantage of different natural species (e.g., the active extension of the tail to lift the body up for drilling in *Erodium* and the three-tailed configuration for beneficial initial angle in *Aristida*).
- The engineered seed carriers with the three-tailed design are superior to a majority of natural seeds with self-burying behaviors in the following ways:
    - Our carrier has an 80% drilling success rate on relatively flat land (perlite soil with a $\log_{10}$ soil microtopographical variance of 0.78 mm^2) after two triggering cycles, partially due to the three active motile awns that provide both the beneficial resting

angle (25° - 30°) and effective torques collectively generated by two tails simultaneously (Fig. 3c-d), whereas the success rate of many natural seeds with motile awns (including *Erodium*, *Aristida*, and *Stipa* species) is nearly 0% in our test detailed in ***Comment #29***.

  - The deployment of the seed carriers with a drone from 5 to 6 m above agricultural land shows a 90% success rate by starting at a beneficial resting angle, whereas the resting angle of *Erodium* and *Stipa* under the same dropping conditions is zero.
  - The five rounds of outdoor self-drilling tests with a total of 136 three-tailed seed carriers in two geographical locations showed an anchor rate of ~66% and establishing rate of ~39%.

Comment #29: The actuators made by the authors indeed seem capable of self-drilling with a very high success rate. However, if we ever want to attach self-propelling tails to seeds we want to disperse over land, why do we not just use seed awns of Erodium or other similar kinds of plant species?

- There are many seeds with motile awns (providing the ability of self-dispersal and self-burial), e.g. black oat grass (Stipa avenacea), wiregrass (Aristida tuberculosa), wheat (Triticum sp.), mouse barley (Hordeum murinum), Erodium and Pelargonium species. Many of them can be easily purchased over the internet.

- The size range is very wide - let alone small seeds of Erodium and Pelargonium species (a few mm long), large awns of Stipa species seeds are as long as 25 cm - so that a wide range of payloads can be covered.

- The authors attribute the high success rate of anchoring or establishing to the three-tailed structure of their actuators. Aristida has three awns (please see figure 1 of Cerros-Tlatilpa et al. Am. J. Botany 98, 1868-1886, 2011), so it is doubtful whether the authors' design is creative.

Our response: we really appreciate that the referee has pointed out many more natural seeds that have motile awns, which was also covered comprehensively by Evangelista, et al. [R1] and Cavanagh, et al. [R2]. We cited [R1, R2] and acknowledged the diverse natural species of various sizes and three-awn designs in the introduction. We emphasize that our main concept and contribution here is to customize the design and fabricate the highly efficient seed carriers inspired by *Erodium* seeds, which are well-studied in literature in terms of their microstructures and the actuation/seeding mechanisms. Therefore, they offer a good example for us to compare against, thus, filling the knowledge gap and performance gap. We have no doubt there are many other examples of natural seeds that may work better than *Erodium* seeds or even better than ours under the conditions they have been optimized for. We do note that natural seeds work in specific habitats [R2, R3]. The seeds with special geometric designs may work best in one specific habitat but not the others. Our intention is not to claim that ours is the best among natural or engineering seed carriers, but rather to present a geometric design strategy inspired by one such natural carrier, *Erodium* seeds, based on wood veneers. By taking advantage of the unique hierarchical structures of wood veneers and their high mechanical strength and moldability under chemical treatment, as well as their hygroscopic nature, the engineered seed carriers could outperform the natural ones.

Intrigued by the species recommended by the referee and mentioned in [R1, R2, R4, R5], we conducted a three-cycle drilling test with five additional species available to us: *Stipa comata*, *Stipa spartea*, *Aristida purpurea*, *Pelargonium reniforme*, *Erodium castellanum* (sample size N = 5 of each species), under the same drilling testing condition as reported in Methods. No successful self-burial was observed during the three triggering cycles except one *Erodium castellanum* established itself and two *Aristida purpurea* seed tips fell into gaps in the granules when dropped. We have learned two important lessons:

- Since biology is often very selective, if we were to leverage biological organisms for aerial seeding, we first need to understand how they work. Then we can propose where and how to use them. There is no guarantee that a chosen type will work for any habitat or that a natural species can be successfully identified for all potential target payloads and soil conditions.

- By observing how different natural species work and how awn morphology and other geometrical factors affect the self-burial, we can design artificial versions to overcome the potential limitations of each individual species and strategically tailor our designs to target payloads and conditions. The interesting coincidence of our three-tailed design with the three-tailed *Aristida* [R5] further validates our design, which can combine different lessons and strengths of natural species, e.g., the design of the three-tail shown in *Aristida purpurea*, the responsive tail that can uncoil and lift up the body in *Erodium guinum*, and the large coiling numbers and elongated body length to increase the rotational speed in *Stipa spartea*.

We have added a supplementary note to share detailed experimental results and reflections.

[R1] Evangelista, D., Hotton, S. & Dumais, J. The mechanics of explosive dispersal and self-burial in the seeds of the filaree, Erodium cicutarium (Geraniaceae). *Journal of Experimental Biology* **214**, 521–529 (2011).

[R2] Cavanagh, A. M., Morgan, J. W. & Godfree, R. C. Awn morphology influences dispersal, microsite selection and burial of australian native grass diaspores. *Front. Ecol. Evol.* **8**, 581967 (2020).

[R3] Garnier, L. K. M. & Dajoz, I. Evolutionary significance of awn length variation in a clonal grass of fire-prone savannas. *Ecology* **82**, 1720–1733 (2001).

[R4] Ghermandi, L. The effort of the awn on the burial and germination of Stipa speciosa (Poaceae). *Acta Oecologica* **16**, 719–728 (1995).

[R5] Cerros-Tlatilpa, R., Columbus, J. T. & Barker, N. P. Phylogenetic relationships of 'Aristida' and relatives (Poaceae, Aristidoideae) based on noncoding chloroplast ('trnL-F, Rpl16') and nuclear (ITS) DNA sequences. American Journal of Botany 98, 1868–1886 (2011).

Our modification to the manuscript:

We modified our Introduction to include more seed types with motile awns:

- On page 4, line 52, we replaced "Erodium" with "Hygroscopic seeds of various natural grass species".
- On page 4, line 55, we added "However, the seed morphology is often evolved to tailor specific natural habitat[22] and other physical constraints, with little flexibility for customization. There is no guarantee that a chosen type will work for the target habitat and payloads. The hygroscopic seeds of *Erodium*, *Stipa* and *Aristida* achieved almost zero anchoring on relatively flat terrain after three triggering cycles in a controlled test (Supplementary Video 1 and Note 1). Additionally, many hygroscopic grass seeds have lightweight seedpods (e.g., ~8 to ~20 mg in Supplementary Table 1), thus limiting the potential to carry heavier payloads such as the ~72 mg whitebark pine seeds, which are important for reforestation[4,23].".
- On page 4, line 66, we added: "Clearly, there is a significant gap that provides us with an opportunity to design and engineer self-burying systems."

We updated Fig. 1d to include more natural seeds to show morphological variations side by side with our engineered systems.

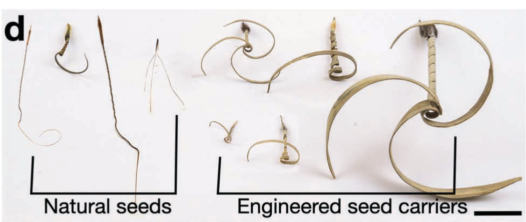

Figure 1. d, Engineered and natural seed carriers of different sizes and geometries. More details in Supplementary Table 4. Scale bar: 20 mm.

On page 5, line 79, we added: "The engineering solution we offer here learns from nature, yet provides flexibility for tailoring (Fig. 1d), according to the specific terrains and payloads including different seeds, symbiotic species, and beneficial nematodes."

We added a new **Supplementary Note 1: Additional Drilling Tests of Grass Seeds with Hygroscopic Awns**

"Comprehensive drilling tests have been performed in the past on different types of grass seeds with hygroscopic awns[19,22]. However, various studies have different testing methods and conditions, depending on the goals of the study. To directly compare an extended body of seeds with motile awns beyond *Erodium* with our engineered seed carriers under the same testing conditions of ours, we carried out additional drilling tests with additional natural species ($N = 5$ of each species, for three triggering cycles), as summarized in Table S1. The testing procedure and conditions were consistent with "Drilling tests under controlled conditions" in Methods.

Table S1: Summary of selective self-burial grass seeds and engineered seed carriers. Data are means ± SD, $N = 3$.

Types	Awn Morphology		Body wet Length (mm)	Seedpod Length (mm)	Seedpod Maximum Diameter (mm)	Seedpod dry Weight (mg)
Stipa comata	• Single awn with one sharp bend and one curve • Twisted body	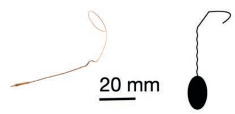	142.6 ± 18.5	11.3 ± 3.1	1.0 ± 0.0	7.9 ± 0.3
Stipa spartea	• Single awn with two sharp bends • Twisted body	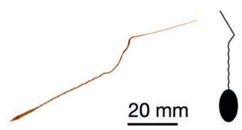	117.7 ± 6.7	18.3 ± 1.0	1.3 ± 0.1	13.0 ± 0.5
Aristida purpurea	• Triple awns with three sharp bends • Straight body	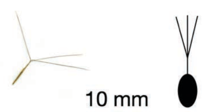	34.9 ± 4.7	8.2 ± 1.8	0.4 ± 0.1	0.9 ± 0.2
Pelargonium reniforme	• Single awn with one curve • Coiled body	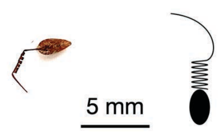	11.5 ± 1.4	4.2 ± 0.3	1.1 ± 0.2	20.3 ± 1.5
Erodium guinum	• Single awn with one curve • Coiled body	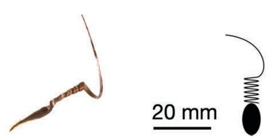	90.4 ± 0.9	15.1 ± 0.6	2.4 ± 0.3	28.3 ± 9.5
Erodium castellanum	• Single awn with one curve • Coiled body	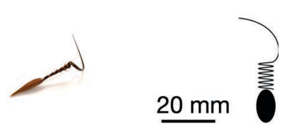	48.2 ± 1.0	9.6 ± 0.2	1.9 ± 0.1	12.3 ± 3.1
Medium-sized Engineered	• Triple awn with three curves • Coiled body		135.3	13.5	3.1 ± 0.3	52.0 ± 10.5
Double-coiled Engineered	• Single awn with one curve • Double-coiled body	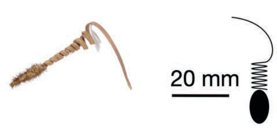	135.3	13.5	3.1 0.3	52.0 ± 10.5

Large-sized Engineered	• Triple awn with three curves • Coiled body	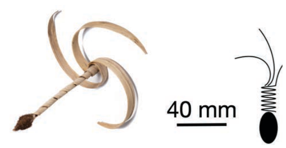	302.7	20.8	9.0 ± 0.5	75.3 ± 0.6

During the seed dropping phase from 35 cm above the soil, the three-tailed and lightweight (~0.1 mg) *Aristida purpurea* has a ~40% chance to anchor its tip into the gaps of the granules. After three triggering cycles, we did not observe any additional successful anchoring except for one *Erodium castellanum*. The originally anchored tips of *Aristida purpurea* did not show further burial either. Our explanation for the low drilling success is that the natural soil conditions, where these grasses survive, are quite different from ours. As shown in the literature[19], after comparing 30 grass species and 10 awn morphological types, the authors concluded that the awn morphology and types have different functional roles in the dispersal and burial stage, and are highly customized to different environmental conditions. Since biology is often very selective, if we were to leverage biological organisms for aerial seeding, we would first need to understand how they work. Then we can propose where and how to use them. There is no guarantee that a chosen type will work for any habitat or that a natural species can be successfully identified for all potential target payloads and soil conditions.

On the other hand, during our controlled drilling test, we observed certain advantages relating to natural motile awns that aligned with our design principles. The body of *Stipa comata* contains many twists (~20), which results in highly effective axial rotation. However, due to its rather short and single tail, it did not form an effective angle between the body and the ground to initiate drilling on relatively flat soil. In contrast, due to the three-tailed arrangement, the body of the *Aristida purpurea* can form an effective (non-zero) angle with the ground. However, unlike the tail of *Erodium* that anchors its tip and uncoils to lift the body upwards for an advantageous drilling pose during the hydration process, the tails of *Aristida purpurea* unbend and lay the body flat when hydrated.

By understanding how different natural species work and how awn morphology and other geometrical factors affect self-burial, we can design artificial versions to overcome the potential limitations of each individual species and strategically tailor our designs to target payloads and conditions. By taking advantage of the unique structure and function of wood veneers, we offer a new engineering solution that allows for accurate control of the morphology and mechanical properties, and thus self-drilling behaviors of the seed carriers. The interesting coincidence of our three-tailed design with the three-tailed *Aristida* further validates our design, which can combine different lessons and strengths of natural species, e.g., the three-tailed design shown in *Aristida purpurea*, the bent responsive tail that can expand and lift up the body in *Erodium guinum* and the large coiling numbers and elongated body length to increase the rotational speed in *Stipa spartea*.

Comment #30: As seen in Fig. 1f of the manuscript, the elastic modulus of existing seed awns is not inferior to that of the veneer used in this work.

Our response: the *Erodium* seed awn indeed has an impressively large elastic modulus (~ 9 GPa), comparable to some hardest wood species as listed in our Supplementary Table 1). The wood veneer we fabricated has an elastic modulus of ~7.2 GPa. In literature and as shown in Fig. 1f, most of the hygromorphic actuators reported had a much lower modulus, ranging from 2 MPa to 2.5 GPa.

Comment #31: To fabricate self-drilling actuators with veneer, the authors used multi-step processes including sawing, cutting, chemical washing, rinsing, drying and moulding. Considering the cost, time, energy and amount of carbon produced to make each actuator, it is questionable whether this kind of work is environmentally friendly and economically viable.

Our response: First, we agree with the referee that since this paper did not conduct any systematic life cycle and cost analysis of manufacturing processes, we should tone down our claim that this manufacturing process is environmentally friendly and economically viable. The focus of this paper is to demonstrate how to rationally design and analyze the seed carriers from wood with a proof-of-concept manufacturing process in the lab. We agree that for scaling up and potentially translating the design into products, optimization of the manufacturing process and life cycle analysis will be needed, which is not the intention of this manuscript. We noted the manufacturing potential of a similar wood sawing and chemical washing method (a common aqueous-based delignification process) has been thoroughly studied in terms of its environmental impact[39], including the life cycle assessment of the wood logging, sawing and drying, the upstream production of NaOH and Na_2SO_3 used in the chemical washing, as well as the water and energy consumption analysis[39]. We cited this work when discussing the future work.

Ref. 39. Xiao, S. et al. Lightweight, strong, moldable wood via cell wall engineering as a sustainable structural material. Science 374, 465–471 (2021).

Our modification to the manuscript:

In Conclusion, we removed “low-cost’ and “scalable”.

On page 15, line 308, we added “For the purpose of scaling up, a further optimization of the manufacturing process and life cycle analysis[39] will be needed.”

Comment #32: (2) A significant portion of the main text describes and explains the curvature change of a bent piece of treated veneer. Although this is an important starting point to understand the shape-morphing of coiled actuators, the actual deformation of the actuator involves the change of pitch as well as curvature of the helix, which leads to coiling and uncoiling. Although numerical simulations with many simplified assumptions and fitting parameters for coiled actuation are presented in Supplementary Note, focusing on the mere curvature of the bent piece in the main text can mislead readers to think that this work has analyzed the shape-morphing with enough depth. The authors need to present theoretical analysis for the pitch and curvature of the helix with drying or to refine their numerical simulations to correlate the internal structure (including MFA) and mechanical properties with coiling deformations.

Our response: we agree with the reviewer that it is important to directly connect the mechanical performances of the coiling actuators and their microstructures. However, the models become very complicated when considering the nonlinear and coupled plastic behaviors and strain-dependent shrinkage induced by moisture change in 3D coils. The multiscale modeling of the effect of MFA is also challenging. Because of the complex design of the three-tailed structures and highly nonlinear interactions between the seed carriers and soils, the drilling process is also very difficult to model and simulate. We note the mechanical behaviors of coiling actuators are generally determined by coiling stiffness and coiling configuration change, including the coiling elongation and rotation (Eq. 1 in Main Text). This motivates us to choose a phenomenological model capable of capturing the configuration change and the associated thrust forces of wood coils during hydration and dehydration cycles. We added one paragraph to better describe the motivation of the current model choice and another paragraph to discuss the model limitations and future improvements.

We have also clarified that our current theoretical analysis of the curvatures focuses on the bending actuators. In addition, we include more discussion to better describe how we calibrate the simulation parameters from experiments.

Our modification to the manuscript: Under Methods, on pages 27-28, lines 634-643, we added one paragraph to discuss the motivation for choosing a simplified model for coiling and drilling:

"The fabrication and actuation of coiling actuators are more complicated to model than the bending actuators, although they share the same fundamental mechanism. The difficulties stem from the nonlinear and coupled plastic behaviors and strain-dependent shrinkage induced by moisture change in 3D coils. On the other hand, the mechanical behaviors of coiling actuators are generally determined by coiling stiffness and coiling configuration change, including the coiling elongation and rotation (Eq. 1 in Main Text). This motivates us to choose a phenomenological model capable of capturing the configuration change and the associated thrust forces of wood coils during hydration and dehydration cycles. A simpler more is also preferred to achieve our goal of simulating the drilling performance of the seed carriers, which requires modeling of the complex structural design and highly nonlinear interactions between the seed carriers and soils. "

On page 29, lines 678-685, we added a discussion about the model limitations and future studies:

"The model is relatively simple and has its own limitations. Nevertheless, it is sufficient for our current analysis, as shown by the agreements between modeling prediction and experimental measurements. More theoretical studies are needed to establish the relationship between the change of pitch and curvature of the coiling actuators and the structures, and the mechanical properties of wood strips. It is also desirable to incorporate the microstructures (e.g., cellular networks and MFA) and their nonlinear interactions into the numerical simulation framework of the coiling and drilling process, to enhance the predictivity of the model for a variety of material systems."

Comment #33: (3) Below equation (5) in Methods, they mentioned that they ignored the modulus reduction effect, which needs to be justified (for other mechanical models in this work, too).

Our response: as seen in the response to **Comment #32**, we choose the simplified model to focus on the key mechanism. Despite being simple, the model was found to agree with experimental results well. This also motivates us to keep this simple model in the current work. To clarify this, we added more discussion on the choice of the simplified models in the current work.

Our modification to the manuscript: Under Methods, on page 25, lines 574-579, we elaborated more on the rationale of adopting a simple model for the analysis:

"Note that we neglect the modulus reduction and irreversible deformation near the outer layer, due to local fiber damage, so as to develop a minimum model to explain the curvature formation after the molding of the wood veneers in the experiments. The current model only requires two fitting parameters, ϵ_{Y_1} and ϵ_{Y_2}, which can capture the nonlinear and non-monotonic bending curvatures in experiments (Fig. 2g). The simplicity and efficiency of the model can serve the purpose of uncovering the key physics governing the bending deformation of the wood veneers."

On pages 27-28, lines 634-643, we add one paragraph to discuss the motivation for choosing a simplified model for coiling and drilling. See response to **comment #32**.

Referee #3 (Remarks to the Author):

Comment #34: This manuscript reports development of seed vehicles inspired by self-drilling plant seeds. They used wood – biodegradable and ecosystem-safe material – to create the hygromorphic machines, achieving 45 times more deformation capacity than previously reported. The new technology is employed to develop sustainable solutions for plant/fungus/nutrients dispersal in soil and vegetation restoration. The work is comprehensive, spanning from material processing to design exploration and functional tests in laboratory and field conditions. Generally, it is done with thoughtfulness and attention to detail and documented and explained clearly in this manuscript.

Our response: We thank the referee for these positive comments.

Comment #35: Major points:

1. The elephant in the room question I had while reading this manuscript is: "This is a very nice and interesting work, but does it have broad significance expected for publications in Nature?".

The wide-reaching significance of this work, I think, lies in being able to make a dynamic water-activated morphing with wood, which has diverse applications. The authors mention this but only one sentence at the beginning and end of the report. Can you elaborate by expanding in the discussion?

Our response:

We thank the reviewer for their appreciation of the contribution to making dynamic water-activated morphing with wood. We have expanded our discussion on potential diverse applications. Based on the reviewer's suggestion, we have made revisions as follows:

Our modification to the manuscript:

To highlight the broad scientific merit, in Conclusion on page 14, line 290-292, we added:

"We uncover the design principle that turns wood veneer into highly stiff (~7.2 GPa) and biodegradable hygromorphic bending or coiling actuators with an extremely large bending curvature (1854 m^{-1})."

To expand our discussion on potential diverse applications, in Conclusion on page 15, line 297-304, we added:

"The design principle along with customized molding can be utilized to create wood-based hygromorphic actuators with versatile shapes and functions, including coiling, bending, linear or radial contraction, twisting and folding for board applications, including sustainable robotics, as well as adaptive structures and environmental monitoring under climate changes. For example, hygromorphic actuators have been used to engineer evaporation-driven engines[45], self-flipping sheets for energy harvesting[46], and self-crawling robots due to the moisture gradient[47] and environmental sensing[24]. Biomass such as wood, offers an alternative to synthetic materials for the engineered hygromorphic actuators with superior performance."

Ref. 46. Chen, X. *et al.* Scaling up nanoscale water-driven energy conversion into evaporation-driven engines and generators. *Nat Commun* **6**, 7346 (2015).

Ref. 47. Shrestha, M., Lu, Z. & Lau, G.-K. High humidity sensing by 'hygromorphic' dielectric elastomer actuator. Sensors and Actuators B: Chemical 329, 129268 (2021).

Comment #36: Throughout the history of materials development, wood and new modifications to enhance its performance (e.g., bent wood, plywood) unlocked whole new ranges of innovations and manufacturing capability. Do you think this could do the same?

Our response:

The reviewer precisely pointed out the importance of developing new modification processes to better use the wood-based materials. We agree that depending on the potential applications, a new range of innovations and manufacturing capabilities can be demonstrated through the modification of various types of wood materials, enabling the advanced performance of hygromorphic actuation. Here, we only showed one possibility by optimizing the manufacturing process based-on wood veneers for self-drilling purposes. In the updated Conclusion, we added more application implications.

Our modification to the manuscript:

We have added the following discussion to the Conclusion on page 15, lines 305-309:

"Furthermore, combining our method with other wood processing methods including lamination[15], impregnation[48] and densification[37] may generate multi-functional wood structures (e.g., programmable response rate, increased energy density and multi-stimuli responsiveness) and new scientific insights as well."

Ref. 48. Wen, M.-Y., Kang, C.-W. & Park, H.-J. Impregnation and mechanical properties of three softwoods treated with a new fire retardant chemical. *J Wood Sci* **60**, 367–375 (2014).

Comment #37: 2. More starting materials? A specific starting material (white oak) was chosen for the best spec – but the observations made may only be relevant for the specific material. Have you tried other types of wood?

Our response: While our goal is to choose an effective wood type (white oak) for proof-of-concept demonstration rather than exhausting all potential wood species, we have investigated a handful of different wood veneers at the beginning, with the goal of balancing stiffness and moldability. To maximize the thrust force, we prefer stiffer wood. However, to produce tight coils, we need the wood to be readily moldable after chemical washing to remove lignin. We also need to choose wood that has relatively uniform fiber alignment so we could cut a strip with a high aspect ratio along the fiber direction and optimize its bending stiffness and integrity during the molding process (some wood can be easily torn apart between fibers).

Our modification to the manuscript: In Methods, on page 19, we add a section "Choices of Wood Types", to provide more analysis behind more types of wood as starting materials:

"To identify a suitable wood type as an actuator, we needed to consider the balance between stiffness and moldability. To maximize the thrust force, we preferred stiffer wood. However, to produce tight coils, we needed the wood to be readily moldable after chemical wash in the wet state. We also needed to choose wood that has a uniform fiber alignment, so we could laser cut a strip with a high aspect ratio along the fiber direction, to optimize its bending stiffness and integrity during the molding process (certain types of wood can easily be torn apart between fibers).

We identified six types of wood that have relatively well-aligned fibers to evaluate their moldability and actuation range. We were not able to mold yellowwood and bamboo into bending samples successfully. White oak has the largest initial dry curvature and actuation range among the four wood types that were successfully molded (Extended Data Fig. 8a). Using the same coiling mold, we tried to mold the seed carrier. Consistent with the bending actuator test, bamboo and yellowwood fractured during the molding process, while the others did not show visible fractures (Extended Data Fig. 8b). Since different types of wood may behave differently under various chemical washing conditions (e.g., chemical mixing ratio and washing duration), further quantitative experiments need to be conducted to optimize the chemical treatment, if we intend to carry out a successful molding process with a wood type other than white oak."

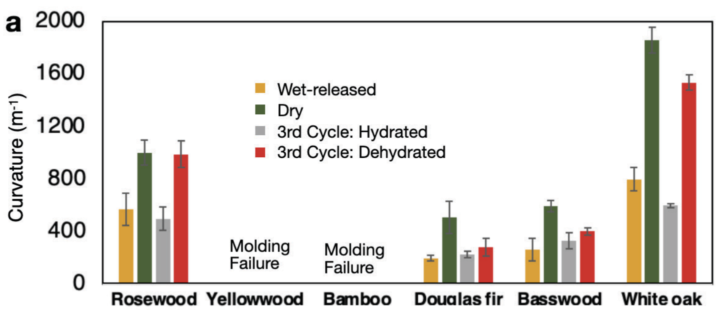

Added **Extended Data Figure 8. a**, Comparison of the moldability and actuation range of bending actuators made of different types of wood. The wood strip is ~0.5 mm thick and the molding diameter is 0.8 mm. Data are means ± SD. N = 3 samples for each type of wood.

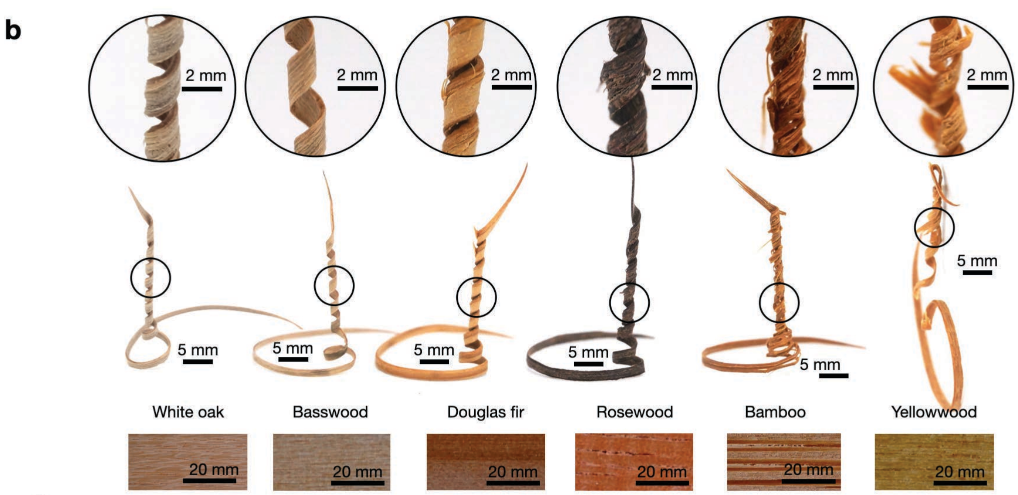

Added **Extended Data Figure 8. b,** Comparison of the moldability of the seed body made of various types of wood. The wood strip is ~0.5 mm thick.

Comment #38: 3. What was the key driver of your innovation? How could you achieve the 45 times better bending curvature? This is critical information and could be articulated with more highlighting. I read that it was because of the chemical treatment – is it the case? If so, please elaborate the development of the method further. Did you try different ways to make to complaisant while maintaining the strength? Why did you choose this method?

Our response: The processing method, the geometrical factor of the sample, and our material choice together drive a large bending curvature (~1854 m^{-1}). First, two critical steps in the five-step process contribute to the large bending curvature: the chemical washing step (as the referee pointed out) and the distinctive wet-release and drying method. As mentioned in the paper and shown in Fig. 2c and d, we achieve a further tightening of the molded structure during the final drying process. A small thickness of the wood strip is also crucial to create a large bending curvature, the limit of which is not only determined by the manufacturing methods but also the required thrust force. Among the three thickness options tested in Extended Data Fig. 8e, we chose 0.5 mm because it reached our desired bending curvature while maintaining a sufficient modulus (7.2 GPa). In addition, choosing an effective wood type (white oak in our case) is critical. As shown in our response to **Comment #36**, some wood types that have well-aligned fibers and relatively large Young's Modulus (at ~10 GPa range) cannot be molded into large curvatures successfully.

In terms of the development of the chemical treatment, we followed a common aqueous-based delignification process reported in literature followed by wood densification through compression[36] and molding[39]. To tailor to white oak and our unique constraints in terms of its mechanical properties, water response speed, and large curvature moldability, we had to optimize the washing time. The optimization process is shared in Methods, on page 20, line 447, under 'Optimization of the chemical washing parameters'.

Ref. 39. Xiao, S. et al. Lightweight, strong, moldable wood via cell wall engineering as a sustainable structural material. Science 374, 465–471 (2021).

Ref. 36. Song, J. et al. Processing bulk natural wood into a high-performance structural material. Nature 554, 224–228 (2018).

Comment #39: 4. Making artificial replica is effective in gaining insights into the why behind biological design. (And such cross-disciplinary impacts could enhance the broader relevance of this work.) You have found the natural form turned out to not so functional (cannot drill as efficiently as three tailed engineered design). Can you discuss why the natural selection has settled on the not so effective form? Do you find double/triple tailed seeds in nature?

Our response:

Our understanding is that nature is highly selective and it settles on an optimized form that adapts to its own environment and other physical constraints. As literature reported, *Erodium* has a high drilling success rate in soil that is relatively rough with crevices, which are critical for the *Erodium* tail to anchor and the body to establish an effective drilling angle with the ground[10]. In addition, *Erodium* seed morphology has evolved towards multiple goals beyond self-burial. For example, it is known that the tail morphology affects the drag which is a critical factor in *Erodium*'s explosive dispersal behavior before landing[14]. In our engineered system, since we leverage machines (i.e. drones) for delivery, we chose to prioritize morphological design to only one goal - self-burial.

Interestingly, in response to **Comment #29**, we further tested five additional species that have motile awns including needle and thread grass (*Stipa comata*), porcupine grass (*Stipa spartea*), and purple three awn – *Aristida purpurea*, under our lab test condition with little success. *Aristida purpurea* has triple tails. It confirms the selectivity of natural systems to a specific habitat and our engineering design has the flexibility to tailor the structure according to different conditions.

Ref. 14. Evangelista, D., Hotton, S. & Dumais, J. The mechanics of explosive dispersal and self-burial in the seeds of the filaree, Erodium cicutarium (Geraniaceae). *Journal of Experimental Biology* **214**, 521–529 (2011).

Ref. 10. Stamp, N. E. Self-burial behaviour of Erodium cicutarium seeds. J. Ecol. 72, 611–620 (1984).

Comment #40: Minor points:

5. Why scalable? The molding procedure and assembly sound quite complex, and it does not sound so scalable.

Our response: We have toned down the claim of scalability by removing "scalable" and "low cost" from the Conclusion, and pointed out that further optimization, life cycle and cost evaluation need to be conducted for scaling. While the manufacturing potential of a similar wood sawing and chemical washing method (a common aqueous-based delignification process) has been evaluated in depth[39], our customized molding, wet-release, and drying process needs further optimization and evaluation for scaled manufacturing. Please refer to our detailed responses to **Comment #31** on the same topic, for more elaborations and changes we have made to the manuscript.

Ref. 39. Xiao, S. et al. Lightweight, strong, moldable wood via cell wall engineering as a sustainable structural material. Science 374, 465–471 (2021).

Comment #41: 6. I read that the samples they used did not pay attention to cellular size differences across the height of the wood piece used. The molding creates the gradient of sizes. It is worth emphasizing, especially because wood is quite heterogenous in cell size and they are arranged in layers across the radius of the trunk.

Our response: We add Supplementary Note S4 to characterize the cellular variability in our samples, describe our manufacturing process to minimize the impact of the heterogeneity in wood samples, and report the performance variability with samples cut from different regions of the wood log.

Our modification to the manuscript:

On page 9, line 186, we added “Note that the cellular size differences are not considered in our analysis. In practice, we try to optimize our manufacturing process to minimize the impact of the heterogeneity in wood samples (Supplementary Note 4).”

We added **Supplementary Note S4: Cellular Size Variability**

“The rather small size of our wood strip (13.5 mm in length and 0.5mm in thickness) compared to the size of the wood log (~500 mm in diameter) helped minimize the cellular size variation induced by the variables in fabrication within a single strip. In addition, a relatively consistent wood log selection (14 – 20-year-old white oak), flat-saw cutting method of the wood sheet and careful selection of cutting strips along the fiber direction were practiced in our sample preparation.

However, due to the heterogeneous nature of wood materials, cellular sizes are inevitably different within one wood strip and among different wood strips. In practice, cellular sizes are likely to have some effect on plastic deformation and hardening deformation, as well as hygromorphic behaviors.

As Figure S5 shows, we have compared the cell size variations within one sample and across different samples with our wood selection and cutting method. Within the same sample, we imaged the wood cells at two distant ends of the strip (Fig. S5a-b) and observed a ~13% change in the cellular size (Fig. S5c). The cell size changes across the thickness (radial direction) were small, as indicated by region 1 and 2 in Fig. S5d. In addition, we carried out random sampling at four different locations of the wood lumber (Fig. S5e-f). While the current cellular size change did not significantly affect the fabrication process, the heterogeneity of the wood and variability of our manual molding process caused variability in the final curvature across samples. With three wood strips cut from randomly selected locations of the wood lumber, the average curvature was measured as $1865 \pm 70.8\ m^{-1}$. Since our current analysis did not take into account the heterogeneity in cell sizes across the height or the radius of the trunk, further study is needed to understand the extent to which the cellular size differences contribute to variations in the maximum bending curvatures.”

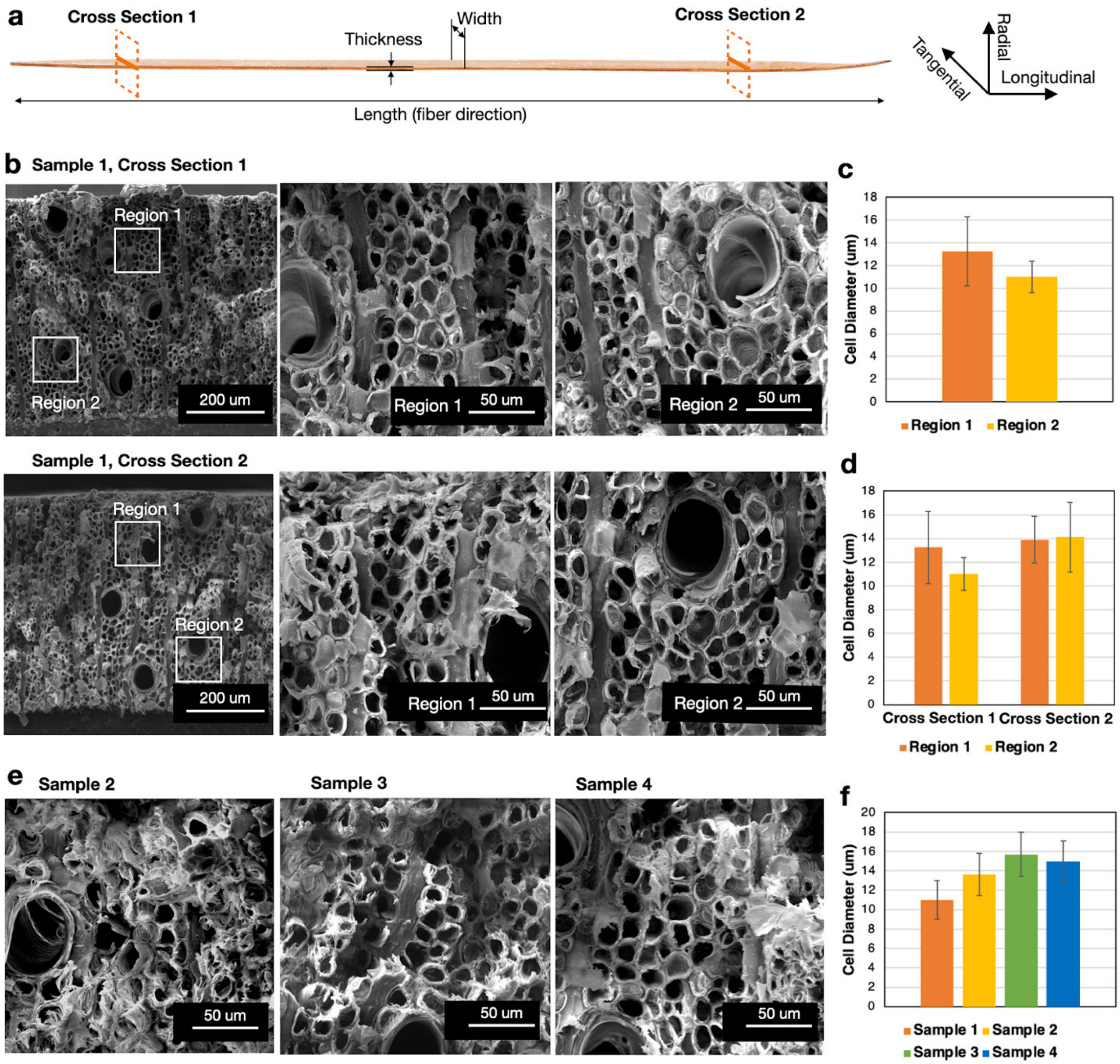

Added **Figure S5**. **The differences in cellular sizes. a**, A single wood strip sample was cut from wood lumber. **b**, SEM images of the cross-sections of a single sample. **c**, Cellular size comparison at two cross-sections at opposite ends of the strip along the length (the longitudinal direction). Data are means ± SD. N = 20 cells per cross-section. **d**, Cellular size comparison across the thickness (along the radial direction) at the same cross-section. Data are means ± SD. *N* = 10 cells per region. **e**, SEM images of the cross-sections of four randomly selected samples at different locations on a white oak log. **f,** Cellular size comparison across four samples shown in (**e**). Data are means ± SD. N = 10 cells per sample.

Comment #42: 7. Quantification is needed in the soil drilling test. Figure 1-3 are done with nice quantitation, while Figure 4 and 5 could have much more.

Our response: Since there is no Figure 5, we respond partially based on our guesses in terms of what the referee was referring to. Related to soil drilling tests:

- To improve the statistical result, we have updated Fig. 3a (the indoor controlled drilling tests) to include tripled numbers of samples, including 15 three-tailed seeds and 15 natural Erodium seeds in 5 continuous hydration and dehydration cycles. The detailed change was included in **Comment #19**.

- For large-sized seed carrying nematodes shown in Fig.4, we added two plots to quantify their drilling performance:

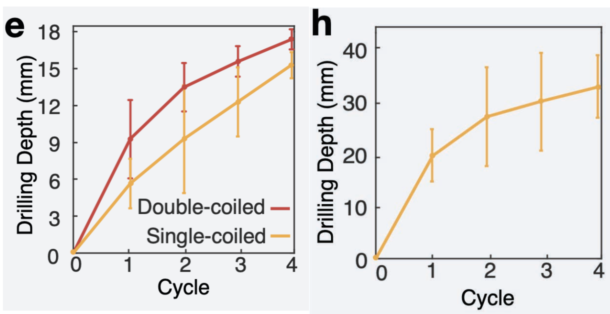

Added **Figure 4. e,** Comparison of the self-drilling depth between the double-coiled and single-coiled seed carriers. Data are means ± SD. $N = 3$ for each type.

Added **Figure 4. h**, Drilling depth of large-sized seed carrier with a body length of ~302 mm. Data are means ± SD. $N = 3$ samples. More details for tests (**b-h**) are included in the Methods.

- In addition, we conducted more field tests under different weather and soil conditions, as well as a germination field test. See response to **comment #44**.

Comment #43: 8. Soil granularity and surface topology – can you specify this for all the conditions you used (in lab and field)?

Our response: We used multiple soils throughout the manuscript. We measure the surface roughness by a pin method adapted from literature[49] that studied self-burying *Erodium*. We further expanded the method description and added a supplementary table to provide more details about the soil.

Our modification to the manuscript:

In Methods, on page 21, line 485, we added a new section named **Soil Characterization**:

"We measured the surface roughness using a pin method adapted from the literature[49]. Ten pins with separated from one other by 1 cm are placed on three sections on each bed. At three randomly chosen locations of the soil surface, we lowered each pin until it touched the substrate. The $\log_{10}$

soil microtopographical variance (LSMV) was calculated as the variance of the vertical pin heights against a measuring board. For soil compaction, we used a soil penetrometer to measure the unconfined compressive strength of the soil. For granular size, we used a light microscope for the measurement. We list all soil types utilized in Supplementary Table 5, in terms of soil type, granular size, quantified surface topology and compactness. ”

Added **Table S5: A summary of the soils used in the drilling and germination experiments.** Measurements of granular size, the LSMV, compressive strength and the experiments in which the soil was utilized.

Soil Types	Granular Size (mm)	LSMV(mm^2)	Compressive Strength (kg/cm^2)	Experiments
Perlite 	3.3 ± 1.3	0.78	0.01± 0.01	In the lab: drilling tests in Fig. 1c, Fig. 3a, Fig. 4e,g,h
Fiber soil (Coconut coir) 	1.4 ± 1.0	1.62	0.05 ± 0.03	In the lab: drilling and germination tests in Fig.3d, Fig. 4b,c,d In the field: drilling tests
Local topsoil (clay soil) 	6.2 ± 6.2	4.61	0.09 ± 0.02	In the field, drilling and germination tests
Steer manure compost and sand (9:1 by weight) 	0.8 ± 2.0	0.70	0.09 ± 0.01	In the field, drilling tests

Comment #44: 9. More field work needed (currently only one field test, which had a surprise storm). More details also needed; for example, what was the germination rate of unlodged and non-lodged seeds (never lodged)?

Our response: To have a better understanding of how the engineered seed carriers behave under different weather conditions, we conducted a few additional drilling experiments in two geographical locations. We have also conducted one more germination experiment to compare the buried and unburied seeds. We shared the additional results in the revision.

We added the Supplementary Table 4 to provide a summary of all the test conditions and added two figure panels to the Extended Data Figure 7 to highlight the capability of continuous drilling and germination after rain.

We have added supplementary data (i.e., photos of 136 seeds before and after rains monitored for two consecutive days) to doi.org/10.5281/zenodo.6541825, and cited it in the manuscript.

Our modification to the manuscript:

We updated the section "Drilling test under natural stimuli" on page 14, to include more field tests:

"We conducted five outdoor drilling experiments with 136 three-tailed seed carriers in two geographical locations over two springs (Supplementary Table 4, Methods). Compared to lab tests, the drilling success rate decreased, with an anchoring rate of 66 ± 16% and an establishing rate of 39 ± 13%. As expected, the drilling success is significantly affected by the varying and unpredictable weather conditions. For example, in drilling test 1 (Extended Data Fig. 7a), two periods of intermittent, light rains on the first day triggered a 95% anchoring rate, yet a heavy rainstorm on the second day dislodged 56% of the previously anchored seed carriers. In drilling test 3, sunlight after the rain was found to promote further seed establishment with a 15% increase (Extended Data Fig. 7b).

Heavy rain can also damage the seed tips, preventing seed carriers from further drilling, despite the fact that the coiled body and tails could later recover from the flood and further functionally coil and uncoil. We expect further optimization of the seed tips[24] could improve their resilience to harsh environments and hostile climate effects, such as extreme flooding or drought. The influence of soil types and surface roughness needs more quantification in the future, to tailor our designs and increase the success rate.

To measure the germination rate, we tracked the seed carriers in drilling test 1-3 and 5. After 14 days, we identified 76 remaining seed carriers with embedded arugula seeds (Eden Brothers, USA). 43 either established or anchored seeds had a 61% germination rate. The rest of the 33 dislodged seeds had a 12% germinate rate (Extended Data Fig. 7c, Supplementary Video 9).

Added **Supplementary Table S4**. Drilling tests under different natural conditions in two geographical locations. Detailed soil information is shown in Table S5 (see our response to # **Comment 43**). The photographs of the 136 seeds, monitored for two consecutive days, before and after exposure to rain are shared at https://doi.org/10.5281/zenodo.6555503.

Field Test	**Month and Location**	**Weather Condition: Temp, Rain (Total Precipitation)**	**Soil Type**	**Sample Size**	**Establishing Rate**	**Anchoring Rate**
Drilling test 1 _Day 1	July 5, Pittsburgh, USA	20 - 35 ºC ~7 hr light rain (~5.5 mm)	Local topsoil (clay soil)	22	68%	95%
Drilling test 1 _Day 2	July 6, Pittsburgh, USA	22 - 35 ºC ~2 hr heavy rain storm (~55 mm)	Local topsoil (clay soil)	22	36%	50%
Drilling test 2 _Day 1	Apr 23, Pittsburgh, USA	10 - 11 ºC ~0.75 hr light rain (~2.5 mm)	Fiber soil	20	30%	60%
Drilling test 2 _Day 2	Apr 24, Pittsburgh, USA	15 - 20 ºC In sun (0 mm)	Fiber soil	20	30%	60%
Drilling test 3 _Day 1	May 1, Pittsburgh, USA	10 - 16ºC ~2 hr heavy rain (~16.5 mm)	Fiber soil	20	30%	55%
Drilling test 3 _Day 2	May 2, Pittsburgh, USA	10 - 22ºC ~5 hr in sun (0 mm)	Fiber soil	20	45%	60%
Drilling test 4 _Day 1	Apr 13, Hangzhou, China	12 - 16 ºC ~1 hr medium rain (~5 mm)	Sandy steer manure compost	18	33%	61%
Drilling test 4 _Day 2	Apr 14, Hangzhou, China	13 -18 ºC Cloudy (0 mm)	Sandy steer manure compost	18	33%	61%
Drilling test 5 _Day 1	Apr 22, Hangzhou, China	25 - 28 ºC ~3.5 hr light to medium rain (~8 mm)	Fiber soil	14	50%	91%
Drilling test 5 _Day 2	Apr 23, Hangzhou, China	24 - 28 ºC ~1 hr light rain (~1 mm)	Fiber soil	14	50%	86%

b

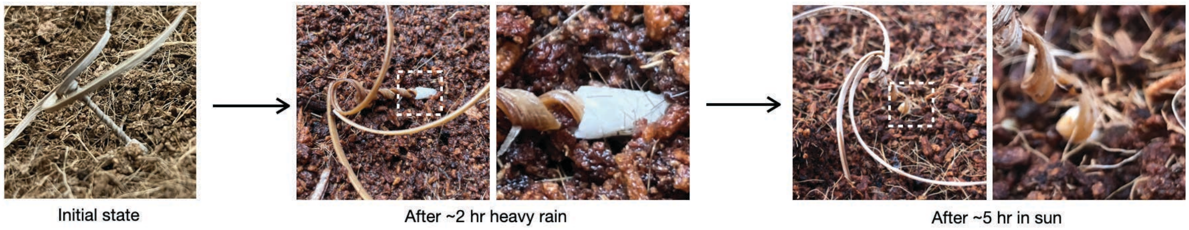

c

Updated **Extended Data Figure 7**. **b,** A rain-anchored seed continues to drill after the sun emerges, as shown in drilling test 3 of Table S5. **c,** Established seed carriers tend to germinate more easily than non-established seed carriers after five days with four periods of rain. The established and exposed seeds had a 100% and 19% germination rate, respectively, in drilling test 1 of Table S5.

Comment #45: 10. Do they tangle with each other upon storage and dispensing? That would be a drawback of the three tailed design.

Our response: We did observe entanglement of the seeds, and that was the reason we used a box with dividers in our drone delivery test. We add an additional supplementary note to discuss the seed entanglement in more detail and share a preliminary deployment solution.

Our modification to the manuscript: we add **Supplementary Note 5: Seeds Entanglement in Drone Deployment**

When multiple seeds are randomly placed together, they entangle (Fig. S6). In our original drone deployment solution, we used dividers in the storage box to prevent entanglement (Extended Data Fig. 3). This was sufficient for our smaller-scale test described in the paper. However, for a much larger scale deployment in the future, further investigation into the entanglement behavior and alternative engineering solution is needed. To date, we have conducted a preliminary test by storing 10 seeds inside one container and dropping them from ~5 m above the local topsoil. We observed entanglement inside the box. When dropped, due to the impact force, the seeds tended to separate after hitting the ground. However, small clusters were still observed from two of the four dropping tests (Fig. S5b-d). Further tests are needed in the future when seeds are dropped onto different soil types and from different heights, which are beyond the scope of this manuscript.

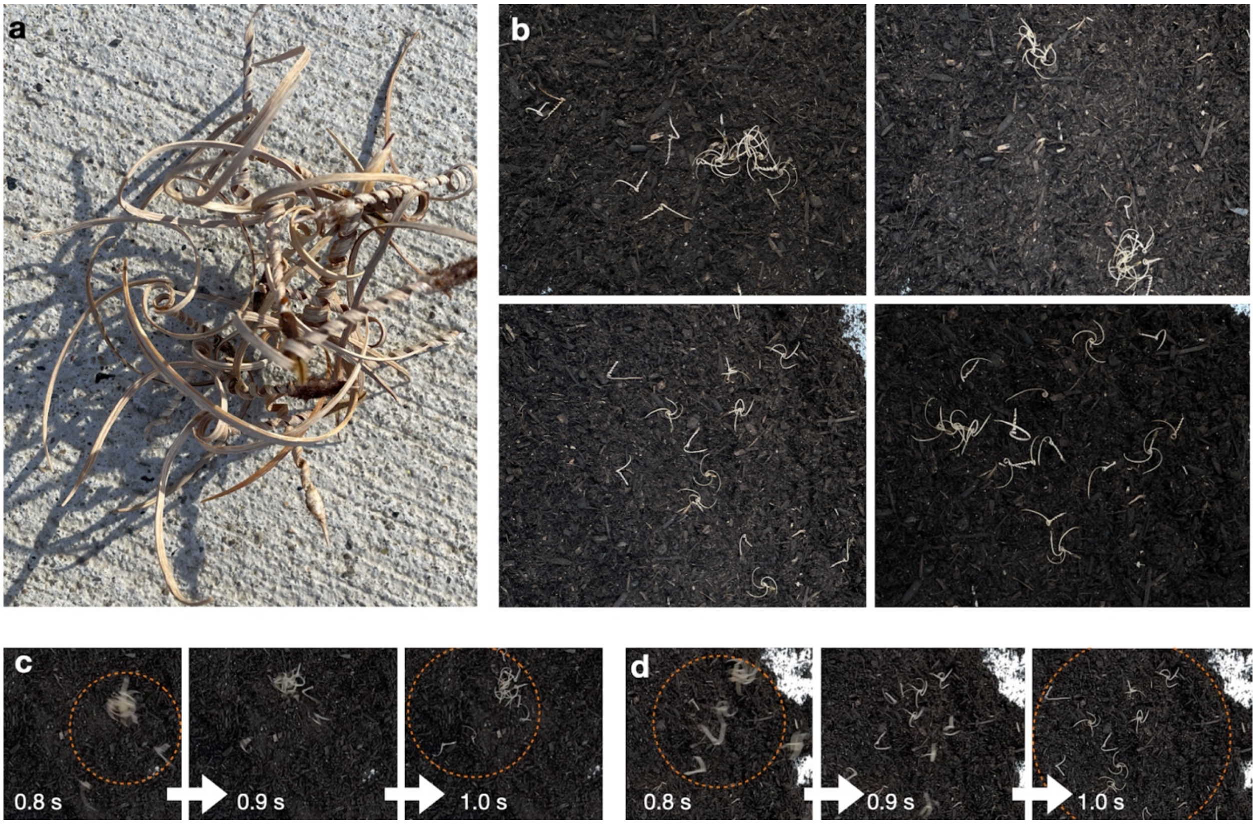

Figure S6. Seed dropping tests. a, Entanglements when seeds are stacked together randomly. **b**, Results of four dropping tests from ~5m above the local topsoil. **c-d**, The degree of separation varies between the two dropping tests.

We also believe that further engineering efforts are needed to design more effective storage and deployment mechanisms that minimize entanglement. For example, Figure S7 shows one potential solution with an extendable accordion structure.

Figure S7. Conceptualized storage and delivery mechanism. a, The assembly of seeds on an extendable accordion structure to avoid entanglement. **b**, The dropping of the seed through the extension of the seed storage device. **c**, Seeds delivered and dropped on the ground. Scale bar: 10 mm.

Reviewer Reports on the First Revision:

Referees' comments:

Referee #1 (Remarks to the Author):

Authors responded comprehensively to most of the comments reported, adding replicated experiments and/or imaging tests and strengthening the manuscript, consequently. However, some inaccuracies or lacks still need to be addressed.

Regarding Comment # 19 the authors reported the experimental data adding information regarding statistical variations (mean value ± standard deviation). However, inconsistencies or points remain to be addressed.
Line 133-134. The authors reports: "for (e-h), each test group contains three samples with an initial thickness of 0.4 ± 0.0 mm, 0.5 ± 0.0 mm and 0.7 ± 0.0 mm, respectively". I suggest reporting the second decimal, since it is quite unusual to have an experimental measurement with a standard deviation equal to 0. Basically, it means that not enough decimals were taken or that the measurement was made with low resolution instrumentation.
Line 235: "Data are means ± SD. N = 2". I suggest adding a third replicate, 2 replicates are not enough for a statistic.
Fig.3f, Line 229-230, Extended Data in Fig.4b, c. Force data should also report standard deviations. Trends (Force vs Time) can be reported individually, but the resulting peak values must be reported as means ± SD for make a significant comparison.

Regarding Comment # 20, the authors explained the nematode dispersion test in more detail in Methods and added a video showing how the nematode moves on day 9 at a distance of 5 cm. In my opinion, a time-lapse would be more convincing, as reported for the germination of radish (Fig. S7). I understand there are magnification issues with respect to radish. Authors should find a way to map and track the movement of the nematode day-by-day.

There is one typo in the revised text that must be fixed, for the correct revision to be consistently implemented. Specifically, when replying to comment#14, the authors clarified that simulation can only provide a qualitative explanation of the experiments, and they aimed to consistently revise the text. However, the revised text reads (line 218): "We conduct further finite element (FE) simulations to quantitatively predict the coiling actuator performance taking into consideration of the frictional interaction between the seed carriers and soil, and the potential anchoring effect (Methods)." Clearly, the word 'quantitatively' should be replaced with 'qualitatively'.
An additional minor point is offered, for check by the authors. I guess that, in the reply to comment#8, namely: "To reveal the underlining mechanism of curvature formation and actuation, we first analyze the deformation behaviors of the bending actuators, made from the three-step molding process (Fig. 2a-d).", the word 'underlining' might be a typo for 'underlying'.

Referee #2 (Remarks to the Author):

Although it is still questionable whether attaching each seed to a wood veneer-based seed carrier will ever prove practically useful, it seems more appropriate at this point to focus on innovations and academic depth this paper delivers. The reviewer still finds that the following points need to be addressed for the paper to be acceptable to scientific community.

(1) Although this reviewer suggested that the authors analyze the mechanics of helical coiling considering the internal structure of the actuator, the authors did not seem to perform further

analysis since the initial submission. This made the reviewer carefully look into the results of current numerical analysis in comparison with experimental data, which brought up the following questions. In Fig. 3, the authors argue that their simulation results match well with experiments (line 232, for Fig. 3f). To claim quantitative (line 218) agreement between simulation and experiment, quantitative data should be presented to compare the results.

(1-1) In Fig. 3d and e, images of experimental and numerical seed shapes are presented. It is necessary to measure the pitch and radius of the coiled part and the curvature of the uncoiled part (end of tail) as functions of time, and check whether the experimental and numerical values match quantitatively.
(1-2) In Fig. 3f, it is hard to agree with the authors that the results of simulation and experiments match well. In what aspects do the authors argue their good agreement? Is the agreement good enough to ensure usefulness and validity of the current simulation model?

(1-3) In Fig. 2i, how were the lines obtained? Are they just fitting curves for visual guide?

(2) Although this reviewer suggested that the authors justify the ignorance of modulus reduction effect when wet, they only mentioned that the simple model agrees with experimental results well. Matching of model and experiment can happen when multiple errors in the model counterbalance with each other, and thus the agreement of model and experiment cannot be an excuse not to check assumptions made in the model. It is suggested that the authors measure the modulus by progressively wetting the material and present the result.

Typo:
Line 641, more -> model

Referee #3 (Remarks to the Author):

The manuscript has been extensively revised reflecting the referee feedback. Now the significance of the work is clear, and the paper is more informative on the design principles, manufacturing process, and functional characterization. I congratulate the authors in achieving this in a short period of revision time.

I do have a few follow up points from my previous review.

Major comments:

#37: Survey of more wood types as the starting material.
I was asking for this survey, because the key design decision is which wood material to use – in other words, certain wood properties matter very much and then the readers should be informed what they are. From this survey, what surfaced as the key parameters? It is mentioned to some extent in the text, but the survey results weren’t used to support the design criteria. Can you clarify better?

#39 (in relation to #29): Survey of natural self-burial seed diversity.
In the Table S1, is the data of their drilling effectiveness missing? I only see the geometrical specs in the table, but the authors say they did the drilling test. Please show the results.

#41: Cell size effect.
I see the cell size is was not that critical, but the data shows the average size. I was more wondering about the number and distribution of larger cells, like the vessels, which have much thicker cell walls and much larger in size. Also, the veneer polarity (the face toward outside of the annual ring would have smaller cells) in general. Did you pay attention to the sides of the wood strips, and/or it did not make a clear difference in the performance of the actuators?

#42: Quantification in the soil drilling test.
Fig 3e and h – error bar is large, and N is small. Please repeat the experiments with more samples.
Also, comparison of germination rates with respect to buried vs unburied (never or resurfaced) is a key result. At the moment such information is mentioned only for a limited number of tests – can you be more comprehensive?

#43: Soil granularity test.
Can you incorporate the finding from this measurement to the results of the drill tests to gain further insights on how strongly soil roughness affect the drilling? Here I especially mean the link to the field tests.

#44: More field test.
I asked for more field tests, so that you could pinpoint what parameters affect the self-burial actuator function the most in realistic conditions. Looking at the data, soil type does not seem to be a dominant factor. Rather, temperature seem to be, and that is not surprising (it is one factor anticipated to affect hydromorphic structural function). I think this is an important parameter to test, and you have a suitable set up to measure the drilling force when the tails are exposed to mist, temperature of which you can modulate.

Minor comments:
The order of the supplementary materials is not in line with the order of mention in the main text.

Author Rebuttals to First Revision:

Response to Reviewers

The responses to the comments and newly added text in the revised manuscript and SI are shown in red.

Referee #1 (Remarks to the Author):

Authors responded comprehensively to most of the comments reported, adding replicated experiments and/or imaging tests and strengthening the manuscript, consequently. However, some inaccuracies or lacks still need to be addressed.

Our response: We thank the reviewer for the insightful comments to improve the quality of our manuscript. We have updated the manuscript and have included a point-to-point response to each individual comment.

Comment #1: Regarding Comment # 19 the authors reported the experimental data adding information regarding statistical variations (mean value ± standard deviation). However, inconsistencies or points remain to be addressed.

Line 133-134. The authors reports: "for (e-h), each test group contains three samples with an initial thickness of 0.4 ± 0.0 mm, 0.5 ± 0.0 mm and 0.7 ± 0.0 mm, respectively". I suggest reporting the second decimal, since it is quite unusual to have an experimental measurement with a standard deviation equal to 0. Basically, it means that not enough decimals were taken or that the measurement was made with low resolution instrumentation.

Our response: We will report to the second decimal.

Our modification to the manuscript: We updated the texts on page 8, line 133 – 134: "for (e-h), each test group contains three samples with an initial thickness of 0.36 ± 0.00 mm, 0.51 ± 0.03 mm and 0.73 ± 0.01 mm, respectively."

Comment #2: Line 235: "Data are means ± SD. N = 2". I suggest adding a third replicate, 2 replicates are not enough for a statistic.

Our response: We believe the review is referring to line 205 instead of 235. We updated Fig. 3g by adding up to three replicates of each coiling number. We have also replaced the y axis title from "total angle changes per coil" to "total angle changes", so as to better highlight the core message directly related to the design guideline: the total coiling number can affect the rotation speed.

Our modification to the manuscript: We updated the Fig. 3g and the figure caption in line 205.

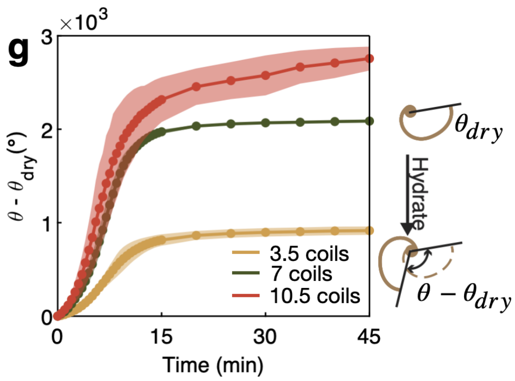

Updated **Figure 3. g**, The rotational range and speed of coiling actuators. Data are means ± SD. $N = 3$ of each coiling number.

Comment #3: Fig.3f, Line 229-230, Extended Data in Fig.4b, c. Force data should also report standard deviations. Trends (Force vs Time) can be reported individually, but the resulting peak values must be reported as means ± SD for make a significant comparison.

Our response: We added additional force vs. time plots demonstrating three repetitions of each coiling type and reported the standard deviations for the peak forces. Indeed, to address other referees' comments related to extension forces, including Comments #9 and #11 (regarding integrating dynamic modulus changes in the simulation in Fig. 3f) and Comments #19 (on testing the extension force under different temperatures), we have tested more samples under different conditions and added a supplementary note to extend greater discussion.

Our modification to the manuscript:

- Added **Supplementary Note 4: Extension Force of the Coiling Actuators**

We compared the extension force profiles of coils of two different thicknesses (0.74 ± 0.06 mm and 0.50 ± 0.02 mm) and three different coiling numbers (3.5, 7 and 10.5 coils) (Fig. S8). The *Erodium* bodies with three coils of uneven diameters were also tested. We observed that the 3.5 coil with a 0.74 mm thickness provided the largest peak extension force, 55.18 ± 6.82 mN, which is ~34% larger than that of natural *Erodium,* 36.57 ± 6.82 mN. However, while we observed a general increase in peak extension forces when increasing the thickness of the strips, the percentage of the increase was not the same: when the thickness increased from ~0.5 mm to ~0.7 mm, the peak force of the 3.5 coil increased ~38%, while that of the 7 coil only increased ~7%. In addition, most peak forces were reached within the first 30 minutes. Therefore, we expect an effective natural rain that can promote self-drilling of a seed carrier should last for at least 30 minutes. Of course, this is only an estimate since other natural conditions, such as rain intensity and temperature, may also play important roles in relation to the extension force of the actuators.

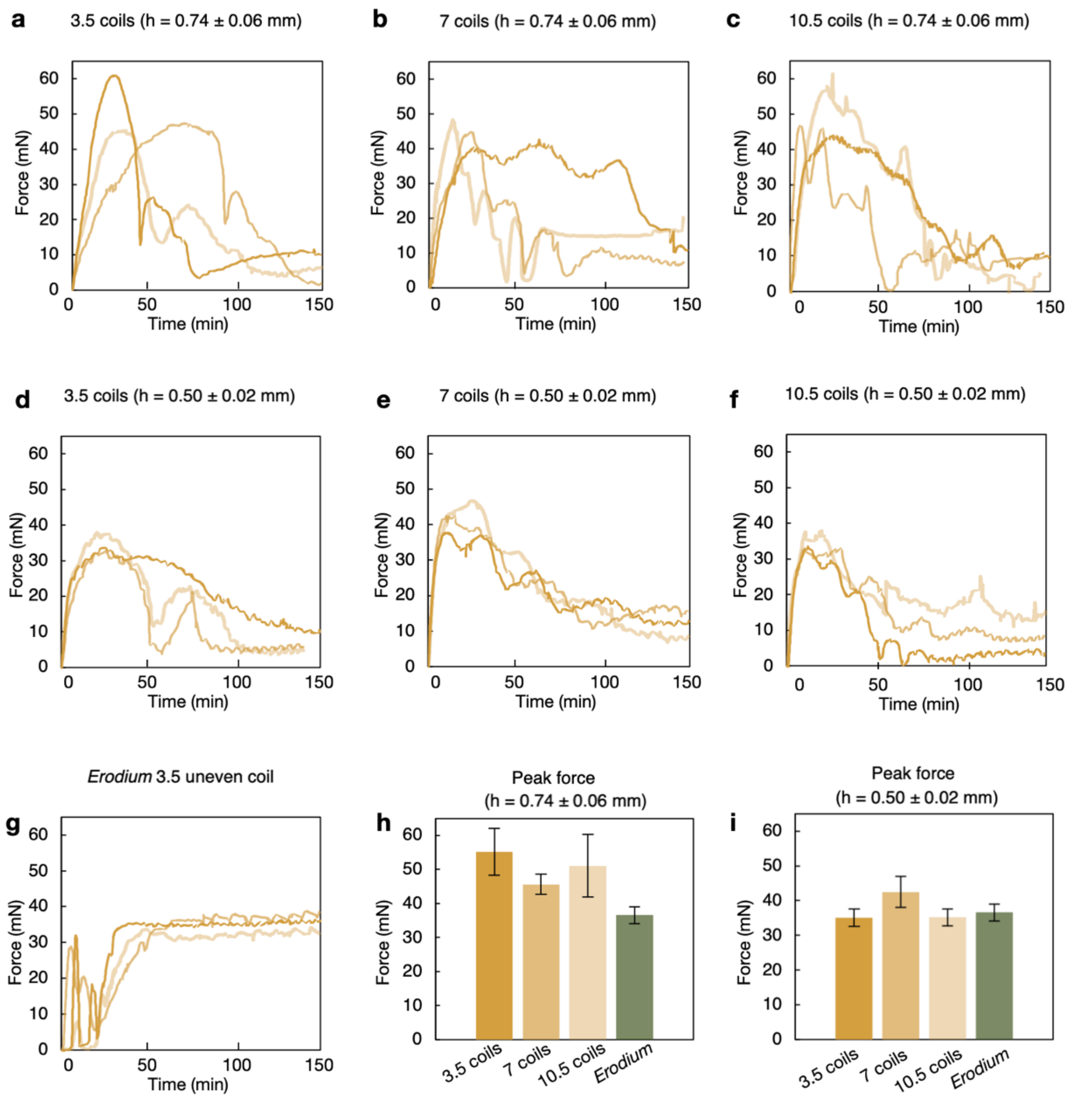

Figure S8. Measurement and comparison of extension forces generated by different coiling actuators. **a-c**, Extension force curves of 3.5 coils, 7 coils and 10.5 coils with a ~0.74 mm thickness. **d-f,** Extension force curves of 3.5 coils, 7 coils and 10.5 coils with a ~0.50 mm thickness. **g**, Extension force curves of *Erodium guinum* coils. Note that the three coils of *Erodium* have varying diameters, with the largest diameter coil touching the load cell. **h-i,** Comparison of the peak extension forces, with data as means ± SD and $N = 3$. In all the tests, the engineered coils are prepared from white oak strips of 2.2 mm in width and molded on mandrels with a diameter of 0.8 mm. The extension force measurement protocol is described in Methods.

- We also updated Fig. 3f, with SD for experimental results, and updated the simulation by adding the dynamic elastic modulus changes during hydration.

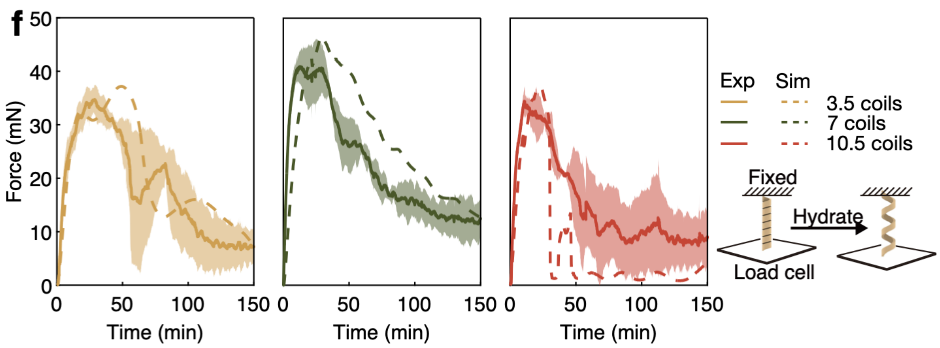

Updated **Figure 3. f,** Experiments and simulation of peak extension forces of coiling actuators with different coiling numbers. Data are means ± SD, N = 3 of each coiling number.

- We updated the texts in lines 228-231: "Among the coiling samples tested in Fig. 3f and Supplementary Note 4, the 3.5 coils with an initial thickness of 0.74 ± 0.06 mm provided the largest peak extension force of 55.18 ± 6.82 mN, which is ~34% larger than that of the *Erodium* seed coils (36.57 ± 2.44 mN)."

Comment #4: Regarding Comment # 20, the authors explained the nematode dispersion test in more detail in Methods and added a video showing how the nematode moves on day 9 at a distance of 5 cm. In my opinion, a time-lapse would be more convincing, as reported for the germination of radish (Fig. S7). I understand there are magnification issues with respect to radish. Authors should find a way to map and track the movement of the nematode day-by-day.

Our response: We chose the centrifugal floatation method [REF1 and 2] to track and sample nematodes in soil samples over time. We discovered that nematodes can be successfully observed in the surrounding soils from the second day after seed deployment. As time goes by, a decrease in the total number of living nematodes in the soil is observed. We shared both images and quantitative data in the update.

[REF1] van Bezooijen, J. *Methods and Techniques for Nematology*. (Wageningen University, 2006).

[REF 2] Freckman, D. W. & Virginia, R. A. Low-diversity Antarctic soil nematode communities: distribution and response to disturbance. *Ecology* **78**, 363–369 (1997).

Our modification to the manuscript:

- We updated the experimental protocol under Methods, in line 519: "For the microbe-delivery experiment (Fig. 4d), we integrated ~0.05 g of beneficial nematodes powder (Steinernema feltiae, BioLogic Scanmask) into each seedpod dough by means of further gentle kneading for ~2 min by hand. We conducted an experiment to track nematode delivery for nine days: we filled 10 separate containers with 20 g of dry coconut coir soil. We then embedded one nematode-loaded seed carrier into each container, which was moistened with 10 mL of water each day. We then extracted and counted the living nematodes from the soil of one container each day using the centrifugal floatation method[50], with sugar water as the extraction fluid, for nine consecutive days (Extended Data Fig. 6). The same set of tests was repeated three times."

[50] Freckman, D. W. & Virginia, R. A. Low-diversity Antarctic soil nematode communities: distribution and response to disturbance. *Ecology* **78**, 363–369 (1997).

- We updated the results from the tests by updating the main manuscript and adding an extended data figure. On page 13, line 263, we added:

"We tracked the delivery of nematodes from our seed carriers to the surrounding soils over a period of nine days in a controlled test (Methods). Living nematodes could be identified from the second day, and the total number continued to increase, reaching a peak of 34760 ± 6525 / kg on day four (Extended Data Fig. 6 and Supplementary Video 8)."

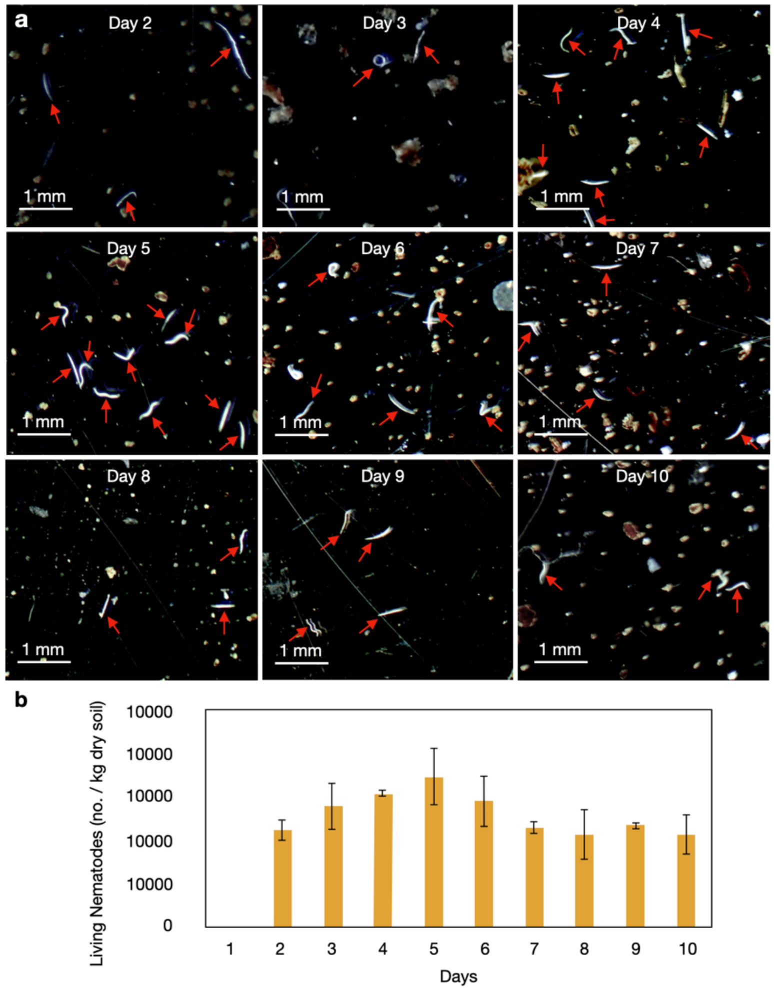

Extended Data Figure 6. a, Representative images of nematodes extracted from the soil (Methods). **b**, Tracking of the living nematodes extracted from the soil. Data are means ± SD, *N* = 3 soil samples each day.

Comment #5: There is one typo in the revised text that must be fixed, for the correct revision to be consistently implemented. Specifically, when replying to comment#14, the authors clarified that simulation can only provide a qualitative explanation of the experiments, and they aimed to consistently revise the text. However, the revised text reads (line 218): "We conduct further finite element (FE) simulations to quantitatively predict the coiling actuator performance taking into consideration of the frictional interaction between the seed carriers and soil, and the potential anchoring effect (Methods)." Clearly, the word 'quantitatively' should be replaced with 'qualitatively'.

Our response: We thank the reviewer for pointing out the typos in Comments #5 and #6. We updated the main texts to correct them.

Our modification to the manuscript: We updated the texts in line 218: "We conduct further finite element (FE) simulations to qualitatively predict the coiling actuator performance…"

Comment #6: An additional minor point is offered, for check by the authors. I guess that, in the reply to comment#8, namely: "To reveal the underlining mechanism of curvature formation and actuation, we first analyze the deformation behaviors of the bending actuators, made from the three-step molding process (Fig. 2a-d).", the word 'underlining' might be a typo for 'underlying'.

Our modification to the manuscript: We have replaced "underlining' in line 144 with 'underlying."

Referee #2 (Remarks to the Author):

Although it is still questionable whether attaching each seed to a wood veneer-based seed carrier will ever prove practically useful, it seems more appropriate at this point to focus on innovations and academic depth this paper delivers. The reviewer still finds that the following points need to be addressed for the paper to be acceptable to scientific community.

Comment #7: (1) Although this reviewer suggested that the authors analyze the mechanics of helical coiling considering the internal structure of the actuator, the authors did not seem to perform further analysis since the initial submission. This made the reviewer carefully look into the results of current numerical analysis in comparison with experimental data, which brought up the following questions. In Fig. 3, the authors argue that their simulation results match well with experiments (line 232, for Fig. 3f). To claim quantitative (line 218) agreement between simulation and experiment, quantitative data should be presented to compare the results.

Our response: We intended to refer to our simulation as a "qualitative" model. Sorry for the confusion. We have now replaced the word "quantitative" (line 218) with "qualitative" in the revision (response to Comment #5). A qualitative model is adopted for the following reasons: firstly, simulations based on the simplified model are beneficial to us in identifying the importance of the tail topology to maintain the inclined drilling angle, the tail tip penetration to increase the thrust force and torques, and seed tip anchoring to enhance the thrust force. These findings are consistent with our experimental observations, which effectively explain the improved drilling performance of the three-tailed coils compared to the single-tailed coils. Secondly, the complicated geometries of our physical seed carriers, such as the non-uniform coiled body and the seed tip, make the simulations difficult to converge. Even in the case of the current simplified model with a uniform coiled body and no seed tip, it took several days to complete the simulation on computer clusters, due to the highly nonlinear deformation and friction between the seed carriers and the ground. Thirdly, the environmental conditions of the drilling experiments cannot be well-controlled even in lab tests. For example, the atomized water spray that was customized to emulate the natural rain conditions in our controlled drilling tests will make non-uniform contact with the seed carriers, as small water droplets are formed. Thus, moisture distribution within the structure is inhomogeneous. Regarding our five field tests, the rain, temperature and soil conditions were all different and were even less controllable. Considering these challenges and the fact that the simplified model can already provide decent guidance to engineer the seed carriers, we would prefer to retain the simple modeling and simulation strategy and use the more comprehensive models for seed drilling experiments in more specialized investigations.

Furthermore, we conducted additional experiments and simulations in response to referee #2's comments below. We really appreciate the referee's critical comments and suggestions to improve our work. More specifically, we incorporated the moisture dependent coil pitch and radius (response to Comment #8) and modulus (response to Comment #11) into the model calibration process and updated all the simulations in the manuscript. The new simulations are consistent with previous simulations. In addition, these new moisture dependent parameters improve the extension force comparison between simulations and experiments (response to Comment #9). To keep the analysis transparent and to enable researchers to reproduce our results, we will make all the simulation codes public. Since all the material properties can be found in the codes, we have removed **Table S6.** Mechanical properties and effective hydration parameters are used in the simulations of the coiled body thrust force calibration and the seed carrier drilling.

Comment #8: (1-1) In Fig. 3d and e, images of experimental and numerical seed shapes are presented. It is necessary to measure the pitch and radius of the coiled part and the curvature of the uncoiled part (end of tail) as functions of time, and check whether the experimental and numerical values match quantitatively.

Our response: The goal of Fig. 3d and e is to show that the seed tail tip anchoring process can be captured both in simulations and experiments. The representative images were identified from the recorded videos of experiments and simulations through a frame-by-frame comparison. We do not claim that the simulation is a quantitative comparison with the experiments. Since there are many uncertainties in the experiments, such as the surface roughness of the soils and non-uniform moisture distribution, the simulations cannot reproduce the exact boundary conditions in the experiments.

We agree with the referee that it is important to confirm the predictability of the coil pitch and radius by the model under different wet conditions. If the moisture changes as a smooth function of time, it is also possible to establish the relationship between the coil geometries and time. To maintain stable and well-controlled experimental conditions, we conducted hydration experiments of uniform coils with seven pitches in a chamber, with feedback closed-loop controls of humidity and temperature (Methods). The experimentally measured data were then used to identify the modeling parameters related to the moisture-induced mechanical deformation. Within the same modeling framework, we showed that the time dependent coil pitch and radius can be captured. For the tail curvature, we did not perform a one-to-one comparison between simulations and experiments, as the tail sizes are smaller in the simulations, due to the missing seed tip in the simulations.

Our modification to the manuscript:

In the Methods section "**Modeling and simulations of the coiling and drilling of the engineering seed carrier**" from line 652 to 654, we included the following discussion relating to the calibration of the coil pitch and diameter:

"The hydration strain field and characteristic time scale are fitted with the coiling configuration (e.g., coil diameter and pitch) of hydrated coils in a controlled humidity chamber (Supplementary Note 11)."

In **Supplementary Note 11: Model Calibrations and Simulations of the Extension Forces** from line 1448 to 1456 on page 80, we added more discussions regarding the shape change parameter calibrations.

"To calibrate the characteristic time scale, t_d, we decreased ξ from 1 following an exponential decay in the simulation to mimic the controlled hydration tests in the humidity chamber, such that:

$$\xi = exp\left(-\frac{t}{t_d}\right). \tag{22}$$

We identified t_d by matching the time variation of the measured coil pitch and diameter in the experiments. We found a set of parameters, namely, $\theta_l = 20°$, $\Psi_0 = 50°$, $\Psi_1 = 70°$, $\epsilon^0_{x'x'} = 0.10$,

$\epsilon^0_{y'y'}$=-0.18, $\gamma = 1.35$ and $t_d = 180\ min$ that could result in a good agreement with the humidity chamber experiments, as shown in Fig. S20. Note that t_d depends on both the material properties and the environment conditions."

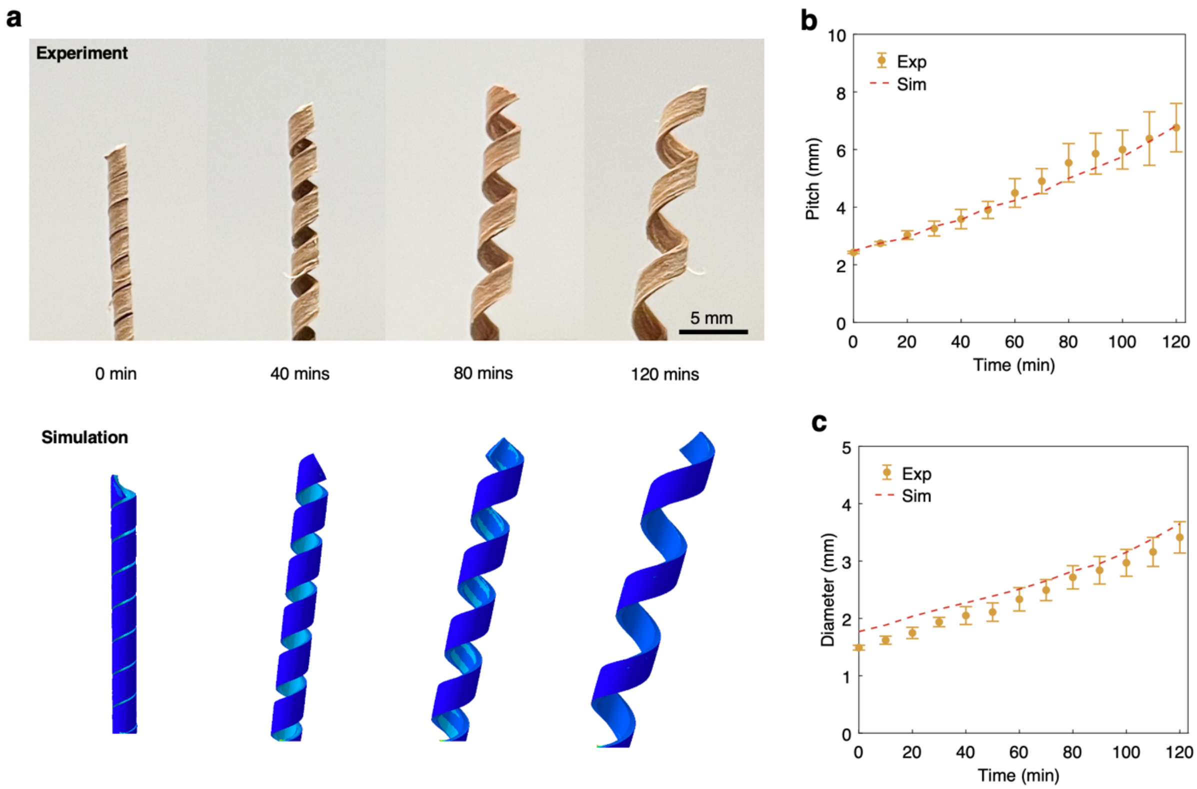

Figure S20. Calibration of the time-dependent variations of the coil pitch and diameter during hydration. **a**, Representative experimental and simulated coil configurations at different hydration time spans. **b**, Comparison of the coil pitch obtained from experiments with that from simulations. **c**, Comparison of the coil diameter obtained from experiments with that from simulations. Experimental data are means ± SD. N = 3 samples.

Comment #9: (1-2) In Fig. 3f, it is hard to agree with the authors that the results of simulation and experiments match well. In what aspects do the authors argue their good agreement? Is the agreement good enough to ensure usefulness and validity of the current simulation model?

Our response: We re-ran all the extension force measurements and updated all the simulations with the newly calibrated model. The comparison between the new experiments and simulations are shown in REF Fig. R1. Although they do not agree quantitatively, the simulations capture the nonlinear force-time relations observed in the experiments for all three coils, including the values and time for the peak forces, initial stiffness and decay over a longer period.

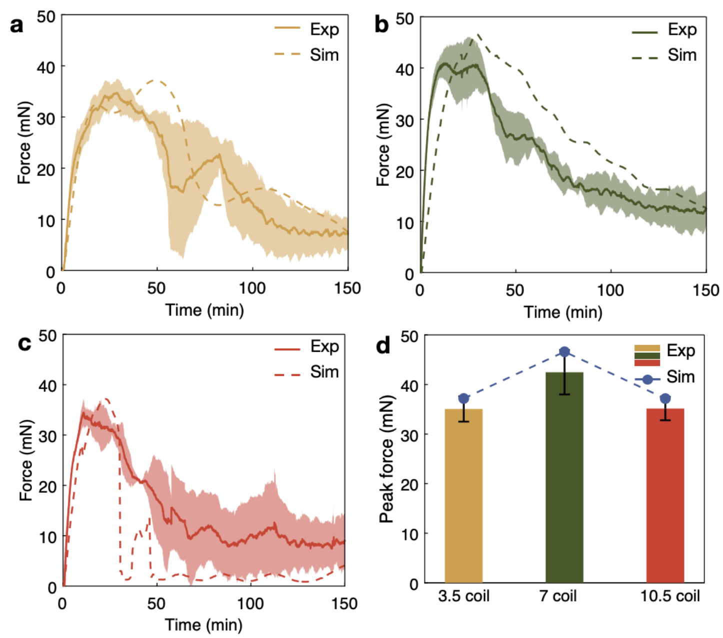

REF Figure R1. Experimental measurements and simulations of the extension forces for three different lengths of coils, including the 3.5 coil **(a)**, 7 coil **(b)** and 10.5 coil **(c)**. The solid lines and shaded areas are averaged data and standard deviation from three experiments, respectively. **d**, The peak forces from experiments and simulations. For **(d)**, experimental data are means ± SD. N = 3 samples.

Our modifications to the manuscript:

- We updated Fig. 3f

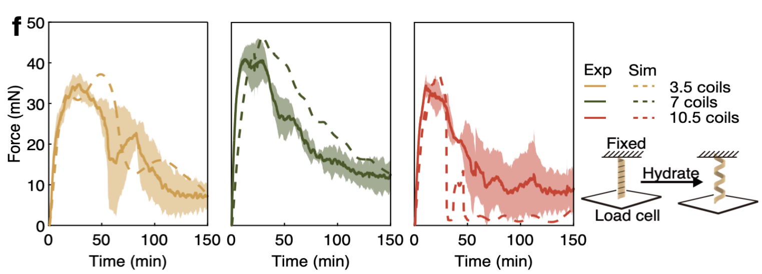

Figure 3. f, Experiments and simulation of peak extension forces of coiling actuators with different coiling numbers. Data are means ± SD, $N = 3$ of each coiling number.

-In **Supplementary Note 11: Model Calibrations and Simulations of the Extension Forces** from line 1513 to 1520 on page 83 and 84, we added more discussions of the extension force simulations.

"To model the contact between the wood and the hard surface, we needed to adjust the coefficient of friction. We found that $E_1^d = 0.33\ GPa$ and a coefficient of friction as 0.45 provided a good prediction for all three coils of different lengths. Using these calibrated materials and contact properties, our model can capture the nonlinear force-time relations for all three coils, including the values and time for the peak forces, initial stiffness and decay over a longer period (Fig. 3f and Fig. S22a-b). The simulations further showed that the peak force of the 3.5 coil is determined by the sliding of the contact tip, and the peak force of the 7 and 10.5 coils are determined by compressive buckling (Fig. S22c)."

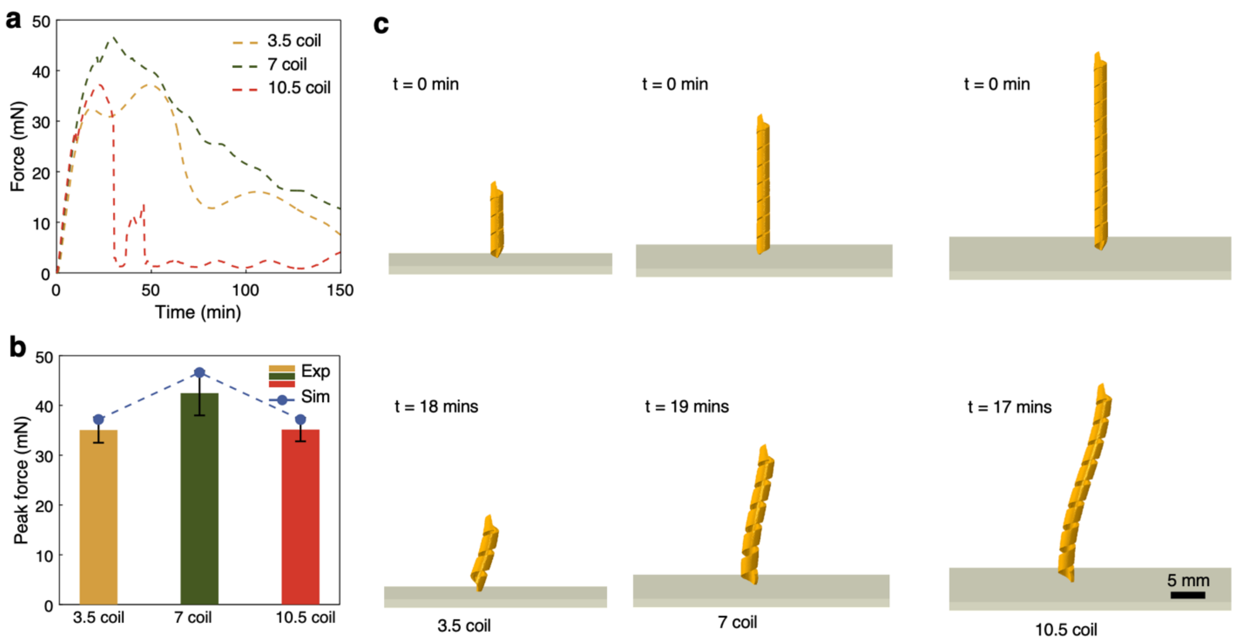

Figure S22. Simulations of the extension force measurements. (a) Simulated extension forces versus time for coils of different lengths. (b) Comparison of peak extension forces in simulations and experiments. (c) Simulation snapshots of the coil configurations near the first peak of the forces. Experimental data in (b) are means ±SD. *N*=3 samples.

- With the new models, we also updated the Supplementary Video S4: Experiment and FE simulation of the uncoiling and self-drilling processes of both three-tailed and single-tailed designs.

Comment #10: (1-3) In Fig. 2i, how were the lines obtained? Are they just fitting curves for visual guide?

Our response: The lines are formed by connecting experimental data points with straight lines (with the 'Line with Markers' style provided by Microsoft Excel). Yes, they are a visual guide only.

Our modification to the manuscript: We added this information into the Fig. 2 caption:

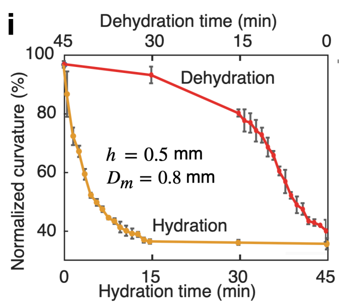

Figure 2. i, Curvature changes of bending samples. The lines provide visual guidance by connecting data points.

Comment #11: (2) Although this reviewer suggested that the authors justify the ignorance of modulus reduction effect when wet, they only mentioned that the simple model agrees with experimental results well. Matching of model and experiment can happen when multiple errors in the model counterbalance with each other, and thus the agreement of model and experiment cannot be an excuse not to check assumptions made in the model. It is suggested that the authors measure the modulus by progressively wetting the material and present the result.

Our response: As suggested by the reviewer, we measured the modulus of the wood strips with a progressive wetting condition, which is controlled by the time in the humidity chamber. More specifically, we placed 39 strips, 80mm long, 20 mm wide and ~0.5 mm thick in a controlled chamber with relative humidity of ~92.98 ± 0.01 %, and at a temperature of 30.84 ± 0.03 °C; we took out three samples every 15 mins during the period from 0 min to three hours, to measure their Young's modulus by means of Instron tensile tests. As the referee suggested, the modulus exhibits considerable change from the dry to the wet state. We recalibrated the FE simulations by incorporating the moisture dependent modulus in the model, and updated all the FE simulations and schematics in the revised manuscript. The new simulations also improved the extension force comparison between simulations and experiments (response to Comment # 9).

Our modification to the manuscript: In Methods, **"Modeling and simulations of the coiling and drilling of the engineering seed carrier"** in line 654**,** we included the following discussion of the calibration of the mechanical properties.

"The mechanical properties of the modeled material were obtained by fitting the measured moisture dependent modulus and the extension forces of the coils (Supplementary Note 11)."

We added experimental measurements and calibration of the moisture dependent modulus in Supplementary Note 11, "**Model Calibrations and Simulations of the Extension Forces**" from line 1463 to line 1491 on page 81 and 82:

It is known that the modulus of wood strongly depends on the water content inside the materials[54]. To study the effect of hydration on the tensile modulus properties of the processed wood samples, we conducted tensile tests on progressively hydrated wood strips in a test chamber, with well-controlled humidity and temperature (Fig. S7). The temperature of the chamber was maintained at ~30°C and the humidity at ~93%. The wood sample size for the test was ~2 mm wide, ~80 mm long and ~0.5 mm thick in the dry state. Multiple wood strips were put in the chamber at time 0. For a period of 180 min, three wood samples were taken out of the chamber every 15 min for tensile testing. The tensile test of the samples was carried out with the universal testing machine (Instron 5969) using 1 kN load cell at 10 mm/min.

Figure S21a shows the representative stress-strain plot of the hydrated samples at different hydration times. Young's modulus was computed from a linear fitting of the stress-strain curve up to a strain of 0.5% (0.005 mm/mm) as shown in Fig. S21b. It was observed that as the hydration time increases, Young's modulus decreases, as seen in Fig. S21b. Young's modulus can be fitted well using the following relationship

$$E = E^d\left(\left(1-\frac{E^w}{E^d}\right)exp\left(-\frac{t}{t_E}\right)+\frac{E^w}{E^d}\right), \tag{23}$$

where E^d and E^w represent the modulus in the dry and wet states, and t_E is a characteristic time scale of modulus change associated with water transport. The best fitted parameters are $E^d = 4.88\ GPa$, $E^w = 1.21\ GPa$ and $t_E = 38.56$ min. Note that the characteristic time scale of modulus t_E is different from that of shape change, which is probably due to nonlinear swelling and mechanical coupling. It was observed that Young's modulus decreases four-fold with respect to the non-hydrated sample. This large change in the modulus cannot be ignored and should be included in the simulations. Note that these measurements are based on unmolded samples and that the exact values are different from the modulus of wood coils, which has been modified by the molding process. During the simulations, we treated the dry modulus, E_1^d, as a fitting parameter to match the extension force measurements, while keeping the experimentally fitted, t_E and the ratio $r_d^w = \frac{E^w}{E^d}$. Then, the modulus E_1 can be expressed as:

$$E_1 = E_1^d\left((1-r_d^w)exp\left(-\frac{t}{t_E}\right)+r_d^w\right). \tag{24}$$

The same time-dependent function is also applied to the rest of the moduli with $E_2^d = E_3^d = G_{12}^d = G_{13}^d = G_{23}^d = 0.1E_1^d$.

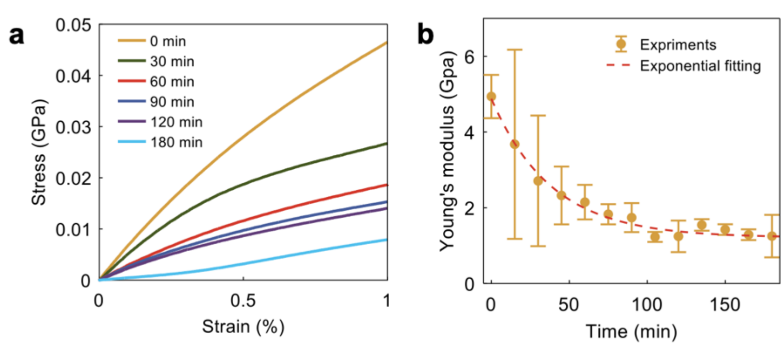

Figure S21. Experimental measurements and calibration of the moisture dependent modulus of white oak. (a) The stress-strain plot of wood strips under different hydrated states and (b) Young's modulus of the hydrate samples at an interval of 15 min. Experimental data in (b) are means ± SD, *N* = 3 samples.

Comment #12: Typo: Line 641, more -> model

Our modification to the manuscript: We have replaced "more" at the current line 640 with "model".

Referee #3 (Remarks to the Author):

Comment #13: The manuscript has been extensively revised reflecting the referee feedback. Now the significance of the work is clear, and the paper is more informative on the design principles, manufacturing process, and functional characterization. I congratulate the authors in achieving this in a short period of revision time.

Our response: We thank the reviewer for the positive comments and suggestions to improve the quality of our manuscript.

I do have a few follow up points from my previous review.

Major comments:

Comment #14: #37: Survey of more wood types as the starting material.

I was asking for this survey, because the key design decision is which wood material to use – in other words, certain wood properties matter very much and then the readers should be informed what they are. From this survey, what surfaced as the key parameters? It is mentioned to some extent in the text, but the survey results weren't used to support the design criteria. Can you clarify better?

Our response: As extensions of the Extended Data Fig. 8a-b, we added additional details for the selection of wood types, by highlighting the critical performance criteria of the wood and clarifying the empirical procedure used to choose the wood. To address the reviewer's comment, we also shared some preliminary analysis in terms of the critical wood properties that may determine the performance of our wood actuator.

Our modification to the manuscript: We added a new "**Supplementary Note 7: Guidelines for Choosing Wood Types**",

"We need wood that (i) is moldable into the large target curvature (a tight coil with a maximum curvature of 1854 m^{-1}), (ii) forms stiff coils to maximize thrust force and prevent bending of the coiled body, (iii) has a large actuation amplitude and good reversibility. We further propose benchmark tests to evaluate these criteria and discuss the potential challenges in choosing wood types to optimize the actuator performances.

Since multi-physics factors are involved in determining the wood choices, we suggest a straightforward procedure experimentally, to identify the suitable wood types that fulfill (i-iii): choosing a few types of wood of interest (in our experiment, we chose four commercially important[72] wood types and bamboo that have relatively parallel fibers, then conducting the test shown in Extended Data Fig. 8a to select the type that provides the largest dry curvature on a target mandrel (0.8 mm in diameter) and the largest actuation amplitude with good reversibility, by measuring at least three actuation cycles. If the design goal is changed, e.g., a larger coiled body with a thicker strip is molded, we would suggest re-doing the benchmarking test to select the most suitable wood types.

To fulfill our criterion (i), it can be observed in Extended Data Fig. 8a-b that certain woods (such as white oak, basswood and Douglas fir) can be molded more easily into large curvatures than others. With regard to the wood types that failed, the fractures often occurred on the outer (tensioned) side of the coil. We suggest choosing a wood type with a large failure strain under tension, which can be obtained through a tensile test. White oak and basswood stood up to larger failure strains among the wood types we tested, following the same chemical washing process (Fig. S12).

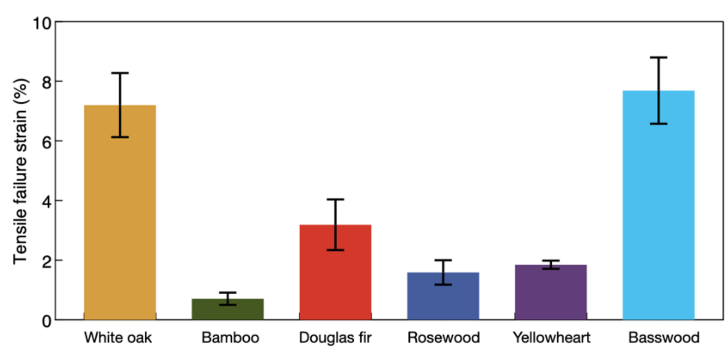

Figure S12. Tensile test to compare the tensile failure strain of the chosen wood types. The samples are 2.2 mm in width, ~0.5 mm in thickness and 80 mm in length. To match our sample molding process, the chemically washed and fully hydrated samples were left in an open environment for 10 min before the tensile test. Data are means ± SD. $N = 3$.

In the case of (ii), in order to achieve stiff coils, we suggest choosing a wood type with a relatively large Young's modulus after chemical washing. However, other factors such as the potential damage during molding (Extended Data Fig. 8e) can also affect the coil stiffness. We recommend further characterization of the molded coils to directly evaluate the effective extension force of the coiling actuators (refer to the extension force test described in Methods and Supplementary Note 4).

In the case of (iii), the large amplitude of the actuation from the wet to the dry state of the coil is determined by the gradient of the moisture shrinkage ratio, caused by deformation during molding. We would suggest choosing wood with strong coupling between the mechanical deformation and moisture induced shrinkage. The good reversibility of an actuator requires little plasticity and minimal local damage under deformation, driven by moisture content change. Since the couplings between moisture and mechanical deformation among wood types are usually highly nonlinear and may also depend on the applied stress state, it is challenging to establish a single criterion that can optimize both amplitude and reversibility at the same time. We recommend measuring the curvature changes of a simple bending actuator for three-cycles as benchmark tests (exemplified in Extended Data Fig. 8a), so as to evaluate the wood materials.

Among the chosen wood materials tested, white oak is the most suitable in terms of its largest initial curvature, actuation amplitude and good reversibility (Extended Data Fig. 8a). However, it should be pointed out that these criteria are based on our experimental observations and serve as guidelines for our design, as it is a challenging, multi-objective optimization problem. In addition, the wood properties are influenced by the chemical washing conditions and manufacturing methods. Our preliminary tests have already shown that rosewood coils also exhibit a promising performance with a smaller actuation amplitude yet better reversibility in three actuation cycles (Extended Data Fig. 8a), showing the possible extensions of the current framework to other wood types and applications. The detailed evaluations and optimizations of the wood materials, tailored to different applications, are important but beyond the current scope, which will be studied in the future."

[72] Miller, R. B. *Characteristics and availability of commercially important woods*. 1.1-1.34 https://www.fs.usda.gov/treesearch/pubs/7141 (1999).

Comment #15: #39 (in relation to #29): Survey of natural self-burial seed diversity.
In the Table S1, is the data of their drilling effectiveness missing? I only see the geometrical specs in the table, but the authors say they did the drilling test. Please show the results.

Our modification to the manuscript: We added the drilling test as a separate column in Table S1. The updated table is shared below:

Table S1: Summary of selective, self-burial grass seeds and engineered seed carriers. Data for dimensional measurements are means ± SD, $N = 3$. The drilling test to obtain the establishment rate (80% tip burial) was conducted for three triggering cycles with five samples of each type. (Testing procedure and conditions are consistent with "Drilling tests under controlled conditions" in Methods).

Types	Awn Morphology		Body wet Length (mm)	Seedpod Length (mm)	Seedpod Maximum Diameter (mm)	Seedpod Dry Weight (mg)	Establishment Rate
Stipa comata	• Single awn with one sharp bend and one curve • Twisted body	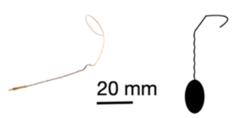	142.6 ± 18.5	11.3 ± 3.1	1.0 ± 0.0	7.9 ± 0.3	40%
Stipa spartea	• Single awn with two sharp bends • Twisted body	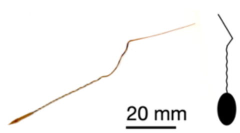	117.7 ± 6.7	18.3 ± 1.0	1.3 ± 0.1	13.0 ± 0.5	0%
Aristida purpurea	• Triple awns with three sharp bends • Straight body	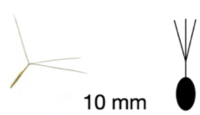	34.9 ± 4.7	8.2 ± 1.8	0.4 ± 0.1	0.9 ± 0.2	0%
Erodium guinum	• Single awn with one curve • Coiled body	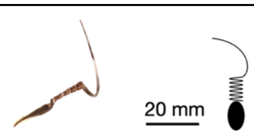	90.4 ± 0.9	15.1 ± 0.6	2.4 ± 0.3	28.3 ± 9.5	0%
Erodium castellanum	• Single awn with one curve • Coiled body	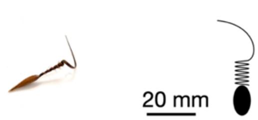	48.2 ± 1.0	9.6 ± 0.2	1.9 ± 0.1	12.3 ± 3.1	20%

Medium-sized Engineered	• Triple awn with three curves • Coiled body	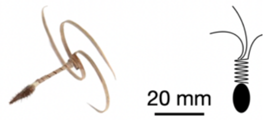	135.3	13.5	3.1 ± 0.3	52.0 ± 10.5	80%
Large-sized Engineered	• Triple awn with three curves • Coiled body		302.7	20.8	9.0 ± 0.5	75.3 ± 0.6	100%

Comment #16: #41: Cell size effect.

I see the cell size was not that critical, but the data shows the average size. I was more wondering about the number and distribution of larger cells, like the vessels, which have much thicker cell walls and much larger in size. Also, the veneer polarity (the face toward outside of the annual ring would have smaller cells) in general. Did you pay attention to the sides of the wood strips, and/or it did not make a clear difference in the performance of the actuators?

Our response: In our original manuscript, since we did not track towards the side to which we molded the strip samples, our data reported in the manuscript revealed the averaged performance without controlling the veneer polarity. We clarified this point in the manuscript. To address the reviewer's question regarding whether the veneer polarity may play a role in the performance of the actuator, we molded samples from the same wood strip towards two opposite sides and compared the curvatures achieved. We did not observe that the veneer polarity played any noticeable role, since the differences between the sides are less than the error ranges of a single side (see Fig. S10 below).

In addition, we greatly appreciate that the review highlighted the vessel distribution issue, as we believe it is an important fabrication detail that we should have added into the manuscript, so as to ensure sample quality and reproducibility. In Extended Data Fig. 4g, we intended to show the manual planning and selection process, to decide where to cut the wood strip for sample preparation. In addition to our recommendation of "laser cutting along the fiber direction," we should have added a second criterion: picking a region that does not have visually identifiable pores (vessels) from the earlywood. These large vessels have an average diameter of ~250 - 500 um[71] and are visible to the human eye. We also conducted a set of experiments to understand how the smaller vessels at ~20-50 um in latewood, which are not identifiable to the naked eye, may affect the actuator performance. It transpired that the vessel number in latewood did affect the maximum curvature of the actuator, while no obvious effects of the vessel distribution were observed. More details are shared below:

Our modification to the manuscript:

- We clarified how we excluded the earlywood region with large vessels through a visual inspection process, visible to the naked eye, by adding additional details in "**Supplementary Note 6: Fabrication Details**": On page 60, line 1106, we added "Note that within each annual ring of white oak, the earlywood has larger vessel diameters of ~250 - 500 um than that of latewood at ~20-50 um[71]. Since our sample is quite thin, relative to the thickness of each annual ring (Fig. S10a), we chose only to use the latewood. We believe that excluding the earlywood with relatively large vessels helps decrease the effects of vessel polarity or the distribution on the bending performance. Before cutting, the exact location of the outlines was visually inspected to avoid the earlywood region with large vessel pores with diameters of ~0.25-0.5 mm in the white oak. As shown in Figure S10b below, the earlywood regions where large vessels concentrate can be identified at low magnification with the naked eye in the case of white oak. In regions where visually identifiable pores exist, these will be excluded for sample preparation."

[71] Maeglin, R. R. & Quirk, J. T. Tissue proportions and cell dimensions for red and white oak groups. *Can. J. For. Res.* **14**, 101–106 (1984).

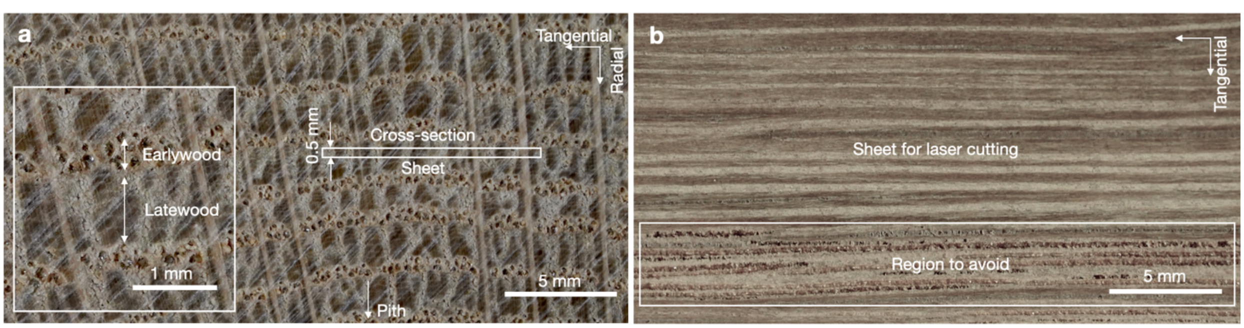

Figure S10. a, The relative size and location of a sample sheet situated on a tangential-radial plane of a white oak lumber. The sheet is prepared from the latewood region with relatively small vessels. **b**, Regions with concentrated large vessels are excluded before the laser cutting and strip sample preparation, through a visual inspection process relying on the naked eye.

- To elaborate how vessel number and distribution may affect the actuator performance, we included additional details in "**Supplementary Note S3: Cellular Size, Number and Distribution**":

The impact of veneer polarity to the molded dry curvature: To further understand whether the polarity within the latewood affects the molding curvature, we molded samples from the same wood strip towards two opposite sides and compared the curvatures achieved. During this test, we used three strips from three randomly selected veneer sheets of latewood. For each strip, we took six samples, with three of them molded towards one side and the other three towards the opposite side (Fig. S5c). The error bar indicates the curvature variations of the three samples on the same side. We did not observe any noticeable role played by the veneer polarity, since the differences between the two sides were smaller than the error ranges of a single side.

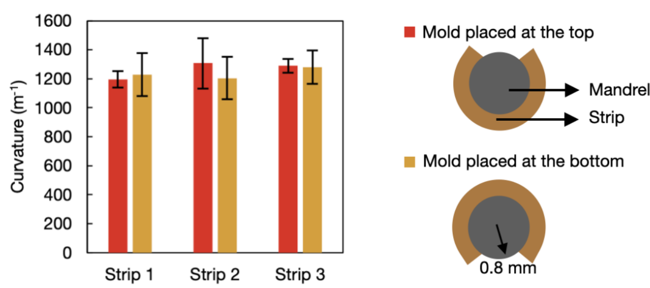

Figure S5. Comparison of the molded dry curvature with samples molded towards two opposite sides. For each strip, ~0.5 mm thick and 2.2 mm wide, six samples of 5mm lengths are prepared, with three of these molded towards one side and the other three towards the opposite side. Data are means ± SD, $N = 3$.

Vessel number and distribution: To understand this aspect, we chose to prepare three veneer sheets from the same white oak lumber, with the sheets ~2 years apart from one other (Fig. S6a). On each sheet, we randomly chose five locations to derive five samples, 5 mm in length and 2.2 mm in width. We imaged one cross-section of each sample under SEM (Fig.S6b), counted the vessels that are larger than 25 um and compared the dry curvature after the samples were molded on a 0.8 mm mandrel.

Figure S6c shows that the total number of vessels decreases as the sample is obtained closer to the center of the trunk. It also shows that the curvature of the molded sample decreases from

1318.4 ± 110.5 m^{-1} to 1079.7 ± 95.5 m^{-1} as the total vessel number increases from 11 ± 3 to 35 ± 7.

To investigate the vessel distribution, we counted a total of five samples from each sheet and mapped them out spatially (Fig. S6d). Since our sample is relatively thin (~0.5 mm), the vessel is relatively evenly distributed across the thickness, especially in the case of sheet 1 and sheet 2 (Fig. S6e). Despite the fact that sheet 3 exhibited a comparably larger difference (with a 17.8% difference) in total vessel numbers between the top and bottom halves, we did not observe a greater standard deviation in curvature than that of sheet 1 in Fig. S6c. Therefore, we do not believe that the gradient of the vessel across the thickness played as significant a role as the other factors (e.g., the unavoidable variations of the manual molding process and the total changing number of the vessels) in the curvature variation, which is also verified in Fig. S5.

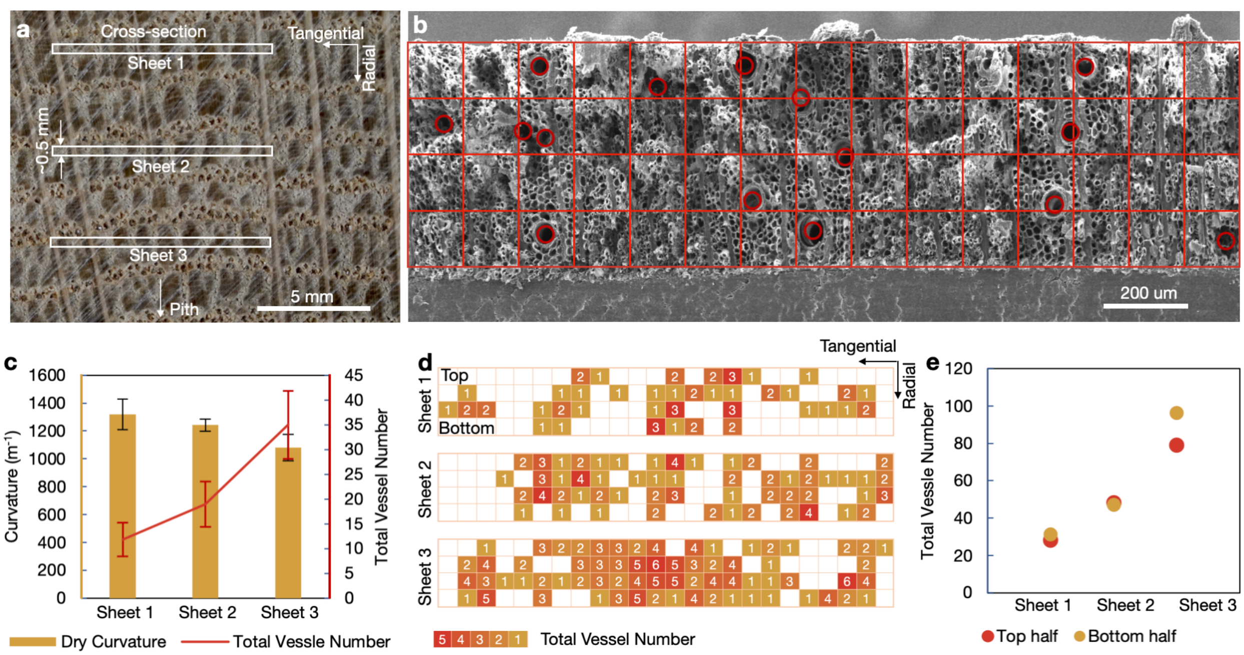

Figure S6: The effects of vessel numbers and distribution. a, The cross-section of the white oak lumber used for our sample preparation. The wood strips used to mold the samples are prepared from latewood, with relatively small vessel diameters of ~25 - 50 um. Five samples, 2.2 mm wide, 5 mm long and ~0.5 mm thick are prepared from each sheet. **b**, Vessels with a diameter larger than ~30 um were identified and counted in the cross-section SEM image of each sample. **c**, Comparison of molded dry curvature and total vessel size of each sheet. $N = 5$ samples from each sheet. Data are means ± SD. **d,** Spatial distribution of the total vessels of the five samples from each sheet. **e**, Comparison of the total number of vessels for the top and bottom halves of all five samples of each sheet.

Comment #17: #42: Quantification in the soil drilling test.
Fig 3e and h – error bar is large, and N is small. Please repeat the experiments with more samples.

Our response: We have increased the testing samples from three to 10, for both tests. Regarding the updated Fig. 3e and h, we obtained smaller error bars compared to the previous plot with only three samples, although they are still relatively large. We believe the variation in drilling depth of each sample is inherent in the testing conditions, despite our best effort to keep these consistent. Aside from the variations induced during the wood selection and fabrication process (see Fig. 2 for curvature variation and Supplementary Fig. S11 in Supplementary Note S6 for coil pitch and length variations), each seed tested may undergo slightly different local soil roughness and hydration conditions. For example, since we test multiple seeds at the same time, even though the average distribution of soil granules is deemed to be relatively even by a standard soil topography test (Methods), the exact size and shape of the granules surrounding each tip of the seed can be different and may cause variations in drilling depth. Moreover, in our test chamber setup (Methods), the atomized water spray, which was customized to emulate the natural rain conditions, induced small water droplets on the seed carriers. Depending on how the small water droplets coalesce on the surface of the seed body, there will be variations in moisture inside the structure.

Our modification to the manuscript:

We have increased the testing samples from three to 10 for all samples, and updated Fig. 4e and h with decreased SD.

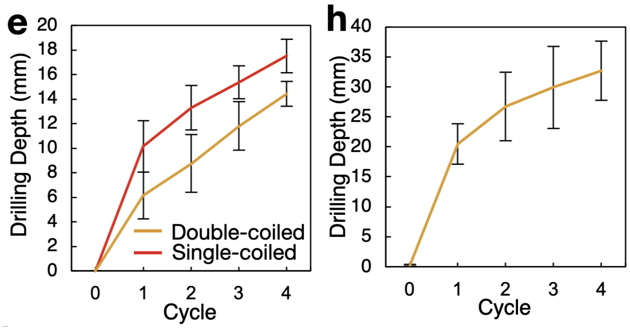

Updated **Figure 4. e,** Comparison of the self-drilling depth between the double-coiled and single-coiled seed carriers. Data are means ± SD, $N = 10$ for each type. **h**, Drilling depth of large-sized seed carrier with a body length of ~302 mm. Data are means ± SD, $N = 8$ anchored ones from a total of 10 samples. More details for tests (**b-h**) are included in the Methods.

Comment #17: Also, comparison of germination rates with respect to buried vs unburied (never or resurfaced) is a key result. At the moment such information is mentioned only for a limited number of tests – can you be more comprehensive?

Our response: First, we shared more details regarding the previous germination tests. We tracked the germination performance across five tests in Table S4. However, we had to give up test 4 as most of the seed carriers, including the ones with tips buried from this test, went missing over the fifth night. We suspect nocturnal animals such as raccoons took the seeds since dug holes were observed. We managed to track the germination performance in the remaining four field tests (tests 1-3 and 5 in Table S4) for 15 days. Initially, there were 47 anchored seed carriers and 29 unanchored ones. Over the testing period, three anchored seed carriers were dislodged, and an additional anchored one went missing (REF Fig. R2a). On day 15, we observed that 26 of out 43 anchored seeds geminated successfully with a 60.5% germination rate, and 4 out of 32 unanchored or dislodged ones germinated with a 12.5% germination rate (REF Fig. R2b). Note that while we embedded five arugula seeds (Eden Brothers, USA) into each seedpod, a seed carrier was considered to have successful germinated if we observed at least one sprout. The sprouts totaled 82 in the 26 anchored seed carriers and 6 in the 4 unanchored ones (REF Fig. R2c).

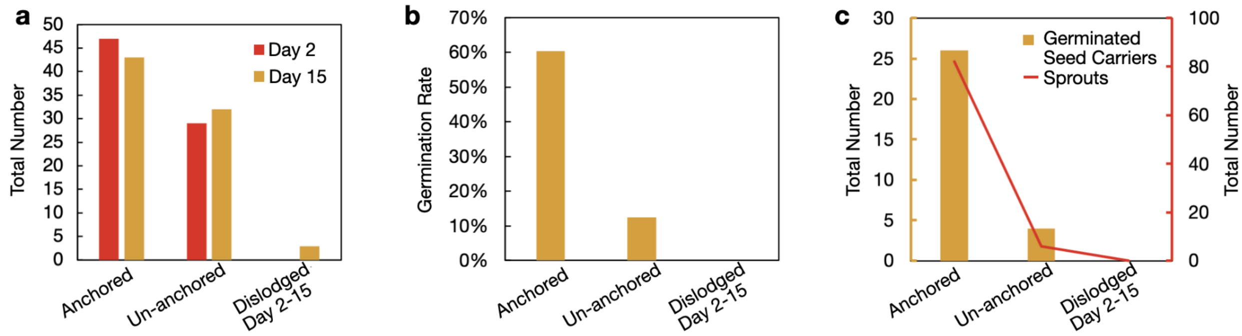

REF Figure R2. Performance from the field germination test as follow-up tests after the initial drilling tests in drilling tests 1-3 and 5 in Supplementary Table 4a, The total number of tracked seed carriers over a period of 15 days after the initial rain-triggered drilling tests. **b**, The total germination rate of initially anchored, initially un-anchored and dislodged seed carriers on day 15. **c**, The total number of germinated seed carriers and sprouts.

A consecutive germination test of 400 seed carriers in the later summer season indicated a consistent advantage of the buried seeds over the unburied ones, yet with an overall lower germination rate than the tests conducted in earlier seasons.

Our modification to the manuscript:

- On page 14, line 293, we briefly describe the test we newly conducted: "A consecutive germination test of 400 seed carriers in the later summer season indicated a consistent advantage of the buried seeds over the unburied ones, yet with an overall lower germination rate than the tests conducted in earlier seasons (Supplementary Note 5)."

- On page 59, line 1068, we added more details regarding both the old and new germination tests in "Supplementary Note 5: Drilling and Germination Performances in Field Tests":

"**Germination Results.** We tracked the germination performance across five tests in Table S4. However, we had to give up test 4 as most of the seed carriers, including the ones with tips buried from this test, went missing over the fifth night. We suspect nocturnal animals such as raccoons took the seeds since dug holes were observed. We managed to track the germination performance in the remaining four field tests (tests 1-3 and 5 in Table S4) for 15 days. Initially, there were 47 anchored seed carriers and 29 unanchored ones. Over the testing period, three anchored seed carriers were dislodged, and an additional anchored one went missing. On day 15, we observed that 26 of out 43 anchored seeds geminated successfully with a 60.5% germination rate, and 4 out of 32 unanchored or dislodged ones germinated with a 12.5% germination rate. Note that while we embedded five arugula seeds (Eden Brothers, USA) into each seedpod, a seed carrier was considered to have successful germinated if we observed at least one sprout. The sprouts totaled 82 in the 26 anchored seed carriers and 6 in the 4 unanchored ones.

The above tests were conducted from April to early July, which is the most suitable season for germinating most vegetable and flower seeds in both of our testing sites. To understand whether the seed carriers could germinate seeds in later seasons with varying seed types, we conducted an additional germination test in fiber soil from August to September, when the average temperature was 35 – 40 °C. 400 seed carriers were deployed in the field. 200 of those had their seedpods 80% buried beneath the soil manually, and the other 200 were placed on the soil surface and unburied. Two hot pepper seeds known to germinate at relatively high temperatures (27 – 32 °C) were embedded in each seedpod. After a month, we observed a 35.5% germination rate for the buried seed carriers and 2% for the unburied ones. While we observed a consistent advantage of the buried seeds over the unburied ones in their germination performance, we obtained an overall lower germination rate than the tests conducted in earlier seasons."

Comment #18: #43: Soil granularity test.
Can you incorporate the finding from this measurement to the results of the drill tests to gain further insights on how strongly soil roughness affect the drilling? Here I especially mean the link to the field tests.

Our response: We analyzed the two-day averaged establishing rate on soils with different granularities in the field tests (Supplementary Table 4) and summarized the data as follows: in fiber soil (tests 2, 3 and 5), the averaged establishing rate of the three tests was 38%; in local topsoil (test 1), the averaged establishing rate was 52%; in sandy steer manure compost (test 4), the establishing rate was 33%. The two-day averaged establishing rate is used to take account of the environmental variations on day 1 and day 2. These data show that the establishing rate has a positive correlation with the LSMV measured in Supplementary Table 5. However, the establishing rate can also be influenced by other factors (e.g., temperature and rains), as the referee pointed out. More controlled field tests are needed to draw a concrete conclusion.

Unfortunately, the ideal season (late spring and early summer) for the field tests has passed. We included a wider discussion on the impact of soil granularity on the field tests in the paper.

Our modification to the manuscript:

We added "Supplementary Note 5: Drilling and Germination Performances in Field Tests" and included a subsection with additional details regarding soil granularity:

"Soil Granularity. We analyzed the two-day averaged establishing rate on soils with different granularities in the field tests (Table S4) and summarized the data as follows: in fiber soil (tests 2, 3 and 5), the averaged establishing rate of the three tests was 38%; in local topsoil (test 1), the averaged establishing rate was 52%; in sandy steer manure compost (test 4), the establishing rate was 33%. The two-day averaged establishing rate is used to take account of the environmental variations on day 1 and day 2. These data show that the establishing rate has a positive correlation with the LSMV measured in Table S5. However, the establishing rate can also be influenced by other factors (e.g., temperature and rains), as the referee pointed out. More controlled field tests are needed to draw a concrete conclusion."

Comment #19: #44: More field test.

I asked for more field tests, so that you could pinpoint what parameters affect the self-burial actuator function the most in realistic conditions. Looking at the data, soil type does not seem to be a dominant factor. Rather, temperature seem to be, and that is not surprising (it is one factor anticipated to affect hydromorphic structural function). I think this is an important parameter to test, and you have a suitable set up to measure the drilling force when the tails are exposed to mist, temperature of which you can modulate.

Our response: We thank the reviewer for the insightful comment. Temperature appears to affect the drilling performance. Tests 2-4 had an average temperature of ~12-17°C, with a 33.5% establishing rate, while test 1 and 5 experienced an average temperature of ~23-32°C with a 51% establishing rate. To understand how temperature may affect the thrust force generated by the coiled body, we conducted a controlled test comparing the extension force of the 7 coils at two different temperatures. This showed that the peak force decreased from 42.47 ± 4.48 mN to

31.45 ± 2.63 mN, when the testing temperature dropped from ~30°C to ~18°C. We integrated these analyses and observations into the updated manuscript.

Our modification to the manuscript:

- On page 14, line 286, we added: "Temperature appears to affect the drilling performance. A higher average temperature in the field tests resulted in a higher (33.5%) establishing rate. In a controlled test, the extension force of the 7 coils decreased from 42.47 ± 4.48 mN to 31.45 ± 2.63 mN when the temperature dropped from ~30°C to ~18°C (Supplementary Note 5)."

- We added "**Supplementary Note 5: Drilling and Germination Performances in Field Tests**" and included a subsection with additional details regarding temperature effects: "**Temperature Effects.** It appears that the temperature affects the drilling performance. Tests 2-4 from Table S4 had an average temperature of ~12-17°C, with a 33.5% establishing rate, while test 1 and 5 experienced an average temperature of ~23-32°C with a 51% establishing rate. To understand how temperature may affect the thrust force generated by the coiled body, we conducted a controlled test to compare the 7 coils extension force under two different temperature conditions (Fig. S9). This showed that the peak force decreased from 42.47 ± 4.48 mN to 31.45 ± 2.63 mN when the testing temperature dropped from ~30°C to ~18°C. The coil under a higher temperature also exhibited a greater rate of force increase within the first 5 mins."

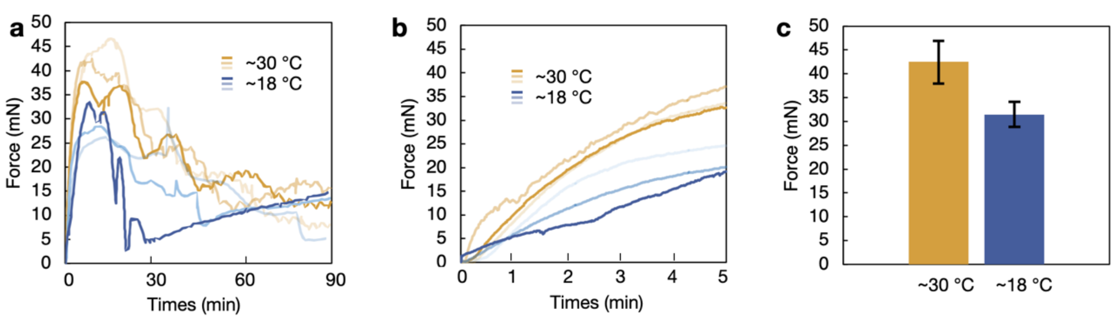

Figure S9. Comparison of coil extension forces under different temperature conditions. a, Extension force profiles during the 90 min hydration process under ~30°C and ~18°C. **b**, The rate of increase in the extension force is larger at ~30°C than ~18°C for the initial 5 minutes. **c,** The comparison of peak forces under two different temperatures. All the tests were conducted in the controlled chamber (Methods), with 7 coils of ~0.5 mm thickness. For (**c**), data are means ± SD, $N = 3$.

Comment #20: Minor comments:

The order of the supplementary materials is not in line with the order of mention in the main text.

Our response: We thank the reviewer for the careful reading of our manuscript. We have double checked the orders of all supplementary materials.

Reviewer Reports on the Second Revision:

Referees' comments:

Referee #1 (Remarks to the Author):

the authors significantly improved the quality of the manuscript. All the reviewers' remarks and feedback have been addressed. The current version is really interesting and shows high potential impact both in science and applied innovation.

Referee #2 (Remarks to the Author):

The authors have extensively revised the manuscript to reflect the referee comments. In particular, the experiments to measure the dependence of Young's modulus on the degree of hydration are impressive and worth of praise.

This referee pointed out that the simulation results were not in quantitative agreement with the experimental results although the authors intentionally inserted the word "quantitative" during the first revision. After the referee's comment in the second round, the authors now change their stance and argue that their comparisons are qualitative, not quantitative. Such a response might have relieved the authors of a lot of burden in the revision process, but leaves a flaw in our constructive peer review process.

Overall, the modeling has been much improved from the initial submission, and now I recommend its publication in the journal.

Referee #3 (Remarks to the Author):

I find the revised manuscript sufficiently reflecting the reviewers' feedback.

One last suggestion is to increase the sample number to at least 10 in all those assays where N is currently smaller than 10. The results are variable (as they are biological materials), but with a higher sample number, the results will become more robust and true to the variations expected.

Author Rebuttals to Second Revision:

Response to Reviewers

Referee #1 (Remarks to the Author):

Comment #1: The authors significantly improved the quality of the manuscript. All the reviewers' remarks and feedback have been addressed. The current version is really interesting and shows high potential impact both in science and applied innovation.

Our response: We thank the reviewer for the insightful comments to improve the quality of our manuscript.

Referee #2 (Remarks to the Author):

Comment #2: The authors have extensively revised the manuscript to reflect the referee comments. In particular, the experiments to measure the dependence of Young's modulus on the degree of hydration are impressive and worth of praise.

This referee pointed out that the simulation results were not in quantitative agreement with the experimental results although the authors intentionally inserted the word "quantitative" during the first revision. After the referee's comment in the second round, the authors now change their stance and argue that their comparisons are qualitative, not quantitative. Such a response might have relieved the authors of a lot of burden in the revision process, but leaves a flaw in our constructive peer review process.

Overall, the modeling has been much improved from the initial submission, and now I recommend its publication in the journal.

Our response: We thank the reviewer for all the comments, especially the integration of Young's modulus changes into our model. Again, we apologize for the initial confusion as we accidentally typed "quantitative" when we intended to say "qualitative".

Referee #3 (Remarks to the Author):

Comment #3: I find the revised manuscript sufficiently reflecting the reviewers' feedback.

One last suggestion is to increase the sample number to at least 10 in all those assays where N is currently smaller than 10. The results are variable (as they are biological materials), but with a higher sample number, the results will become more robust and true to the variations expected.

Our response: We thank the reviewer for the positive comments and suggestions to improve the quality of our manuscript. For the suggestion of potentially increasing the sample number, we have highlighted the intrinsically heterogeneous nature of the biological materials and the uncontrolled field conditions in our tests, making variations of the measurements inevitable.